



An Investigation into The Effect of a Soft Tissue Stabilising Mesh Within Elastomeric Liners for Lower Limb Prosthetics

Bernardo Mateus Bastos Teotónio Pereira

Thesis to obtain the Master of Science Degree in
Bioengineering and Nanosystems

Supervisors: Dr Arjan Buis
Prof. Miguel Tavares da Silva

Examination Committee

Chairperson: Prof. Gabriel António Amaro Monteiro
Supervisor: Prof. Miguel Tavares da Silva
Member of the Committee: Prof. Rogério Anacleto Cordeiro Colaço

October 2018

ACKNOWLEDGEMENTS

First and foremost, I would like to thank Dr Arjan Buis, for the opportunity he gave me to work at the University of Strathclyde in association with the Legbank Project. I especially want to thank him for his help, support and advice throughout this project.

I express my sincere gratitude to Dr Nicholas Roberts, his teaching and help on finite element analysis was critical for the completion of this thesis.

I would like to express my appreciation to all members of the staff from the National Centre for Prosthetics and Orthotics (NCPO), for the warm welcome I received and for the constant willingness and patience to teach me, that each one demonstrated.

I would like to thank Richard Copeland, for the support handling the Instron machine.

I also want to thank Professor Miguel Tavares da Silva for his support and contributions in the last months of the project.

Finally, I want to thank Professor João Folgado, for his support and help at the final stages of the finite element analysis.

ABSTRACT

A suspension or locking prosthetic liner, is a prosthetic component that functions as an interface between the skin of a lower residual limb and a rigid prosthetic socket. The ultimate purpose of a liner is to improve amputee safety and comfort. Although prosthetic liners for lower-limb amputees are broadly commercially available, no academic studies have been found that evaluate the effect of different configurations of imbedded reinforcement structures within the matrix of liners, preventing pistoning (longitudinal displacement) occurrence.

The aim of this investigation is to create tools to produce a liner that provides prosthesis suspension, by reducing pistoning and subsequently avoid deep tissue injury and to guarantee acceptable levels of comfort for the patient, by allowing an easy insertion and use of the liner.

In this work, after a commercial liner's development analysis and a scientific literature review, a set of design goals was created to achieve such a liner and matrix reinforcement.

A finite element model (FEM) was created with two main goals: proving the necessity of a reinforcement within the matrix, evaluating where the main areas of stress in the reinforcement mesh configuration are present and what was its effect on the liner pistoning occurrence.

To compare the reinforcement mesh configuration produced in this project with the state of the art commercial liners, utilising mechanical tests mimicking the conditions of the swing phase of the gait cycle, the effect of the liners when stump volume variations occur, and if the liners were resilient enough to maintain contact with the stump while its volume varied, during swing phase conditions has been investigated. The "Majicast" prototype liners, produced in this project, showed a state of the art response to the test conditions.

Key-words:

Reinforcement mesh; Matrix; Liner; Pistoning; Deep Tissue Injury; Finite Element Model; Swing Phase.

RESUMO

Um liner de suspensão, faz parte dos componentes de uma prótese e atua como uma interface entre a pele de um coto de membro inferior e o componente de encaixe rígido da prótese (“socket”). O objetivo último de um liner, é o de aumentar o conforto e segurança do paciente. Apesar de já serem amplamente comercializados, não foram encontrados estudos acadêmicos que avaliem o efeito de diferentes configurações de reforço, dentro da matriz dos liners, de maneira a evitar a separação longitudinal do liner com a perna no momento em que o pé não está em contacto com o solo (efeito de “pistoning”), tendo assim uma boa suspensão.

O objetivo desta investigação, é criar as ferramentas necessárias para a produção de um liner que providencie a suspensão desejada da prótese, reduzindo o efeito de “pistoning”. Consequentemente, o liner evitará lesões de pressão, garantindo ao mesmo tempo níveis de conforto ao paciente, permitindo uma boa inserção e remoção do liner.

Para atingir este liner, uma série de objetivos de design foram implementados para a criação de uma matriz reforçada de silicone, depois de uma análise ao desenvolvimento comercial dos liners e de uma revisão da literatura científica.

Um modelo de elementos finitos foi criado com dois objetivos principais: demonstrar a necessidade de um reforço da matriz, avaliando as áreas onde esse reforço é mais crítico, e avaliar o efeito que o reforço tem na redução da deslocação longitudinal do liner.

Para comparar a configuração da rede de reforço da matriz desenvolvida neste projeto, com os liners presentes no mercado, realizaram-se testes mecânicos simulando as condições da fase de balanço da perna durante uma passada. Um parâmetro simulado simultaneamente foi a variação de volume do membro residual, verificando-se a eficácia dos diferentes liners ao longo de tais variações. Os protótipos de liners “Majicast”, produzidos neste projeto, demonstraram uma resposta equivalente aos liners comerciais, face as condições de teste mencionadas.

Palavras chave:

Rede de reforço; Matriz; Liner; Pistoning; Lesão de pressão; Modelo de elementos finitos; fase de balanço

CONTENTS

ACKNOWLEDGEMENTS	iii
ABSTRACT	v
RESUMO	vii
CONTENTS	ix
List of Abbreviations and Glossary	xi
LIST OF TABLES	xiii
LIST OF FIGURES	xv
CHAPTER 1 - Introduction.....	1
1.1 Motivation	1
1.2. Objectives.....	2
1.3. Literature Review	2
1.3.1. Socket fit – A biomechanical and medical problem	2
1.3.2. The interface – a socket and a residual limb.....	5
1.3.3. Load transmission and pressure distribution	6
1.3.4. Soft tissue injury: DTI and skin stretching	8
1.4. Main Contributions	10
1.5. Structure and Organization	10
CHAPTER 2 - Lower-Limb Prosthetic Liners.....	13
2.1. Liner’s material mechanical tests.....	13
2.2 Heat transfer properties and moisture permeability.....	15
2.3 Clinical evidence for liners performance.....	16
2.4. Suspension elastomeric liners development	17
2.4.1 Prosthetic silicone rubber liner	18
2.4.2 Dual Stiffness Membranes	19
2.4.3 Other mesh configurations.....	19
2.4.4 Alternative approaches	23
2.4.5 Summary	25
2.5. Product design considerations	25
CHAPTER 3 – The Need for An Anisotropic Matrix.....	29
3.1. Model Geometry – 1 st stage.....	30
3.2. Material Properties - 1 st stage.....	32
3.2.1. Silicone material properties	32
3.2.2. Soft Tissue material properties	34

3.3. Boundary conditions and applied load - 1 st stage:	35
3.4. Mesh the model - 1 st stage	40
3.5. Finite Element Analysis Results - 1 st stage.....	42
3.5.1. First stage results.....	42
3.5.1.1. Linear Model	44
3.5.1.2 Hyperelastic/non-linear model	46
3.6. Reinforced liner VS Non-reinforced liner – 2 nd Stage.....	49
3.6.1. Geometry and Mesh.....	49
3.6.2. Material Properties	53
3.6.3. Boundary Conditions	53
3.6.4. Second Stage Results.....	55
3.6.4.1. Reinforced liner – ABAQUS model	55
3.6.4.2. Non-reinforced liner – ANSYS model	58
3.7. Finite Element Analysis Discussion.....	59
3.7.1. 1 st Stage Discussion – Pistoning effect:	59
3.7.2. 2 nd Stage discussion – Reinforced VS Non-reinforced liner:	60
CHAPTER 4 - Liner’s Mechanical Tests	63
4.1. Objective	63
4.2. Materials.....	63
4.4 Mechanical tests results	67
4.4. Mechanical tests discussion	70
CHAPTER 5 - Conclusions and Future Developments.....	75

List of Abbreviations and Glossary

DTI – Deep Tissue Injury;

FEA – Finite element analysis;

FEM – Finite Element Model;

FE mesh – finite element mesh – Set of elements and nodes, describing a geometry;

Reinforcement mesh – Structure composed by fabric, embedded in the silicone matrix;

Matrix – The binder of the composite (reinforcement plus binder);

PTB – Patellar Tendon Bearing;

TSB – Total Surface Bearing;

HS – Hydrostatic;

VAS – Vacuum-Assisted Suction;

COF – Coefficient of Friction;

CS – Compressive Stiffness;

H – Finite Element Model criterion for the separation between the liner and the soft tissue;

LIST OF TABLES

Table 3.1: Silicone material properties for the linear model	33
Table 3.2: Soft tissue linear elastic properties.....	34
Table 3.3: Comparison between the mesh metric and the size functions available. The goal is to find the size function that combines the highest minimum value for element quality, the smallest maximum value for the aspect ratio and smaller maximum value for the Jacobian ratio. Highlighted in bold are the best values according to these criteria, and the size function that have the best match overall.	41
Table 3.4: Silicone material properties used for second stage analysis. Linear elastic model used. ...	53
Table 3.5: Polyester fibres material properties. Linear elastic model.	53
Table 3.6: Node magnitude of deformation and liner's region	56
Table 4.1: Tests description	66
Table 4.2: Maximum displacement in each test. It is also show the percental change between each volume variation and the total change between the first volume and the last.....	67
Table 4.3: Mean minimal displacement. Highlighted are the values were the offset was higher than 1mm.	69
Table 4.4: Mean maximum tensile force. Highlighted are the values where the offset was higher than 9N, considering the value of 49N as reference.	69
Table 4.5: Mean maximum compressive force. Highlighted are the values where the offset was higher than 10N, considering the value of 0N as reference	70
Table 4.6: Amplitude of the displacement, using maximum and minimum value of displacement of each test. Also % variation is shown between the immediately previous stump volume tests realized.	70
Table A. 1: Parameters evaluating the quality of three different meshes for the reinforced model.	84

LIST OF FIGURES

Figure 1.1: A scheme of the stump-liner-socket system. Adapted from [2].	1
Figure 1. 2: Gait Cycle representation, where stance and swing phase can be observed. Image adapted from reference on footnote	3
Figure 1. 3: Reswick-Rogers diagram (1972) [12], “safe” pressure below the curve.	4
Figure 1.4: Representation Adapted from [1]. The graphic represents the pressure level and the shear stresses that result from a pressure gradient. This shear stresses within the soft tissue are especially likely to occur at bony prominences.	7
Figure 1.5: Residual limb finite element model. Donning pressures [kPa] are predicted for a transtibial residual limb in a PTB socket [13].	8
Figure 1.6: Proposed sequence of events during tissue compression [24].	9
Figure 2.1: Liner worn by amputee for pressure and shear sensing test [52].	17
Figure 2.2: 1 - Representation of the liner proposed by Klasson <i>et al</i> (1987); 2 and 3 – fixation system; 4 – reinforcement fabric laminated within the liner [54].	18
Figure 2.3: Donning of the liner representation: 5 – inside surface of the liner; 6 – outside surface of the liner; 7 – stump; 8 – skin; 9 – soft tissue downward drawing effect; 10- neutral line for stretching/compression of the liner; T – portion of the liner stretched; K – portion of the liner compressed; [54].	18
Figure 2.4: Configuration: Number 11 – elastic material matrix; 13 – distal attachment; 14 – open end; 16 – side wall; 18c – convex short arms imbedded inside the matrix; it includes elongated arms (20) that extend themselves longitudinally, both are made of silk or fibreglass cloth for ex. Adapted from [58]	20
Figure 2.5: Fibres orientation when stretched in direction 14[60].	21
Figure 2.6: Non-stretched fibres. Two possible directions of stretching: 12 and 14 [60].	21
Figure 2.7: Embodiment of the structure within the liner [60].	21
Figure 2.8: 2 – layers; 4 – liner material (silicone or other elastomeric); 6 – fibres; 8 – first fibres layer; 10 – second fibres layer; [60]	21
Figure 2.9: Spiral fibres embedded in two different pats liners. Adapted from [60]	22
Figure 2.10: Hexagonal shape mesh. [60]	23
Figure 2.11: OWW liner configuration showing the knee panel. [62]	24
Figure 2.12: Number 25 shows the knee panel described by [62]	24
Figure 3.1: Model sketch with dimensions shown:	30
Figure 3.2: Interior core that will be composed by soft tissue;	31
Figure 3.3: The exterior shell, that will be the silicone liner.	31
Figure 3.4: The steel plate, used to apply the force in a realistic way.	32
Figure 3.5: Fixed support highlighted, fixing the top surface of the soft tissue and liner’s geometry....	35

Figure 3.6: Remote force (highlighted in red) of -49 N applied parallel to the Y direction, at the centre of the top surface of the rigid plate under the liner.	35
Figure 3.7 Lower limb schematic drawing representing the angle of rotation of the knee during swing θ_k [74].....	36
Figure 3.8: Force diagram for the pendulum. Adapted from reference in footnote.	37
Figure 3.9: Frictional contact, with COF = 0,6.	39
Figure 3.10: Bonded contact between liner and plate.	40
Figure 3.11: Mesh representation	41
Figure 3.12: Region of interest amplified at the hyperelastic model. The labels on to are the deformation vector values for 2 different nodes at the surface of soft tissue ($U_{st}=5,3$ mm). The label at the liner is the deformation at a single node at the surface of the inside core of the liner ($U_l=16,8$ cm). $H=U_l-U_{st}=16,3$ cm.	43
Figure 3.13: Region of interest at the hyperelastic model, with deformation vectors shown in arrows. The blue vectors and red vectors are parallel with the Y axis.	43
Figure 3.14: Pattern of deformation in the soft tissue. The maximum value of deformation in the soft tissue is of 7mm; An absence of necking is also observed, although separation between soft tissue and liner occurs.	44
Figure 3.15: Deformation pattern across the liner.	45
Figure 3.16:Region of interest. Here the values that set the criterion are labelled. On the soft tissue, the $U_{st}=5,7$ mm, and on the liner, the value $U_l=3,13$ cm. The resulting separation criterion is $H=2,56$ cm.	45
Figure 3.17: Linear model showing Von Mises stress, the stress areas at the silicone liner with maximum value of 93 kPa at the contact region, and the increase in stress at the region where the separation between soft tissue and the liner surface occurs (no necking observed tough).	46
Figure 3.18: Linear model Von Mises stress, showing the stress distribution at the soft tissue with the maximum value of 10kPa and the minimum value of 143 Pa.	46
Figure 3.19: deformation pattern at the hyperelastic model liner. The maximum deformation is considerably higher compared to the linear model. It is also observed necking of the liner were the separation between the liner and the soft tissue occurs. Maximum value at the liner approx. 16 cm; Max deformation at the soft tissue approx. 5,3 mm	47
Figure 3.20: Region of interest. Here the values that set the separation criterion can be seen. On the soft tissue, the $U_{st}=5,3$ mm, and on the liner, the value of $U_l=16$ cm. The resulting separation criterion is $H=15,5$ cm.....	47
Figure 3.21: Hyperelastic model Von Mises stress, the stress distribution in the soft tissue is homogeneous, it also has a maximum value of 12,3 kPa and a minimum value of 173 Pa.	48
Figure 3.22: Highlight of the necking area, were the maximum von Mises stress is obtained. It shows the stress areas at the silicone liner with maximum value of approx. 109 kPa at the necking region.	48
Figure 3.23: Hyperelastic model showing the full von Mises stress pattern across the liner.	49
Figure 3.24: Mesh representation in FreeCAD 0.17 software. The liner dimensions are:	50
Figure 3.25: Beam elements representation in ANSYS.	51

Figure 3.26: Highlighted in red are some (not all) beam elements (the solid elements of this region were removed to visualize the beams). It is visible that they cross the solid elements in the middle of both layers of solid elements.	51
Figure 3.27: Again, highlighted in red are the beam elements, in this figure however the inner layer is shown, to understand the disposition of the beams with the matrix, and that they are coincident with some solid elements edges.	52
Figure 3.28: Side view of the geometry, with the reinforcement beam elements imbedded in the matrix highlighted in red.	52
Figure 3.29: Bottom view. Highlighted in red are the nodes that can be manipulated to develop the different mesh configurations. In this case, it is visible the “24 node” mesh.	52
Figure 3. 30: Fixed support on top surface of liner (highlighted area) – Ansys representation	54
Figure 3. 31: Force representation. 49N applied at the distal end opening of the liner.	54
Figure 3. 32: Boundary conditions in Abaqus. The top surface is fixed, and the distal end opening as an applied force in the same conditions as reported in Ansys.	55
Figure 3.33: Total deformation magnitude at the reinforced liner. Maximum value of node’s deformation at the distal end ($\approx 3\text{cm}$) equivalent to pistoning value.	55
Figure 3.34 Graphical relation between the total node’s deformation and the liner’s length. A high increase in deformation occurs in the first 25 mm of liner. [0 value of liner’s length starts at the distal end].	56
Figure 3.35 Von Mises stress - Exterior view of reinforced liner. Maximum value of stress shown of 278 kPa in a reinforcement beam. The blue colour shows how the silicone doesn’t sustain any considerable stress.	57
Figure 3.36: Von Mises stress representation at the reinforcement beams – bottom view. Isosurface representation.	57
Figure 3.37: Lateral view of Von Mises stress sustained by the beams. Blue dots are visible on the cylindrical region of the liner.	58
Figure 3. 38 Von-Mises stress, lateral view – Non-reinforced liner. Maximum value – 192 kPa.	58
Figure 3.39: Total deformation for Non-reinforced liner, lateral view. Maximum value of total deformation was at the distal end with a value of 6,7 cm. More than twice the value of the reinforced liner.	58
Figure 4.1: A - Silicone membrane covering the model shown. Its purpose is to allow air pushing out when the liner is donned, causing this way a realistic suspension. B – Exterior representation, with tube connecting the syringe to the interior visible ; C – Stump model without silicone cover, 35 cm length, with syringe connected to the interior of the model; D – Cavity with transtibial amputation bone replica shown. E – Bag inserted inside the cavity shown in image D, and after that filled with fluid by the syringe.	63
Figure 4.2: Liners tested. From left to right: Iceross Original, Iceross Comfort, Iceross Clear, Majicast non-reinforced liner, Majicast reinforced liner.	64
Figure 4.3: Instron machine experimental setup – A - No stump model; B - Stump Model and Non-reinforced Majicast liner prototype.	65

CHAPTER 1 - Introduction

1.1 Motivation

The purpose of a prosthetic device is to replace the normal functions of the missing body part. It generally, consists of a socket that surrounds the residual limb, a terminal device, and an apparatus to connect and adjust the position of the socket relative to the terminal device [1]. The load supporting structure of the human body is the skeleto-muscular system, and so a prosthesis is intended to behave like an extension of this system. When a prosthetic device is used, after a lower limb amputation, all external loads are transferred from the socket prosthesis to the skeleton through the residual soft tissue. This load transfer is problematic, as the soft tissues are not designed to transfer these loading conditions. To achieve enhanced performance with minimal discomfort and no soft tissue damage, it is necessary to guarantee an adequate fit between the prosthesis and the residual limb. Therefore, the study of prosthetic liners is fundamental.

A suspension or locking prosthetic liner, is a prosthetic component that functions as an interface between the skin of a lower residual limb and a rigid prosthetic socket (figure 1.1). The ultimate purpose of a liner is to improve amputee safety and comfort. Although prosthetic liners for lower-limb amputees are broadly commercial available, no academic studies have been found that evaluate the effect of different configurations of imbedded reinforcement structures within the matrix of liners, preventing pistoning occurrence. The investigation has mostly been developed on the study of the single material properties, without taking into account the stump/socket interface has a whole system.

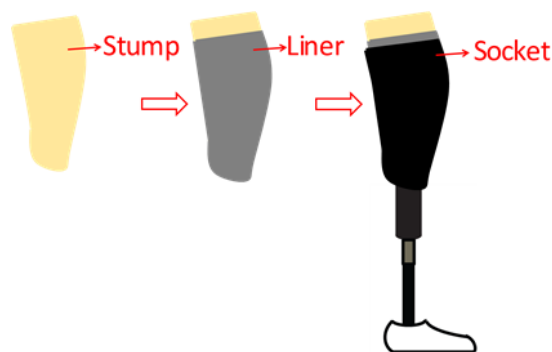


Figure 1.1: A scheme of the stump-liner-socket system. Adapted from [2].

The introduction will describe how an elastomeric liner attempts to achieve those goals and what the problems are that need to be addressed to achieve them.

1.2. Objectives

The aim of this work is to investigate the use of an embedded fabric mesh within an elastomeric matrix of a liner. The objective of this investigation is to allow the production of a liner that provides a good prosthesis suspension, by reducing pistoning, avoids deep tissue injury, through a good pressure distribution, and reaches acceptable levels of comfort for the patient, by allowing an easy insertion and use of the liner.

To achieve the mentioned objectives, there is the need to study how a fabric mesh embedded within a liner, achieves a solution that fulfills a “surface matching” concept. This concept was described by Klasson and Buis [1] and it helps the achievement of the fitting criteria just described before, through a local pressure equalization at the limb, while it tackles the problems described ahead.

The occurrence of pistoning, causes the loss of this surface matching concept. As it is compromised, pressure equalization is no longer possible. The stump volume variations are also a threat to the loss of surface matching, as they can cause pistoning.

With this said, the main goals to look for in a liner and in this project are:

- Full contact with the stump, capable of avoiding pistoning and maintain the surface matching concept. As described in section 1.3.1, a good mechanical coupling stiffness.
- To avoid pistoning, the liner’s matrix must have an anisotropic behaviour. The liner can’t stretch in a longitudinal direction, but it must stretch radially, to allow the donning of different stump sizes.
- Local pressure distribution around bony prominences, using an elastomeric material, that avoids peak pressure due to its viscoelastic behaviour akin to soft tissue behaviour, and that deforms at constant volume.

1.3. Literature Review

As it has been previously said, prosthetic liners have been developed in order to allow a good fit between the prosthesis and the residual limb. However, what is the definition of a good fit? How can it be quantified the fit quality? To achieve this, an investigation of the literature available about socket fit is required. The following literature review as the goal of, through its analysis, allow the setting of parameters and criteria that can guide the design of such a prosthetic liner.

1.3.1. Socket fit – A biomechanical and medical problem

According to Buis and Klasson (2006) [1], to achieve a good coupling between the body/device interfaces, two points of view should be taken into care: the medical and the biomechanical/engineering one.

On a medical point of view, the concern is related with soft tissue safety. When the tissue is under pressure it can be at risk at the cellular level or at the tissue level [1]:

- At the cellular level, by cell breakdown, due to restricted oxygen and nutrients supply, caused by restricted blood flow [1].
- At the tissue level, due to abrasion, mechanical overload or tissue breakdown due to repeated overloading. The last one is also called “fatigue” but different from normal material’s science fatigue. In this case, the cause is probably related to thermo coagulation following heat development, or tissue inflammation [1].

Several studies have been conducted to quantify the relationships between interface stresses and tissue breakdown. It was initially proposed in 1942 [3] an inverse relationship between pressure and time for the development of a pressure ulcer. The following studies [4-11] demonstrated a second order relationship between the threshold pressure for ulcer formation and the duration of pressure application. However, these studies focused in a long pressure time environment and for a short duration pressure, as during the stance phase (see gait cycle in figure 1.2, with stance and swing phase visible), soft tissues can sustain moderately higher pressures [1].

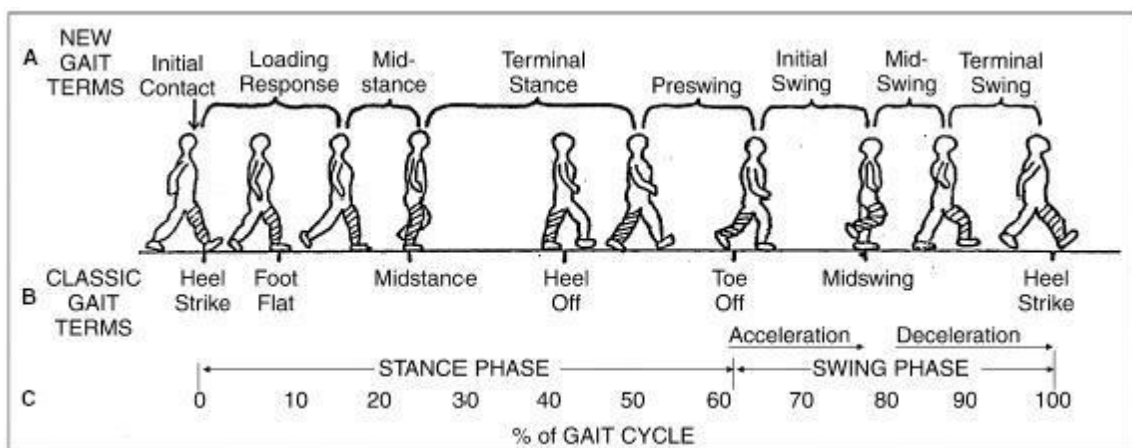


Figure 1. 2: Gait Cycle representation, where stance and swing phase can be observed. Image adapted from reference on footnote¹

Knowing that the goal is to avoid blood flow restriction and following the general guidelines proposed by Reswick-Rogers diagram (1972) (figure 1.3) [12], it can be stated that nowhere in the stump should the local pressure be higher than 20 mmHg, for a long duration of time [2]. To accomplish this, one needs

¹ <https://upload.orthobullets.com/topic/7001/images/gait%20cycle.jpg> consulted on the 22/11/2018

to make sure that high pressures developed in the stump during the stance phase are relieved during the swing phase.

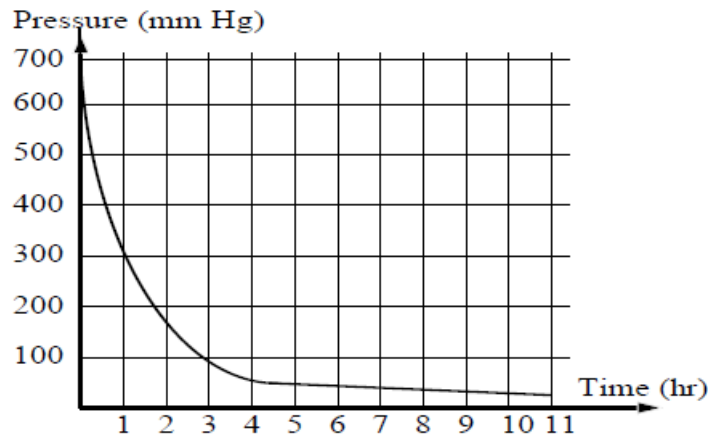


Figure 1. 3: Reswick-Rogers diagram (1972) [12], “safe” pressure below the curve.

On a biomechanical/engineering point of view, considering the coupling system between the mechanical prosthesis and the skeletal system, the concern is about the performance of the layers of soft tissue and the socket components, meaning, as the fit quality is dependent on the response of the soft tissues to the mechanical elements action.

To understand the coupling system, one needs to understand the concept of coupling stiffness. This is a mechanical quality criterion described by Buis *et al.* [1] of the coupling between the skeleton and the prosthesis. This mechanical quality is accessed by the minimum relative movement between the two parts and in this situation the stiffness can be defined as the unit of load per unit of movement [1]. Stresses at the skin surface, can be applied in two directions – pressure, being perpendicular to the skin surface, and shear stress, being tangential to the skin surface [13]. This way there can be two relative movements – longitudinal displacement (also called pistoning), that occurs typically between full weight bearing and swing phase, and transverse or rotational movement (instability, shift or angulation). Both stress directions can provide support to the coupling system, but above a certain level and duration they will induce tissue breakdown [1,13].

The benefits of an enhanced coupling stiffness, according to [1] include:

- An increase in patient's comfort, and pressure symptoms prevention at the stump surface.
- Increase proprioception;
- Reduced pistoning, that way decreasing the risk for sores, eczema or ischemic problems, and also reduce the risk that the foot touches the ground during the swing phase.

Having the mechanical and medical considerations in mind, it can be set quality criteria for a good prosthetic fit. That would be: as stiff a coupling as possible, with no tissue damage. To achieve this, it is created an interface that distributes the stresses in such a way that the prosthetic limb is stably coupled but doesn't overstress the soft tissues. This might be difficult to achieve because a stable coupling

requires that high interface stresses are applied, but interface stresses cause skin trauma and possibly deep tissue injuries [1,13].

1.3.2. The interface – a socket and a residual limb

Rigid sockets

It is misleading to talk about liner properties focusing the interest prematurely on the liner, not considering the broader interface system, which has a relatively stiff socket on one side, and a surface-changing environment with different and variable properties on the other side (the residual limb, that does not have a constant shape and volume and is not homogenous). Therefore, it is important to understand the current prosthetic socket designs, as these designs are directly related with the use of liners. For people with transtibial amputation (this work focus), the designs can be characterized in four different categories: patellar tendon bearing (PTB), total surface bearing (TSB), hydrostatic (HS), and vacuum-assisted suction (VAS) sockets. PTB claims for the residual limb to be loaded proportionally to the gait biomechanics and soft tissue “pressure tolerance limits” [14], applying and relieving the pressure in different areas of the stump, according to its tolerance to pressure. When elastomeric liners were introduced, TSB sockets became available. TSB claims to do a more even pressure distribution over the entire residual limb, comparing with previous PTB sockets [15]. For TSB, the liner mechanical properties are essential, as the effectiveness of this design depends mainly on it [15].

Hydrostatic sockets (HS) were introduced based on the idea that if the volume of the soft tissues of a stump can be contained in a socket of the same volume, a hydrostatic weight-bearing system could be established, according to Pascal’s law in fluid mechanics, i.e. “a change in pressure at any point in an enclosed fluid at rest is transmitted undiminished to all points in the fluid”. Then in the absence of motion, there is no shear stress as the pressure at a point is the same in all directions. This system aims to be able to have at the same time, surface matching and uniform adjustable pressure distribution, through pressure casting method in combination with an elastomeric liner material [16]. Without surface matching this system losses efficiency as a hydrostatic system is stable only as long as it is tight.

VAS sockets on the other hand, secures the limb within the socket using elevated negative pressure, applied between the liner and the rigid socket [17].

Residual limb

The residual limb is also a complex environment. The soft tissue between the skin and the bone isn’t uniform, composed by muscles, tendons, vessels, fat, etc... Each one of these different components, distributes the load from the limb surface to the bone. However, this load distribution is different according to the mechanical properties of each type of tissue, with the force flow choosing the stiffest available path.

It is known [18], that soft tissue has a fibrous structure, and according to [1], the stress-strain relationship of soft tissue can be expressed as a “quasi-elastic” or viscoelastic behaviour. This means that if soft

tissue is considered as a homogeneous material, its shear modulus would be very low while the fibres are being reoriented in the stress direction, with a sudden increase when fibre reorientation is achieved. The fibre reorientation step allows us to consider that until a certain degree, soft tissues compensate for limited local mismatches on pressure distribution.

Soft tissues not only rearrange on a fibre order of magnitude as seen just before. Changes in residual limb shape occur for a number of reasons and to varying degrees. It depends on the patient's activities, weight, amputation procedure, health and other factors. There are two-time courses differences: daily and long-term. Generally, during the day, the stump shrinks [1]. Likely due to the pumping effect of the socket on the soft tissues, leading to a drive out of fluid from within the interstitial spaces over the course of a day [19]. At night when the socket is out, the limb is no longer compressed, and fluid flow enters interstitial spaces, leading to a volume expansion.

Long term shape changes are probably due to soft-tissue remodelling. It can be caused by changes in vascular condition, muscle atrophy, large weight changes and limb maturation. These changes tend to be more localized, than diurnal changes [20].

All these variables must be taken into account on prosthetic design.

1.3.3. Load transmission and pressure distribution

This concept presents the main difficult on prosthetic comfort and tissue protection. The subject is worth a full description, but here it will be given the basic understanding in order to have a critic view over the following liner properties analysis.

Buis and Klasson [1], by applying basic engineering principles to create a model that describes how the load transmission is made through the stump, show two major approaches:

- An elastic load transmission, causing an uni-directional compression;
- A quasi-hydrostatic load transmission;

The difference between these two models is that a quasi-hydrostatic behavior doesn't allow for shear stresses in the soft tissue to appear. This load transmission can only be accomplished if the volume of the stump equals the socket volume. It is called "quasi" because soft tissues have anisotropic behavior, due to its fibrous nature.

The elastic unidirectional compression is a drastic simplification of reality, but it can be a good starting model for deformation and pressure distribution on living tissue, as it may remain sufficiently valid if it is considered only the short-term loads during the gait cycle.

Using elastic theory to explain how pressure is applied, and how pressure peaks can appear in bony areas, one of the variables that one needs to know is that when the thickness of an elastic material decreases, the pressure increases in that region. Considering living tissue, the thickness is not constant all along the skin and the mechanical behavior of the tissue constitutes a statically indeterminate system, this way, it requires to not be considered as a whole material, but has a number of small finite elements. To add complexity to this problem, there is also the problem of varying stiffness along the surface, causing gradients of high stress concentration, as the force chooses the path of higher stiffness available. [1]

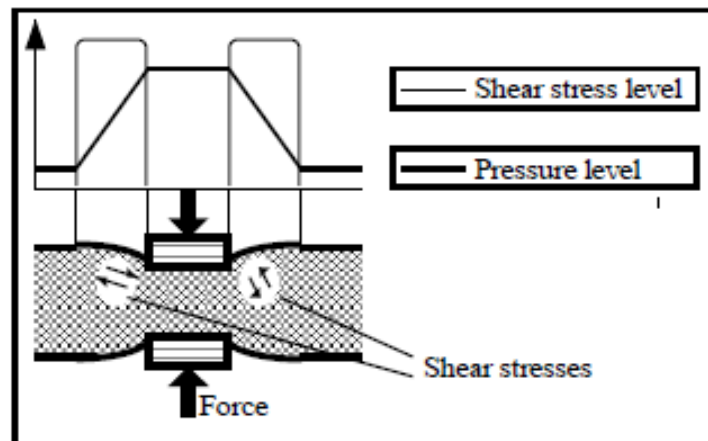


Figure 1.4: Representation Adapted from [1]. The graphic represents the pressure level and the shear stresses that result from a pressure gradient. This shear stresses within the soft tissue are especially likely to occur at bony prominences.

The problem of having uneven pressure distributions (peak pressure spots), is that this will try to push material from high pressure areas to low pressure areas, creating undesired shear stresses within the tissue (figure 1.4). To avoid this phenomenon, surface matching and volume matching sockets and liners are applied, at full load, in order to create a uniform pressure distribution under this condition, or at least a modest pressure gradient distribution. Surface matching aims to offer local pressure distribution at full load, with modest pressure gradients, over the entire stump surface, this way avoiding peak pressure areas, and all the problems that come from those peak pressures, like the ones just mentioned of shear stresses within the soft tissue. Local pressure distribution with modest boundary pressure gradients is specially intended to be possible around bony prominences, where the risk for its rising is higher.

It must be noted that the pressure peaks spots, are not areas where the tissue is more sensitive to pressure. Instead, they are simply areas where, for geometrical reasons or stiffness gradients, tissue is more exposed to compressive loads (like bony prominences) [1]. As already discussed, soft tissue, due to the high presence of collagen and resultant fibre composite behavior, is capable of a certain degree of pressure equalization. The increase of this ability, through a surface matching liner, that acts like an artificial “second skin”, is one of the main goals of a prosthetic liner.

Finite-element modeling has been the most common computer modeling method used to predict stresses and pressure distribution at the stump-liner-socket interface [13].

The elastic theory, was assumed for the soft tissue finite element models in several studies from 2000-2007 [21], especially for limb surface stresses only. However, more recent models [22, 23, 24] used hyperelastic soft tissue models to respond to the large strains and non-linear stress-strain behavior observed by indentation studies [23], especially when investigating internal soft tissue stresses [23].

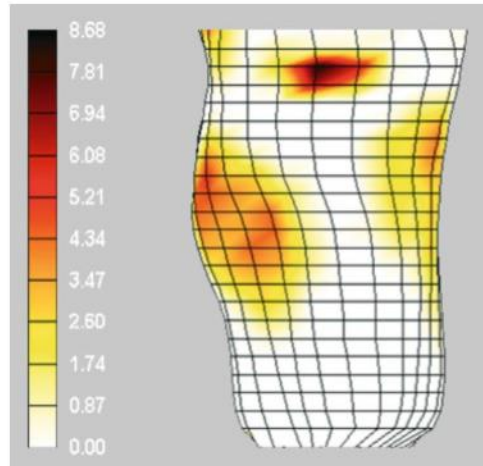


Figure 1.5: Residual limb finite element model. Donning pressures [kPa] are predicted for a transtibial residual limb in a PTB socket [13].

Although the software is increasing its complexity capacity and a better understanding of soft tissue is gradually taking place, each amputation and each stump is different, due to the complexity that is explained in the previous section. This way, finite element models see their utility constrained to a certain level. They are useful enough to describe approximations and analyze different approaches to the resolution of this problem, but an individual, patient by patient analysis, is not possible, as it is not possible to describe the individual soft tissue composition of each patient.

1.3.4. Soft tissue injury: DTI and skin stretching

According to the U.S National Pressure Ulcer Advisory Panel, deep tissue injury (DTI) is defined as “a pressure-related injury to subcutaneous tissues under intact skin”. This injury is typical in weight bearing soft tissues [25], and it has been long known that tissue pressures are higher internally near bony prominences than at the skin surface (might be 3-5 times to that of the pressure measured at the skin surface) [26]. The cause of DTI is still under investigation [27]; also, there is the need to investigate the stress and strains inside the muscle flap of the limb. It is long known that one of the mechanisms of pressure ulcer formation implicates localized ischemia as the primary cause of the onset damage [5, 8, 10, 28].

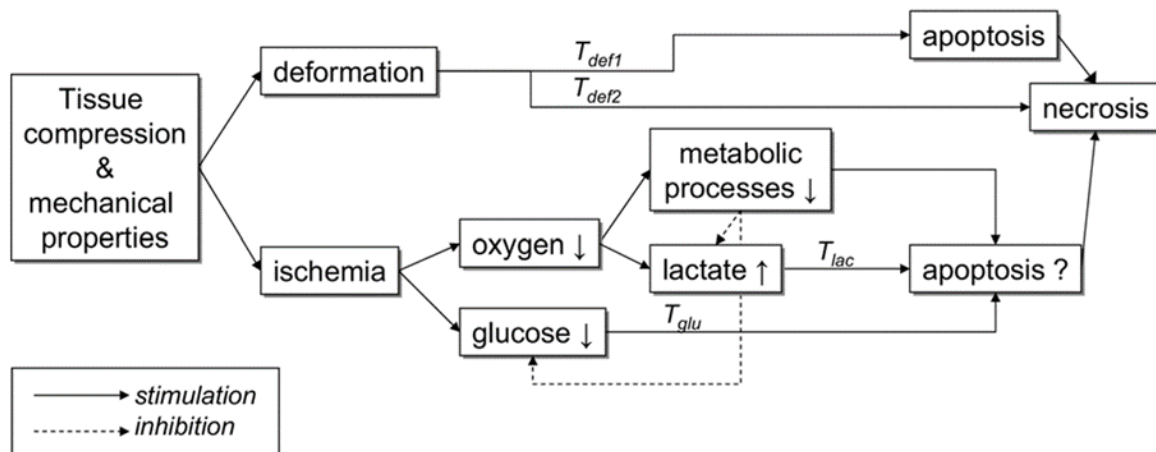


Figure 1.6: Proposed sequence of events during tissue compression [24].

In trans-tibial amputation patients, DTI results from compression of the muscle flap by the truncated bones against the socket [25]. This way, as it is impossible to invasively measure internal strains and stresses in the muscle flap, computational models have been trying to be incorporated. Finite element analysis was used by Portnoy *et al.*, 2007 to develop a 2D real-time approach. To develop a 3D model, it is necessary to know the internal mechanical conditions of the limb. Developing such a model, would help to prevent DTI and aid surgical planning and rehabilitation, however the difficulties of such a model have just been discussed in the previous section.

It was seen in the previous section, that shear stresses and their appearance near pressure gradient areas are a problem, and it might even be related to DTI cause, although that's still under investigation. However, shear stresses are not a major component in load bearing if, while donning a silicone roll-on liner, the soft tissues are pulled down along the stump creating headroom. This headroom allows the skin to slide in bony areas and if the bone is parallel to the skin in this area, the shear stresses will not be transferred to the bone surface.

Due to the nature of wound healing, the new epithelium formed at the surface of a wound is smaller than the original. Orthopedic surgeons agree that shear stresses in the soft tissues, notably those tissues in vicinity of wounds, are extremely dangerous and should be avoided [1]. Either by overstretching of the new epithelium in the vicinity of wounds, inducing tissue breakdown, or by the occurrence of friction, that leads to heating of the surface and quickly leading to blister formation.

The skin response for shear stress depends if there is slip between the two surfaces ("friction"), or if it is applied without slip, let's call it "tangential shear". Friction can lead to blister formation by heating up the interface [29,30]. With tangential shear the applied force is distributed through a greater volume of tissue. This way local stress concentration and heat build-up are reduced. Skin can thus tolerate greater shear stress without slip of one of the surfaces [31]. It is necessary to take into account what Naylor (1955) [32] also stated, that small amounts of fluid added to the interface, as might occur during sweating, will increase shear stresses, but if the interface is extremely wet, the shear stress will decrease.

1.4. Main Contributions

The main contributions of this dissertation are:

- The development of a computational model that predicts the behaviour of a silicone prosthetic liner under longitudinal stretch, that mimics the tension that the prosthetic device exerts in the liner during the swing phase of the gait cycle. This model justifies the need for an imbedded fabric mesh within elastomeric liners;
- The development of a computational model that compares an imbedded reinforcement mesh within a silicone matrix with the absence of it, enabling prediction of the soft tissue stabilization effect that a liner has.
- The development and creation of an imbedded fabric mesh within an elastomeric liner, creating an anisotropic composite able to control pistoning.
- Creation and development of a residual limb model, capable of being used to compare the effectiveness of different liners and their effect to avoid pistoning.
- Development of a liner's testing methodology, that compares the effectiveness (regarding pistoning decrease) of different liners in a realistic model.

1.5. Structure and Organization

This dissertation is composed by five chapters:

In Chapter 1, the motivation and objectives for this work are presented. The literature review that follows gives the reader a contextualization of the subject in study. The challenges and the investigation already developed that provide the background for this work. Finally, in this chapter, the main contributions of this work for the field of investigation are described.

Chapter 2 starts with a review on several studies conducted with prosthetic liners focusing on their mechanical properties, heat transfer properties and the clinical evidence of their performance. It is also presented a review of several commercial patents, with the purpose of drawing a general picture of the available prosthetic liners in the market. This chapter seeks to highlight the relevance of an imbedded fabric mesh within a liner for soft tissue control and strives to demonstrate the variety of configurations that exist. Finishing this chapter and making use of the information acquired with these two chapters, are the product design specifications regarding liners. These design specifications were used and adapted since the beginning of this project.

Chapter 3 describes the methodology, results and discussion of the computational model created with two main objectives: to prove the need of an anisotropic matrix and the effect of an imbedded fabric mesh within a silicone liner.

Chapter 4 describes the experimental work made. It consisted in the creation of a stump model, the development of a protocol to compare how effective 5 liners are, regarding the effect they have in avoiding pistoning (3 commercial liners from Össur and 2 liners produced at the University of Strathclyde).

Chapter 5 presents the final considerations of the project, the main conclusions and the future work that still needs to be developed.

CHAPTER 2 - Lower-Limb Prosthetic Liners

2.1. Liner's material mechanical tests

A large portion of research about prosthetic liner properties has been focused on the mechanical properties of the materials used in liners. Several materials were tested and used before companies have reached the materials most commonly used nowadays: silicone, polyurethane or other copolymers synthesized by each company, as will be discussed further ahead.

Sanders *et al* [33] have studied in 1998 the mechanical behavior of eight different materials commonly used for liners at the time. The materials were Spenco, Poron, silicone, soft Pelite, medium Pelite, firm Plastazote, regular Plastazote and Nickelplast. Spenco used was a silicone-based, neoprene with a fabric membrane on top; Poron is an open-cell urethane foam; the silicone was nylon reinforced; Pelite is a closed cell polyethylene foam, Plastazote is a closed-cell crosslinked polyethylene foam and Nickelplast a closed-cell polyethylene foam, with an alloy of ethylene vinyl acetate.

These materials influence the pressure and shear distribution along the stump's skin and underlying tissue principally via their elastic properties and their frictional characteristics with the skin [33]. This way it was characterized the static coefficients of friction (COF) between the materials and the skin, and the compressive stiffness (CS) of the different materials. Where CS is defined as the instantaneous slope of the stress-strain curve under compression loading, and COF is defined as the ratio of shear force to normal force necessary to initiate movement of the material relative to the skin. Sanders *et al.* propose that a material with low CS will attenuate the stress concentrations on bony prominences and a low COF value will induce low shear stresses. It would then be expected that, materials with low COF and CS would be perfectly fit for the use in liners, as the risk of tissue breakdown would be lower. However, it can be unsafe because of a lack of adequate mechanical coupling between the soft tissues and the prosthesis. The challenge is then to select a material that provides an interface pressure and shear stress distribution that induces adequate stability but not excessive risk of tissue breakdown.

Based on compressive stiffness tests and the consequent load displacement data, this study concludes that:

- Spenco, Poron and silicone are recommended for situations where it is desirable for the liner to maintain thickness and volume since these materials had the least non-recovered strain.
- Soft Pelite, medium Pelite, regular Plastazote, and firm Plastazote had all the highest non-recoverable strains. Also, stiffness increased with displacement, just like it happens with biological tissues, and so these materials may be of use when it is wanted to match liner properties with biological tissues properties.

- Nickelplast behaved linearly but will not give much of a cushioning effect as it had a very high stiffness.
- Spenco and Poron had the lowest COF, which could be problematic in maintaining suspension in order to avoid common pistoning.

Emrich and Slater [34] studied also four materials used in liners: Bock-lite, Pedilin, Polyurethane and silicone. These four materials were tested to access changes occurring during end-use brought about by extensive application of compressive or shear force, and to predict the ability to retain contact with the body and socket. These mechanical properties were assessed through cyclic compressive loading, cyclic shear abrasive loading, and frictional loading.

- About the number of cycles of compressive loading required for failure, Block-Lite and silicone had the higher number of cycles, while Pedilin and polyurethane lasted orders of magnitude less.
- Under abrasive loading Block-lite survived 15 times as many cycles as the Pedilin. Silicone and polyurethane were not able to be tested under these conditions due to tearing of the samples.

Covey and others [35] performed a study where the compressive mechanical properties of four prosthetic liner materials (urethane, two silicone liners-ICEROSS and Alps Easy Liner, and a thermoplastic elastomer) were compared to human muscle as a function of geometric flow constraint and loading rate. The conclusion of this work was that urethane was the optimal liner material since it was the stiffest (and so a best response was obtained, although a stiffer material requires careful socket design and liner fit), provided the best impact protection (via lowest impact forces), and the lowest residual displacement 8 seconds after unloading (giving rise to be the least thinning). However, it needs to be taken into care that the manufacturer of the urethane samples used (TEC systems) financed the study.

To further understand the mechanical behavior of liners, Sanders *et al* [36] tested 15 commercially available liners under compression, friction, tension, and shear. All the load levels were compared to interface stress measurements reported on transtibial amputees. The liners included samples made of silicone elastomer, silicone gel and urethane². All these four different types of tests were conducted with

² In this paper [36], a distinction is made between silicone elastomers and silicone gels with Silicone elastomers being extensively crosslinked and containing little free polydimethylsiloxane (PDMS) fluid. Silicone gels have lightly cross-linked polysiloxane networks, swollen with PDMS fluid. Since the PDMS fluid is not chemically bound to the network in silicone gels, fluid can bleed out of the gels. The classification of a liner as a silicone elastomer or silicone gel was made upon manufacturers' product literature.

specimens of the material retrieved from the liners. The compression tests had short cylinder specimens of 11.1 mm diameter, the friction, tensile and shear stress tests used square samples.

In general, silicone gel liners were of lower compressive, shear, and tensile stiffness than the silicone elastomer products, consistent with their lightly cross-linked, high-fluid content structures (fluid that bleeds under compression). These silicone gels were the most similar to biological tissues suggesting that they would be most appropriate for cushioning bony prominences, according to [36]. Silicone elastomer products demonstrated a wide range of compressive, shear, and tensile stiffness values. This material is highly cross-linked, and was the stiffest in compression, suggesting that these would be an advantage for residual limbs with excessive soft tissue, as the liner will not cause deformation on top of the tissue. For compressive stiffness the urethane sample (it was just one) had a similar value to some of the silicone elastomer samples.

About the coefficient of friction (COF) data, Urethane had the highest value (by a large margin), suggesting that it would adhere well to weak skin sites and protect them from breakdown. For the silicone materials, it is suggested that COF is controlled more by manufacturing than by content for the silicones.

Shear stiffness trends were similar to the compressive tests, suggesting that silicone elastomers and urethanes would be most appropriate for residual limbs with excessive residual limb soft tissues to prevent the limb from sliding into the socket, while silicone gels would be appropriate for limbs with bony prominences to provide some cushioning effect. The silicone gels and urethane were soft in tension as were three of the silicone elastomer samples though most of the elastomers had higher tensile stiffness. This suggests that the elastomers with higher tensile stiffness would provide better suspension [37].

2.2 Heat transfer properties and moisture permeability

The socket and the liner create a warm and humid microenvironment that encourages growth of bacteria and skin breakdown [38,39], as the liner/socket behaves as a heat capacitor, and heat is retained even after activity is ceased [40]. Because of this, there is a concern to investigate the liner's transfer properties of heat and moisture.

However, the research on the thermal behavior of the socket and liner materials and their effect on stump skin temperatures is limited. Klute *et al.* [41] have done an investigation on different liners and socket materials thermal conductivity. They concluded that there was no large variation on thermal conductivity for typical used socket materials (carbon fiber and thermoplastic). On the other side of things, different liner materials showed a large variation on thermal conductivity, and so liner material selection has a considerable effect on the residual limb skin temperature, compared with socket material selection. These way different liner materials will lead to a different limb skin temperature, which leads to different microenvironment and the possibility to avoid several skin problems [42,43].

To understand how prosthetic sockets and liners may influence the retention of the expected perspiration caused by the heat increase between the interface skin/liner, Hachisuka and others [44] investigated the moisture permeability of liner and socket material. In this study they observed that the liners were more than 80 times less permeable than tests without a sample material, suggesting that liner materials are highly impermeable to moisture transfer.

According to [37] there is an opportunity to improve amputee comfort by finding a way to remove heat and moisture from perspiration, out of the skin/liner interface. Future research should focus on improving heat transfer coefficients in liners, as well as finding a way to remove moisture without affecting suspension. The urgency of this problem became even clearer with Klute *et al.*, 2014 [45] that concluded that rest alone after a walk is insufficient to provide thermal relief without doffing the prosthesis. They also observed that skin temperature varied through the limb, suggesting that the development of location-specific technology would be advantageous.

There are several studies under development in order to achieve this. One study of interest was the thermoregulatory system [46], which kept a thermal equilibrium between the inside and outside surfaces of a silicone liner. However, this system was not tested in a real situation. These way further investigations to improve the design of thermoregulatory system and its application in clinical set up are necessary.

2.3 Clinical evidence for liners performance

To evaluate the effect of liners on interface pressure distribution, Sonck *et al.* [47] have measured the pressure at four sites of the sockets of 26 amputees in three different test conditions: no liner, a soft insert called Kem-Blo, and an elastomeric silicone liner. The results observed a decrease of the pressure at all the socket sites with the silicone liner, compared with the other test conditions. This suggests that silicone has the ability to distribute pressure evenly to the residual limb.

Another study was made [48] to investigate residual limb pain threshold and tolerance. With the patients using a Pelite liner, or a polypropylene socket material, at all locations on the residual limb, the patients could withstand a higher force with the Pelite than with the polypropylene, suggesting that Pelite distributes load over a greater surface. This study also found out that pain is tolerated differently according to the tissue under load. For a soft thick layer, the pain is less tolerated comparing to a stiff layer of tissue. This suggests that liners that have different geometries or material properties according to different tissue areas could perhaps provide additional functionality.

There is also a review from 2014 [49] that was a systematic review on the more general topic than liners: "Transtibial prosthesis suspension systems". Referring to suspension systems as diverse socket types: the silicone suction suspension socket and the ICEROSS socket; but also referring to liners as an alternative suspension system. This paper stated that clinicians still select the suspension systems, and

liners, based on subjective experience [50], and that there is no consensus on selection criteria [50,51]. It also stated that thicker liners are more comfortable and can distribute the pressure more evenly over residual limb.

While the material properties of prosthetic liners have been well studied, how those properties affect function *in situ* is not well understood. This is caused by an absence of papers that analyse on a quantitative way the performance of liners. Instead there are plenty of survey studies that through mainly PEQ (Prosthesis Evaluation Questionnaire) evaluate on a subjective and qualitative way the liners and other suspension systems performance. Although mainly qualitative, it helps to identify the areas where more clinical environment liner research would be useful: donning and doffing procedures, sweating problems and durability are examples of it.

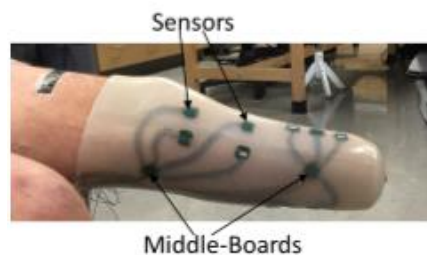


Figure 2.1: Liner worn by amputee for pressure and shear sensing test [52].

Some recent studies have been found to be moving in this direction. One is the pressure and shear sensing liner developed by Wheeler *et al.*, 2016. [52]. It was already possible to sense pressure *in situ*, based on thin-film pressure sensors based on piezoresistive or capacitive principles. However, these sensors are not entirely accurate as they can't measure shear stress. Sanders [53] had measured in the 90's shear stress using three-axis load cells in a modified socket, however the amount of data that can be collected with this technique is limited to the use of elastomeric liners between the socket and the skin. Here they have developed an elastomeric liner with sixteen integrated pressure and shear sensors, along with necessary wiring and acquisition data electronics. Maintaining the properties of liner's typically used in clinical practice and successfully tested. This development will be able to bring quantitative tests on liner performance *in situ*.

Although this work goes in the direction of quantification, it is some researcher's opinion that there is no need in measure superficial shear stress. This because the shear stress that one should take into care is the shear inside the soft tissue [1], caused by pressure gradients, which has nothing to do with the superficial shear stress measured.

2.4. Suspension elastomeric liners development

The following section wants to draw a general picture of the available prosthetic liners in the market through the selection of a few relevant patents. It wants to highlight the relevance of an imbedded fabric mesh within a liner for soft tissue control, and provide insight into the variety of configurations that exist.

2.4.1 Prosthetic silicone rubber liner

In 1987, B. Klasson and O.Kristinsson [54] published the invention of a prosthetic liner (or a sleeve-shaped article as it was called at the time), working as a suspension system that was intended to be used with a rigid socket. The novelty this device demonstrated was maintenance of the suspension of the prosthesis, by maintaining the contact between the full surface of the stump, even when the volume of the stump varies during the day. This was not possible before with the single use of rigid sockets. In this invention Klasson *et al.* had already developed an anisotropic liner that would control the soft tissue in the longitudinal direction, avoiding pistoning and allowing enough radial stretch, essential to accommodate residual limbs of different diameter [55].

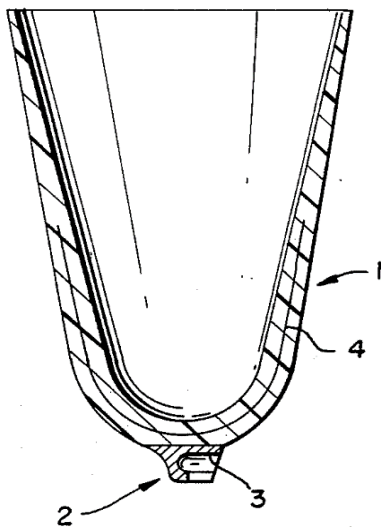


Figure 2.2: 1 - Representation of the liner proposed by Klasson *et al.* (1987); 2 and 3 - fixation system; 4 - reinforcement fabric laminated within the liner [54].

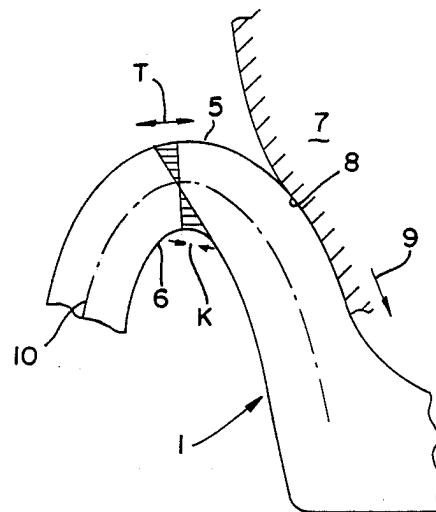


Figure 2.3: Donning of the liner representation: 5 - inside surface of the liner; 6 - outside surface of the liner; 7 - stump; 8 - skin; 9 - soft tissue downward drawing effect; 10- neutral line for stretching/compression of the liner; T - portion of the liner stretched; K - portion of the liner compressed; [54]

To reach the anisotropic effect, it is proposed to laminate an inelastic material within the elastic material that constitutes the liner. This lamination only occurs at the distal end of the liner, allowing the knee bending and avoiding pistoning. The elastic material proposed is already silicone, although other rubbers may be used. Due to its elastic properties silicone can adhere to the skin, allowing surface matching across the entire skin, even when there are small volume variations. It also receives the shear forces transmitted by the socket, between the socket liner interface, acting like a “second skin” and protecting the skin itself. The donning of the liner is of extreme importance for the adhesion to the skin, and with that the suspension of the prosthesis. This liner is capable of being turned inside out, for the insertion of it onto the limb. This turning compresses the exterior wall (represented by number 6 and K in figure 2.3) and stretches the inside wall (stretching represented by T and inside wall represented by 5 in figure 2.3), with this, when the sleeve is unrolled onto the stump, the skin will be dragged downwards into the

sleeve. The higher thickness at the distal end of the liner, increases this effect at this end, improving the suspension effect. When the reinforcement (in figure 2.2 represented by 4) is applied at the outside of the liner, by preventing longitudinal stretching, it also displaces the neutral line (represented by 10 in figure 2.3) towards the outside, increasing the stretching amplitude and this way increasing even more the downward dragging effect. This effect is represented in figure 2.3.

Since then, several new approaches have been developed, mainly within the same general concept created by these two authors (Klasson and Kristinsson), as the 100 number of citations by other patents confirms.

2.4.2 Dual Stiffness Membranes

Laghi *et al.* [55], created a liner that would not use the fabric used by Klasson *et al.* embedded into the silicone membrane to have the anisotropic effect necessary. Instead they reinforced the elastomeric material itself, this way they avoid the tearing of the elastomeric material caused by the concentration of stresses at the end of the fabric insert [55], something they claimed that occurred with Klasson *et al.* invention. It also avoids the opacity created by the fabric embedded in the silicone, this way allowing a clear view of the distal end, which assists the correct donning of the prosthesis without air entrapped. [55]. Their invention consists in a dual hardness elastomer, with a softer interior membrane (Shore A hardness rating between five to twenty), and a stiffer outer membrane (Shore A hardness rating between thirty to eighty). It is claimed that this configuration substantially eliminates shear and friction forces against the skin, and that the outer membrane at the distal end reduces pistoning in patients with great amounts of excess soft tissue.

In 1997 Össur [56] brought together the concept of different stiffness membranes with the use of a fabric reinforcement to maintain the anisotropic behaviour. The fabric reinforcement consisting in a white woven polyamide stockinette. The silicone has a soft inner silicone elastomer layer and a relatively harder outer silicone elastomer layer, keeping however a viscosity low enough to allow rapid injection moulding. This dual stiffness membrane concept is still used in more recent inventions [57] by “Össur hf”.

2.4.3 Other mesh configurations

Fay (1999) [58] developed a new mesh fabric imbedded configuration. His purpose was to develop a liner that exhibits the same ideal properties as proposed by Klasson *et al.* but which doesn't include a wire or fabric that only covers the lower third or half of the liner [58]. It is claimed by Fay (1999) that Klasson *et al.* configuration doesn't spread the pressure generated along the swing phase in such a way that it avoids the “milking” effect (distal tissue stretch caused by the pin and the lock) [59]. This way Fay's configuration intends to increase the area that supports the prosthesis weight, without constraining the knee bending movement, for a transtibial liner.

The configuration proposed by Fay consists generally in several longitudinally extending elongate arms that are substantially non-stretchable in that direction, attached to a distal plate (for reference called here an umbrella) in a distal-to-proximal direction. These arms are equidistant and circumferential apart from each other. With this configuration they claim to allow the radial movement of the liner, as the arms material is flexible in a radial direction. The length of these so-called arms can cover the entire inner surface of the liner, rationale of offering a significantly better suspension capable of supporting the weight of the prosthesis during the swing phase without “milking” [58]. This length can also be of half the liner size, or even a combination of half size and full-length arms might be used [58].

The fabric can be embedded into the elastomer used for the liner, or it can be secured into the surface of the liner. The fabric material used is preferably formed of silk, fibreglass cloth, or other substantially non-stretch material according to Fay [58].

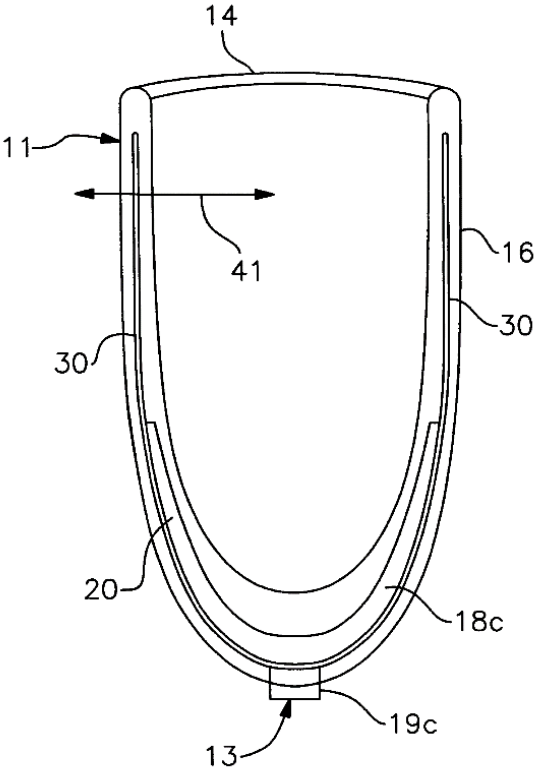


Figure 2.4: Configuration: Number 11 – elastic material matrix; 13 – distal attachment; 14 – open end; 16 – side wall; 18c – convex short arms imbedded inside the matrix; it includes elongated arms (20) that extend themselves longitudinally, both are made of silk or fibreglass cloth for ex. Adapted from [58]

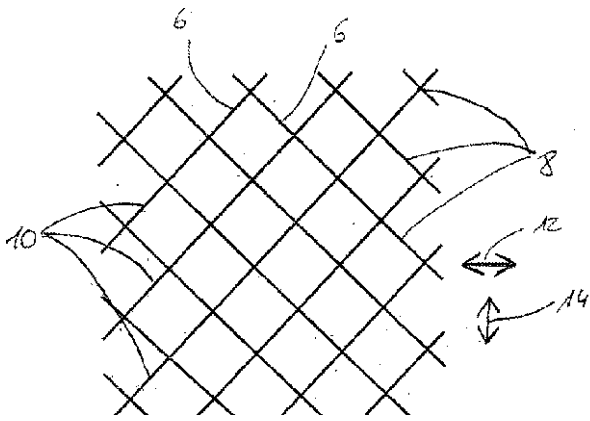


Figure 2.5: Non-stretched fibres. Two possible directions of stretching: 12 and 14 Adapted from [60].

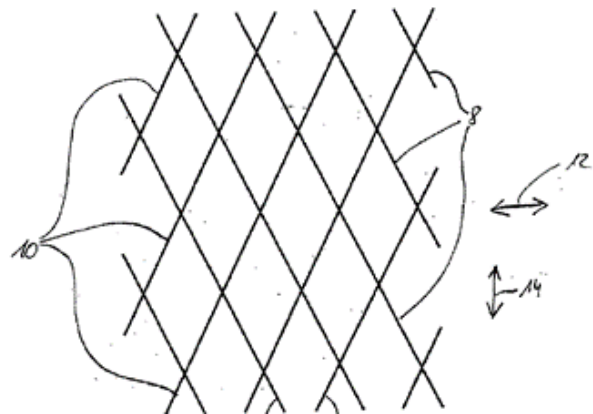


Figure 2.6: Fibres orientation when stretched in direction 14. Adapted from [60].

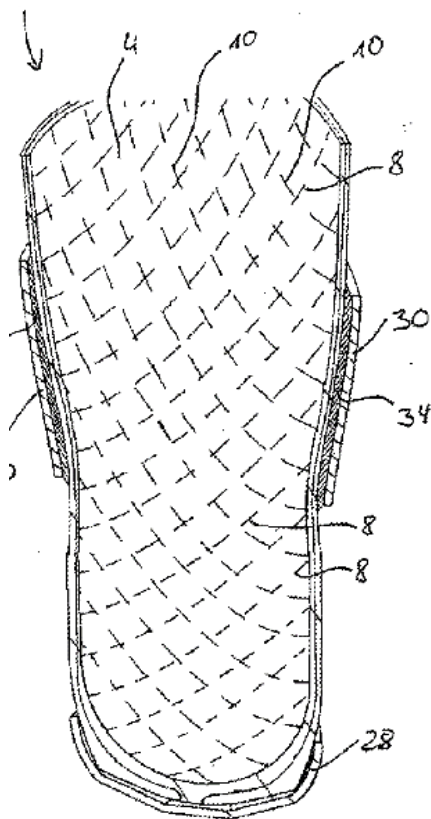


Figure 2.7: Embodiment of the structure within the liner. Adapted from [60].

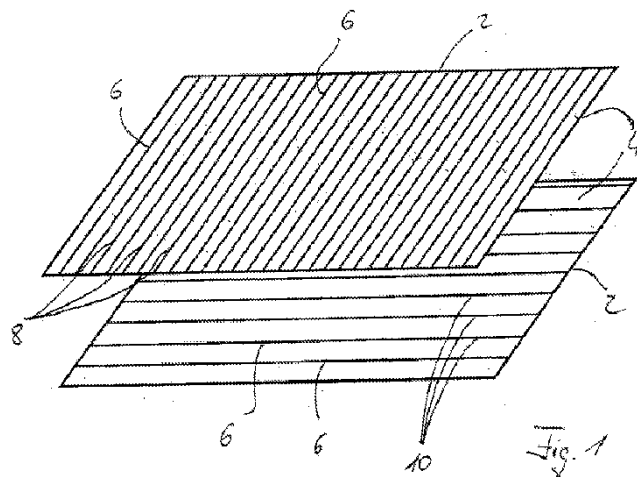


Figure 2.8: 2 – layers; 4 – liner material (silicone or other elastomeric); 6 – fibres; 8 – first fibres layer; 10 – second fibres layer; Adapted from [60]

From “Otto Bock Healthcare GmbH”, Mosler *et al.* (2012) [60], studied different configurations for the inelastic fabric fibres within the liner. Their goal was to achieve a product that when stretched longitudinally, it would result in a shortening of the liner in the radial direction and vice versa. It is also claimed that this liner can avoid slip from the stump, even though stump volume variations may occur along the day, with the use of a highly adhesive surface to the skin. With this they wanted to reach volume stability and shape adaptation. The combination of both these properties would avoid the pistoning effect and will result in an anisotropic behaviour.

To achieve this, they came upon several configurations that they claim to be particularly advantageous.

The first one consists in at least a first fibre and a second fibre layers that cross each other at a rhombic pattern in which the internal angles of each rhombus are right angles and the fibres enclose an angle of 45° or -45° with the longitudinal direction of the liner (figure 2.5 and 2.7). These first and second fibres can be in separate layers or in the same layer (figure 2.8.).

The embodiment of this mesh arrangement results in a configuration as shown in figure 2.7.

Other embodiments created by this group using the same general idea is represented in figure 2.9. Here there are two layers of fibres, each one with a perpendicular orientation between each other, but where each fibre is parallel to its own pair in each layer. Each layer forms a spiral mesh, with opposite orientation to each other. The liner is this way divided in two parts, where the first part is inserted first, and when the second part is rolled on secondly, it overall forms a mesh like structure with the desired properties.

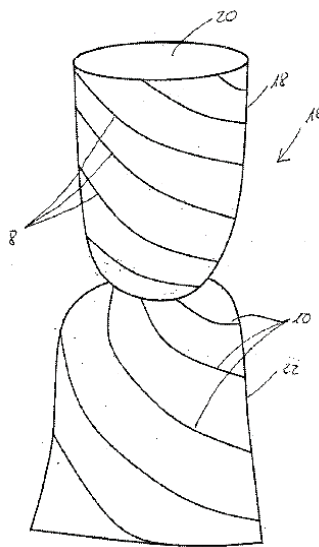


Figure 2.9: Spiral fibres embedded in two different parts liners. Adapted from [60]

Another arrangement of the fibres, that is not parallel in this case, is represented in figure 2.10. It is claimed with this configuration that a shortening of the fibres occurs in the opposite direction from the stretched direction, when stretching of the liner occurs, achieving the desired effect. However, the embodiment of such a mesh within the liner's matrix is not shown. Something that would be of interest specially at the distal end of the liner.

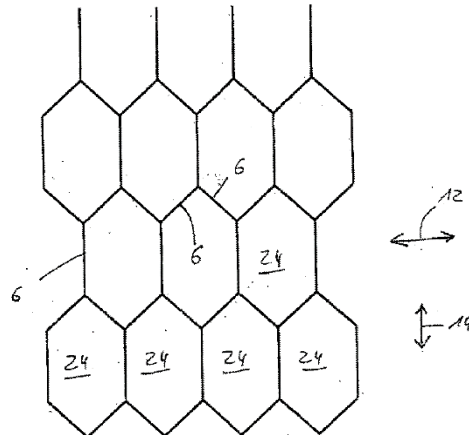


Figure 2.10: Hexagonal shape mesh. [60]

2.4.4 Alternative approaches

Other companies and inventors have not followed so closely the work of Klasson *et al.* as Fay or others have done. Instead they have developed new composite polymers, and used fabric on the outside of its surface, instead of having a fabric embedded within the elastomer.

Kelley *et al.* [61] create a cushioning block copolymer and plasticizing oil gel composition, which is surrounded on the outside by a fabric covering for the Ohio Willow Wood Company (OWW).

This so called polymeric gel material is highly stretchable, which allows it to conform to the stump shape, but it allows an undesirable stretch in the longitudinal direction. The fabric on the outside has the purpose of avoiding this directional stretch, with the claim of having an anisotropic behaviour, this way controlling longitudinal stretch and allowing radial stretch. This fabric has the same length of the polymeric material underneath it, covering the entire surface. When trying to reduce the stretching ability of this gel polymeric material, these authors added Kevlar in the form of fibres, powders and nano particles or other materials that increase the strength and reduce the elasticity of the polymer. They also might reduce the amount of plasticizer present [62]. According to Kelley *et al.*, based on mechanical testing data and data from on patient tests of prototypes of their product, it is desired for a fabric to have a range of elasticity in the longitudinal direction between 10-40% and in the radial direction a range between 70-250%. The liner they presented is claimed to have an elasticity below 30% in the longitudinal direction, and between 140-190% in the radial direction.

Although the fabric described by Kelley *et al.* [62] covers the entire liner, it's configuration claims to allow the bending of the knee joint by having a specially designed knee panel (figure 2.11 and 2.12). They use different materials and different configurations along the liner, and also in the knee panel (number 25 in figure 2.12) where the fabric can stretch in both radial and longitudinal directions, with a claimed elasticity of 100-130% in both directions. These values of elasticity and all the other mentioned above

were obtained from tests that followed the ASTM D4964-96 (2008)e1—Standard Test Method for Tension and Elongation of Elastic Fabrics (Constant-Rate-of-Extension Type Tensile Testing Machine).

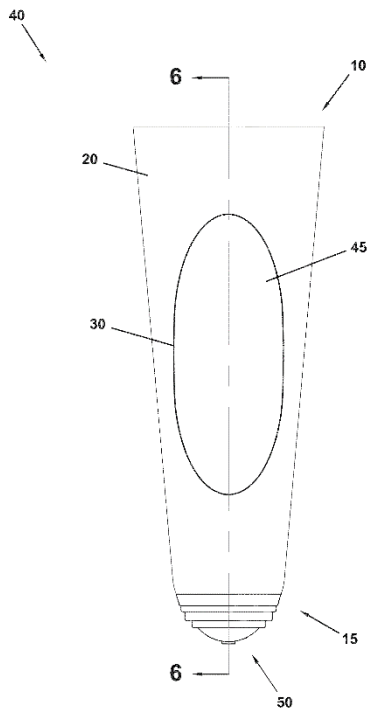


Figure 2.11: OWW liner configuration showing the knee panel. [62]

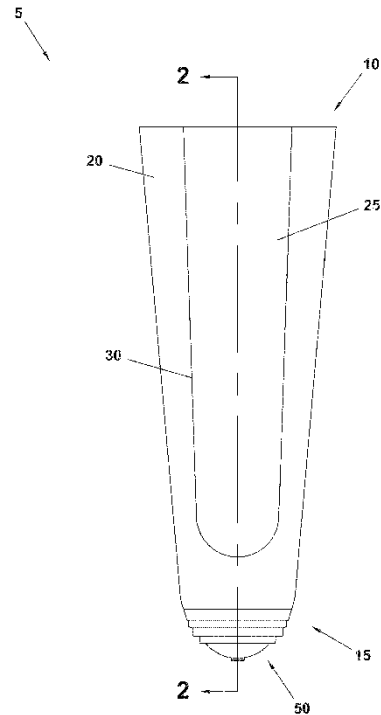


Figure 2.12: Number 25 shows the knee panel described by [62]

Kelley *et al* also claimed the importance of other parameters concerning the fabric, beside the stretching ability. One is the elastic modulus at the radial direction, that they recommend having a 50% elongation with a force applied between 2,2N and 53N and for the longitudinal direction a 50% elongation for a force between 2,2-9N, all this to avoid an excessive tightness of the stump. In the tests ran for the prototype described by this group, the best comfort reported by patients was obtained with a fabric that observed a 50% elongation for a 4N force applied in the non-limited direction.

They also state that the weight of the fabric material influences the abrasion resistance and the polymeric material thickness of the liner. For the product described here, the recommended weight is of 712 g/m² of fabric.

Based on the physical properties mentioned above, the fabric material for stretch control may be CORDURA (Nylon 6,6), Taslan nylon, Stretch nylon, Spun nylon, Polyester and Celliant with a rib knit pattern (for example a 1x1 rin knit). One combination that performed well was CORDURA/Nylon blend with 54% CORDURA, 37% Nylon and 9% elastic. This elastic cord material may be inserted during the manufacturing of the fabric through ribbing, every course, our every 2, 3, or 4 courses, etc., of the stretch-controlling fabric, this way affecting the elastic modulus of the fabric and allowing the optimization of the stretching control. Examples of material used are synthetic elastics (such as Spandex, Lycra, or Elastane), natural rubber (such as Latex) or a combination of both [62].

2.4.5 Summary

Summarizing the works presented here and their intention to improve stump soft tissue control:

- In 1986 Klasson *et al.* presenting a patent, showing the development of the first elastomeric liner, creating the idea of a prosthetic liner as it is broadly known today. Acting as an alternative suspension system, maintaining a full surface match even through stump volume variations along the day. The liner was already anisotropic, by laminating a general inelastic material within the silicone matrix, allowing a reduced longitudinal movement, but not conditioning the liner so much that it would not stretch radially to accommodate different diameter stumps.
- The work presented by Laghi *et al.* (1996) showed how the reinforcement of the elastomeric material itself could be a good strategy for pistoning reduction. They created a dual hardness elastomer, with a soft interior membrane and a harder outer membrane, without substantially increasing the viscosity.
- Kristinsson *et al.* (1997) merged his own work with Laghi's creating a dual hardness silicone liner with a fabric reinforcement to improve anisotropy. The material used for the inelastic reinforcement was a white woven polyamide stockinette.
- Fay (1999) created a different configuration for the imbedded reinforcement mesh, with the purpose of increasing the anti-milking effect, without affecting the bending of the knee.
- Kelley *et al.* drifted away from using silicone and created their block copolymers with a plasticizing gel composition, reinforced with Kevlar. They also didn't imbed a fabric within the matrix of the liner, instead they covered the outside of it, using mainly different types of nylon, ribbed with a small elastic material concentration to try to optimize the stretching ability control.
- Other mesh configurations were also proposed by Mosler *et al.* but the general concept is still the same as previously seen.

With these examples, the reader can have a clear idea of the state of the art in the prosthetic industry. The materials used for the liners matrix are mainly elastomers like silicone rubber [54] and low density nonfoamed nonporous polyurethane [63], or copolymers with a plasticizing oil gel composition [58]. This matrix can be reinforced, either by adding components to itself (Kevlar powder, fibres or nano-particles [61]) or by incorporating a mesh fabric, either imbedded within the matrix, or attached on the outside surface, that has the main goal of limiting longitudinal stretching, while allowing radial stretch to accommodate different stump shapes. This mesh is mainly composed by an inelastic material.

2.5. Product design considerations

Taking into consideration the objectives proposed for this work and the liners development history and investigation previously presented, a product design specifications document was written and adapted

while the project was ongoing. That is shown in the following section, taking into special care the stabilizing mesh design requirements.

Product: An elastomeric silicone liner for lower limb prosthetics, including a stabilizing mesh fabric imbedded within it, integrated between two membranes of silicone, in the thicker distal area of the liner. It allows the liner to stretch radially, but constrains its movement longitudinally, contributing for an effective suspension at the same time it counteracts the shear forces during suspension. This is the same concept as is described by [16].

The following section presents the product design specifications (PDS) for this product. It is divided into the following headings:

1. *Expected product size:*

Right now, there are several liners with different sizes, according to different stump sizes. The product proposed on this design wants to have three unique standard sizes, Small, medium and large. With thickness varying from 6mm to 3mm and height between 18cm to 45 cm.

The mesh fabric is embedded for the full length of the liner or only at the distal area. However only the full-length liner was tested.

2. *Expected product performance requirements*

- Local pressure equalizing properties over the stump surface, especially bony prominences;
- Surface matching adaptability
 - Material requirements for optimal function:
 - Low initial shear modulus, to allow initial hydrostatic behavior, as present in elastomers.
 - Deformation at a constant volume.

Expected performance requirements for the imbedded fabric:

- Allow easy donning and doffing of the liner by allowing radial movement;
- Don't allow pistoning, by not allowing vertical displacement of the matrix;
- Manufacturing ease caused by a good configuration and easy appliance on the mold;
- Good integration with the silicone matrix.

3. *Environment*

The liner is required to be in full contact with the skin, behaving almost like a second skin, between the stump and the socket. The liner and the socket behave like a heat capacitor, and heat increases during activity [45], being even retained after activity stops. The temperature in

the liner is a function of ambient temperature, and ranges roughly from 22°C to 31°C, considering ambient temperatures of 10°C and 25°C [64].

The product should withstand the conditions supra mentioned.

It should be resistant to UV degradation.

4. *Maintenance*

The liner must be kept clean to avoid skin infections. The cleaning process of silicone shouldn't require expensive products

5. *Materials*

The fabric material must be a mesh that adheres to silicone. The elastomeric liner described uses a medical grade silicone.

6. *Ergonomics*

Easy to handle: The amputee himself carefully rolls the liner onto his limb, without pulling.

7. *Aesthetics*

The silicone can have colour to avoid an unpleasant transparent liner.

8. *Customers*

High demand on low income countries affected by war and with a non-existing or severely damaged National Health Service.

9. *Life in service*

One year of service, at least. ³

³ <https://www.delatorreop.com/faq/how-long-will-this-prosthesis-last-how-long-will-my-liners-last/> consulted in 13/03/2018

10. Marketing

The liner should be marketed towards Non-Governmental Organizations.

11. Packaging:

Packaging costs should be minimal, and any packaging used should be recycled and reusable.

12. Customer requirements

The customer requirements are that the liner enables a comfortable gait and helps the overall success of the prosthetic device of a return to a normal, functional, working life. Avoiding discomfort over the interface between the skin and the liner, as well in the soft tissue.

13. Standards and Specifications

There are no standards applied to prosthetic liners. To assure CE marking, as a liner is classified as a Class I medical device, it should comply with all the requirements of the "COUNCIL DIRECTIVE 93/42/EEC of 14 June 1993 concerning medical devices".

14. Testing

Two kinds of tests were made in this work: a computational and a mechanical one. First a finite element analysis (FEA) was conducted. This FEA intends to be a study that shows the importance of the existence of an embedded mesh fabric within a silicone liner. It is wanted to be divided into two stages: a first stage where a model is developed that will predict the behaviour of a silicone prosthetic liner under longitudinal stretch, that mimics the load that the prosthetic device exerts in the liner during the swing phase of the gait cycle. The second stage of this FEA is intended to be the embedment of a reinforcement mesh that controls pistoning, within the model generated in the first stage. This FEA is described in detail in Chapter 3.

The mechanical test was made on three commercial liners, and on two prototypes produced at the University of Strathclyde. The main goal of this tests is to analyse the different pistoning control that each liner observes. The tests are described in detail in Chapter 4.

CHAPTER 3 – The Need for An Anisotropic Matrix

Objective

On a first approach (1st stage) a model that will predict the behaviour of a silicone prosthetic liner under longitudinal stretch is developed. This model will mimic the force that the prosthetic device exerts in the liner during the swing phase of the gait cycle.

On a second approach (2nd stage) the goal is to insert an imbedded reinforcement mesh into a silicone prosthetic liner model and evaluate the effect that such a reinforcement has in the silicone liner, regarding pistoning prevention.

The goal of these steps is to predict the soft tissue stabilization effect that a liner has.

Method

The steps for the development of this model and a general finite element analysis are:

- To define the model geometry and dimensions;
- Define the material properties;
- Mesh the model;
- Specify the boundary conditions and the loads applied;
- Run the model conditions;
- Analyse and improve the model.

The description of the 1st stage analysis is as follows: The analysis of the effect of a non-reinforced silicone liner in soft tissue during the swing phase of gait cycle.

3.1. Model Geometry – 1st stage

On the purpose of having an imbedded reinforcement fabric mesh within the silicone matrix liner model, the geometry of the model on a first approach is extremely simple. This, because to imbed a reinforcement mesh into a silicone matrix (the binder) model, the reinforcement mesh needs to be regular and constant and to do so, the geometry created is also regular. The dimensions were based on the dimensions that regular commercial liners present⁴.

The sketch shown in figure 3.1 was revolved, creating the three bodies that compose the model: the steel plate for application of the force, the silicone matrix liner and the soft tissue stump.

The force application requires a steel plate to simulate the real behaviour. If the force was applied at a single point in the liner the material would not stretch in a realistic conformation.

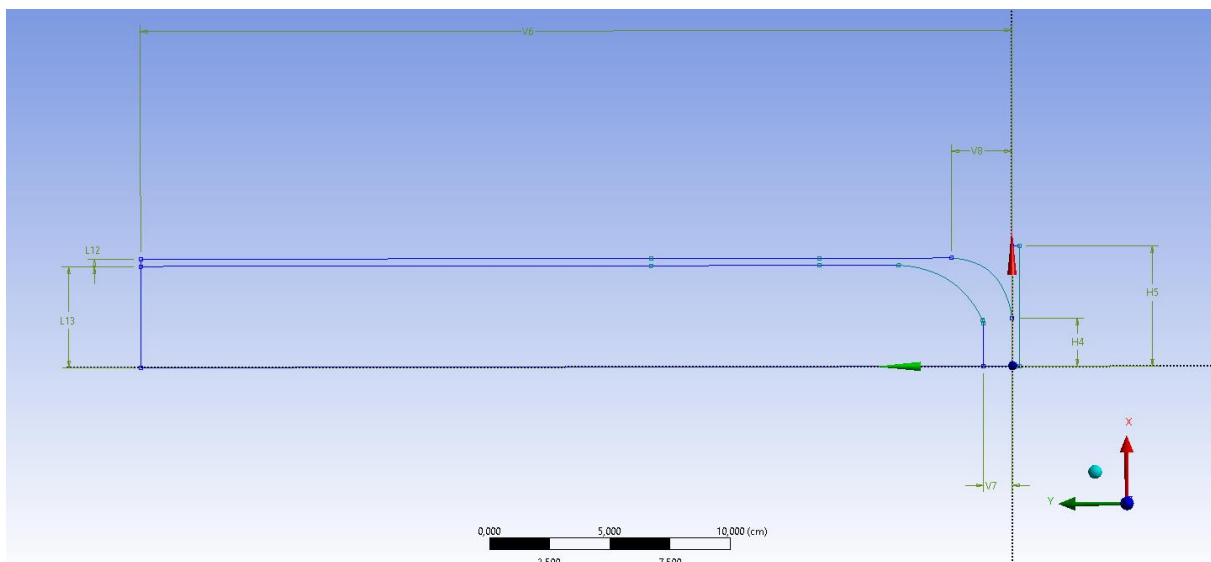


Figure 3.1: Model sketch with dimensions shown:

- **Liner's dimensions:** L12=3mm (thickness at top), V6 (total height) = 36,2 cm; H4 (contact between liner and plate) radius =2 cm, V7 (thickness at the bottom) =1,19 cm;
- **Inside core dimensions:** L13 (cylindrical part radius) = 4,2 cm;
- **Steel plate radius:** H5=5cm

⁴ <https://www.willowwoodco.com/products-services/liners/transtibial/alpha-classic-liners/#tab-2> consulted on 15/04/2018

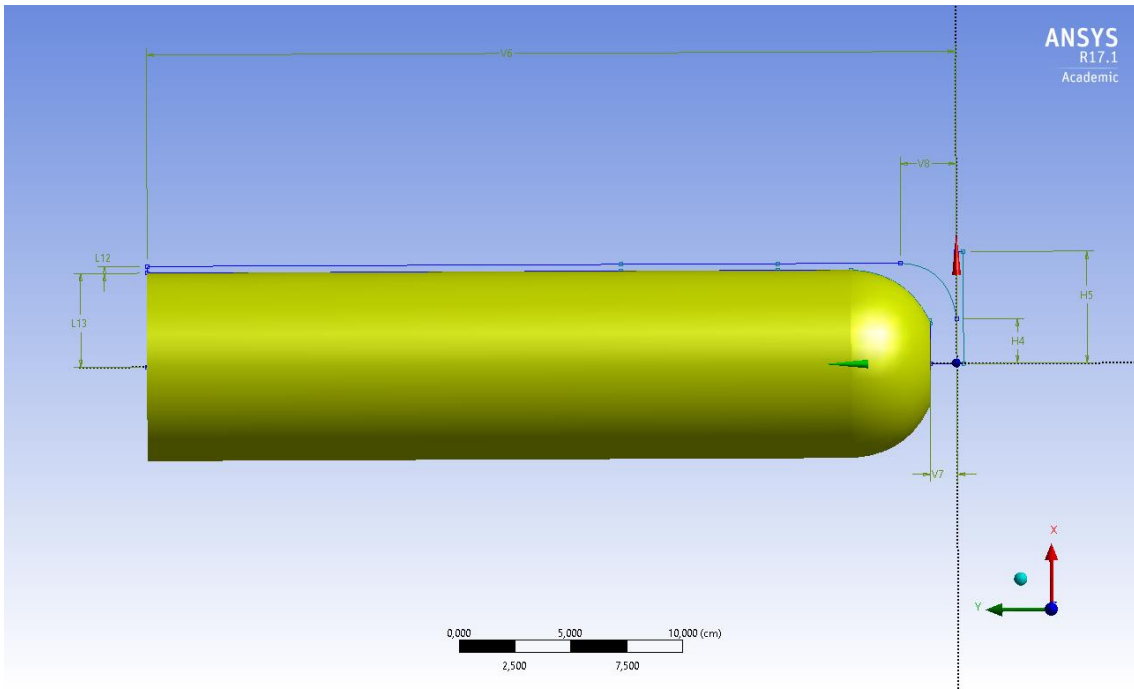


Figure 3.2: Interior core that will be composed by soft tissue;

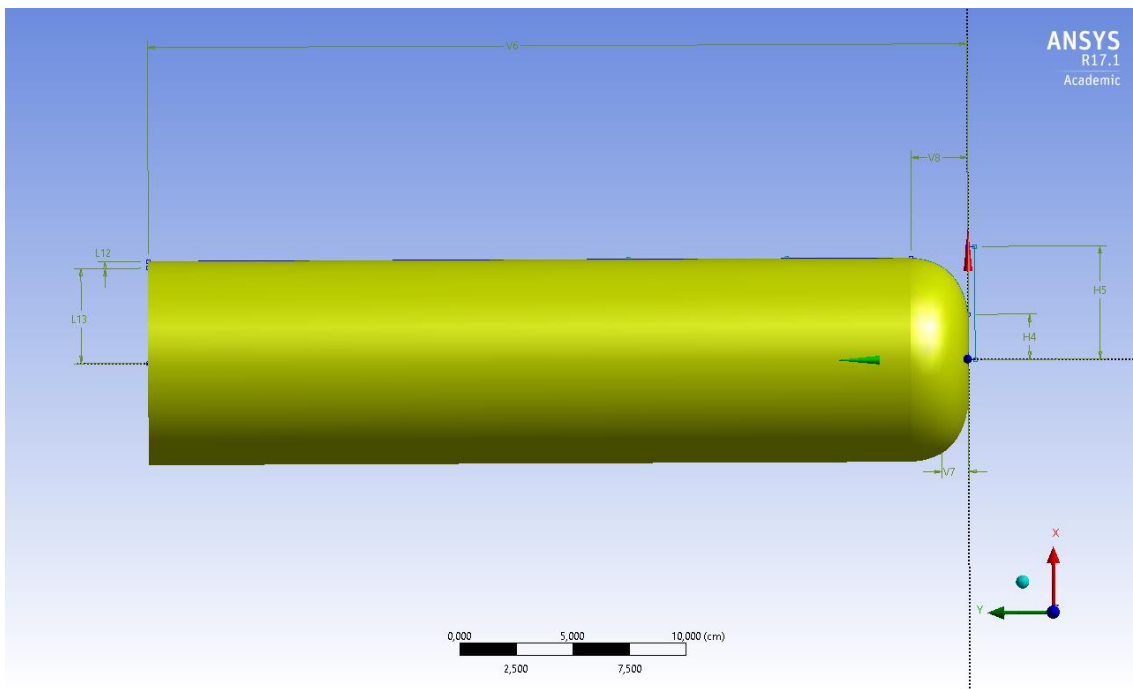


Figure 3.3: The exterior shell, that will be the silicone liner.

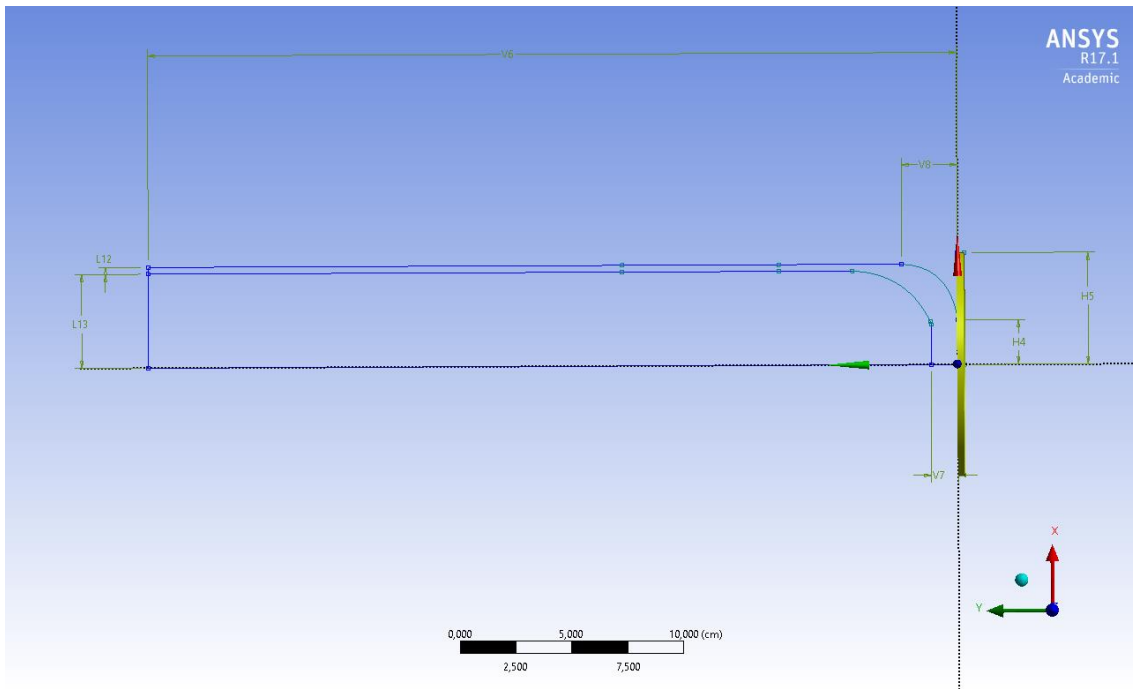


Figure 3.4: The steel plate, used to apply the force in a realistic way.

3.2. Material Properties - 1st stage

The material properties defined in this study, for the soft tissue and liner were adopted from the literature. To apply a force in a realistic way a steel plate was bonded to the bottom of the liner, but this was considered a rigid body, which, will therefore, not be analysed by the software.

3.2.1. Silicone material properties

There were two analyses performed, a linear and a non-linear one. These were performed in order to assess what was the material response, if it was linear elastic or if it was loaded beyond the elastic limits of the material.

In the linear analysis, the material is only defined in ANSYS by Young's modulus and Poisson's ratio, calculating a Bulk and shear modulus for the material from those two values. This means that the relationship between stress (force/area) and strain is linear elastic and the element will return to its original configuration once the load is removed. An isotropic behaviour was preferred because at this first stage there is no reinforcement mesh imbedded and this way the composite material mechanical behaviour is the same in any direction.

The material properties for the linear model are stated in table 3.1.

Table 3.1: Silicone material properties for the linear model

Property	Value	Unit
Density	2,3	Kg m ⁻³
Isotropic Elasticity		
Young's modulus	4E+05	Pa
Poisson's Ratio	0,45	
Bulk Modulus	1,333E+06	Pa
Shear modulus	1,3793E+05	Pa

Density was adopted from the footnote⁵, considering the maximum density value of a silicone rubber range of value.

The Young's modulus and Poisson's ratio were adapted from [65]. It is important to consider for this simulation that one is looking for any 10A shore hardness range of silicones, as this was not only used in this project but also in many state of the art silicone liners. A technical datasheet for a silicone like the one mentioned is given in the footnote reference⁶.

In the non-linear analysis, a hyperelastic material model was used for the prosthetic liner. The chosen model was the Yeoh constitutive model. This is a phenomenological model that follows a reduced polynomial form of the strain energy density function, to describe the elastic properties of the material [66]. In ANSYS, this model is given by:

$$W = \sum_{i=1}^N c_{i0}(I_1 - 3)^i + \sum_{k=1}^N \frac{1}{d_k}(J - 1)^{2k} \quad (1)$$

Where:

W = strain energy potential

I₁ = first deviatoric strain invariant of the Cauchy-Green deformation tensors

J = determinant of the elastic deformation gradient

N, c_{i0}, and d_k = material constants

⁵ <https://www.azom.com/properties.aspx?ArticleID=920> consulted on 4/04/2018

⁶ <http://www.renewmaterials.com/products/silicone10.php> consulted on 07/06/2018

The material constants were taken from [67]. In this work [67], d2 and d3 constants were absent, probably considering both values 0, and so was followed in the reported work.

The Yeoh model showed the best combination of stability and accuracy in the preliminary simulations run by [67], and the smaller root mean square error for the model fit, in comparison with the Money-Rivlin model [67]. The liner under study by [67] was modelled with the following Yeoh model coefficients:

$$N=3;$$

$$c_{10} = 2.014E+04 \text{ [Pa]},$$

$$c_{20} = -1.541E+03 \text{ [Pa]},$$

$$c_{30} = 4.094E+02 \text{ [Pa]},$$

The material incompressibility of the prosthetic liner was simulated through the D1, that is inversely related to the material's bulk modulus. With:

$$d_1 = 3.0E-06 \text{ [Pa}^{-1}\text{]}$$

That approximates a Poisson ratio of 0.48, according to [67]. These values provided the best convergence stability with the closest possible representation of an incompressible material and where all used in this thesis.

3.2.2. Soft Tissue material properties

The soft tissue is neither homogeneous or isotropic and although investigators have speculated that a precise representation of the soft tissue is essential to the model accuracy [68], many studies have considered soft tissue properties to be elastic, isotropic and homogeneous [68-73]. What most studies do, is to either to use properties from literature data, or to experimentally evaluate it through in vivo indentation studies of the residual limb [70, 73].

Considering this, the soft tissue properties used in this study were adopted from [68], considering a linear isotropic elasticity, being the values used similar to the ones observed in other studies [65] and stated in table 3.2.

Table 3.2: Soft tissue linear elastic properties

Property	Value	Units
Density	1,1	g/cm ³
Isotropic Elasticity		
Young's Modulus	3E+05	Pa
Poisson's Ratio	0,45	
Bulk Modulus	1E+06	Pa
Shear Modulus	1,0345E+05	Pa

3.3. Boundary conditions and applied load - 1st stage:

The boundary conditions applied were the following:

- 1 Fixed support at the top of the soft tissue and liner.

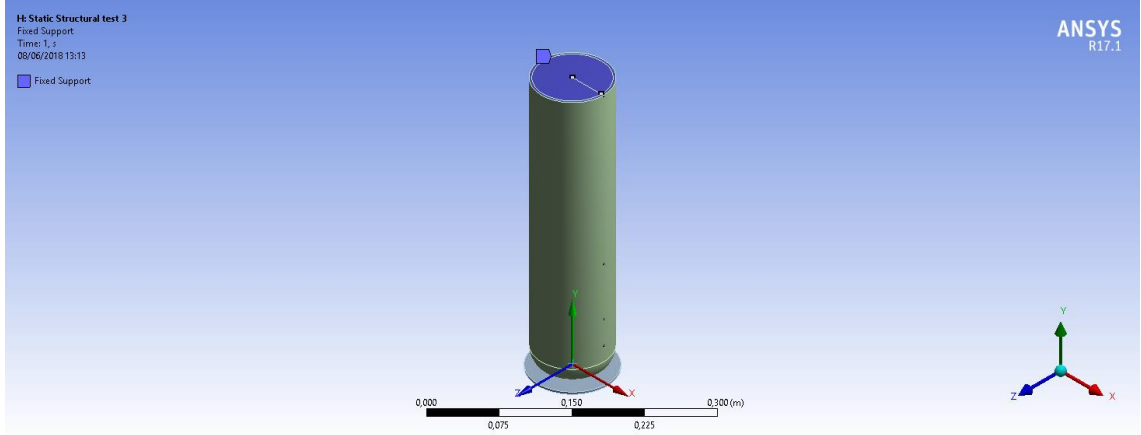


Figure 3.5: Fixed support highlighted, fixing the top surface of the soft tissue and liner's geometry.

- 1 Remote force at the rigid plate. With a remote force being equivalent to a regular force load on a surface, plus some momentum and is used to apply a force load to a rigid body, as it is the case. The remote force is supposed to simulate the force that the prosthetic device exerts in the pin of the liner during the swing phase. The approximation made to calculate this force is justified and shown next.

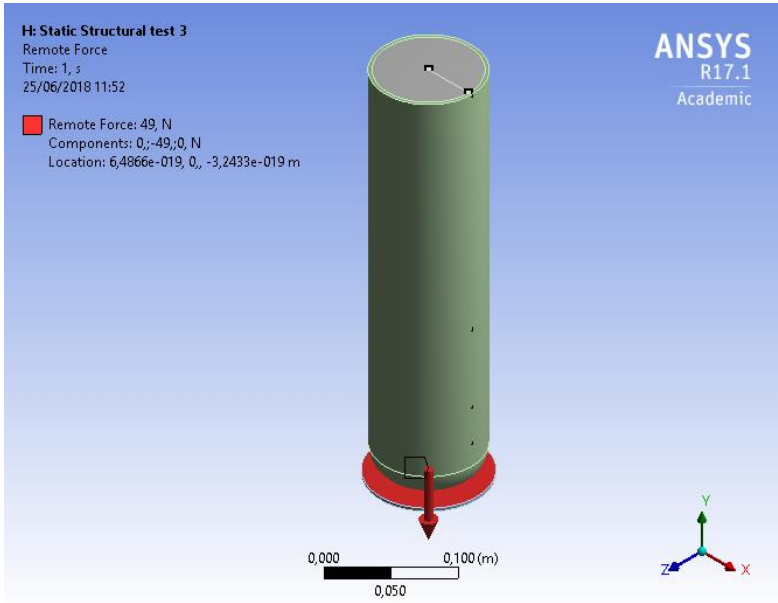


Figure 3.6: Remote force (highlighted in red) of -49 N applied parallel to the Y direction, at the centre of the top surface of the rigid plate under the liner.

Applied load at the liner's pin during the swing phase – A static approximation

This model is a static approximation to a dynamic problem. Considering this, the following calculation was made to derive a load to be applied at the plate of the model.

This force wants to mimic the maximum real force that a prosthetic device of a certain weight, exerts at a liner's pin during the swing phase. For this, a simple pendulum model was created. This pendulum mimics the below knee rotation occurring during the swing phase, using the knee flexion angle.

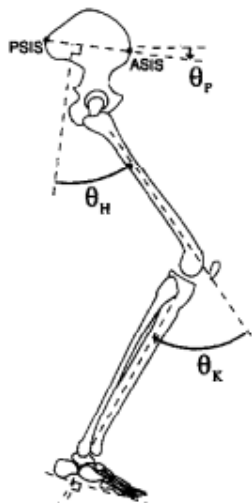


Figure 3.7 Lower limb schematic drawing representing the angle of rotation of the knee during swing θ_k . Adapted from [74]

The study from Piazza *et al.* [74] describes knee flexion angles during the swing phase. The knee angle is defined by the angle between the shank axis and the long axis formed by the thigh, as can be seen in figure 3.7, where knee angle is referenced by θ_k .

During the swing phase, the maximum knee angle reported by this work [74] and others [75, 76] is around $\theta_k=60^\circ$ and the minimum angle is of $\theta_k=0^\circ$.

For the pendulum approximation (figure 3.8), the axis of reference considered is the line that goes from the knee to the ground, perpendicular to the ground. The angle between the shank and this axis is represented by θ , with positive direction of rotation being clockwise. Considering this, the shank at the initial position of $\theta_k=60^\circ$ corresponds to a $\theta=+30^\circ$ at the pendulum, and a final position of $\theta_k=0^\circ$ corresponds to a pendulum angle of $\theta=-30^\circ$.

In figure 3.8, "m" represents the mass of the prostheses (in this case 3,5 kg, an average value between a heavy and light prostheses [77]), at its centre of mass. The distance l, is the distance between the liner's pin and the centre of mass of the prosthesis. Taking as reference the distance from the knee to the centre of mass of a regular shank [74] this distance was set to 15cm.

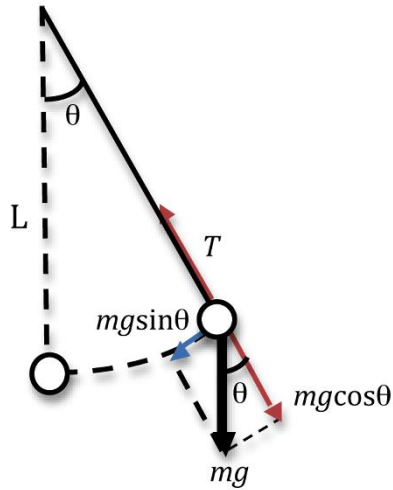


Figure 3.8: Force diagram for the pendulum. Adapted from reference in footnote.

Referring now to the force diagram in figure 3.8⁷, there are two directions: a radial and a tangential one. In the radial direction, there is the tension (T) along the string and the radial component of the gravity force ($m g \cos\theta$). In the tangential direction, there is the tangential component of the gravity force ($m g \sin\theta$). Considering also that the height of the bob is given by:

$$h = l - l \cos \theta \tag{2}$$

With the maximum height at a $\theta_{\max}=30^\circ$:

$$h_{\max} = l - l \cos(\theta_{\max}) \tag{3}$$

and a minimum height at $\theta=0^\circ$:

$$h_{\min} = l - l \cos(0^\circ) = 0m \tag{4}$$

⁷ Image Adapted from http://www.webassign.net/question_assets/ncsucalcphysmechl3/lab_7_1/manual.html consulted in 21/6/2018

Conservation of energy can be considered, as the velocities are low and air resistance can be neglected, giving the following:

$$E_{phmax} + E_{khmax} = E_{phmin} + E_{khmin} \quad (5)$$

Since the bulb can't rotate due to the string, the kinetic energy is only related to the translational movement associated. This way:

$$mgh_{max} = mgh_{min} + \frac{1}{2}mv^2 \quad (6)$$

$$mgl(1 - \cos \theta_{max}) = 0 + \frac{1}{2}mv^2 \quad (7)$$

Where v is the translational velocity modulus.

The goal is to calculate the maximum tension in the string of the pendulum. Considering the centripetal/radial forces, with the positive sign for force pointing inwards and the negative pointing outwards the pendulum's centre of motion, and Newton's second law ($F=ma$), it results in the following equation:

$$\frac{mv^2}{l} = T - mg \cos \theta \quad (8)$$

T will be maximum when the velocity, v , is maximum and it can be easily seen that is at $\theta=0^\circ$, that the velocity is maximum. To consider the maximum force exerted in the liner's pin, the calculation made for the Tension (T) was at that exact moment, to have an approximate value for the future tests.

With $\theta_{max} = 30^\circ$; $l = 0,15$ m; $m = 3,5$ kg; $g = 9,8$ m/s the maximum velocity can be calculated with:

$$v = \sqrt{2gl\left(1 - \frac{\sqrt{3}}{2}\right)} = 0,63\text{m/s} \quad (9)$$

And now with this value of velocity, the Tension (T) at its maximum value, when $\theta=0^\circ$, can be calculated:

$$T = \frac{mv^2}{l} + mg \cos \theta = 49\text{N} \quad (10)$$

- 2 Contacts: A frictional one between the soft tissue and the liner, with a coefficient of friction⁸ (COF) of 0,6. This value for the COF was taken from [78], although higher COF between skin and liners has been reported in amputee skin studies [32] and benchtop measurements of prosthetic liners [33]. Those reported values are for kinetic/dynamic coefficients of friction. As this analysis is a static structural one, the coefficient of friction used by Ansys is a static one based on Coulomb's law, although the static coefficient of friction is harder to measure as its measurements are less repeatable than the dynamic CoF measurements [79].

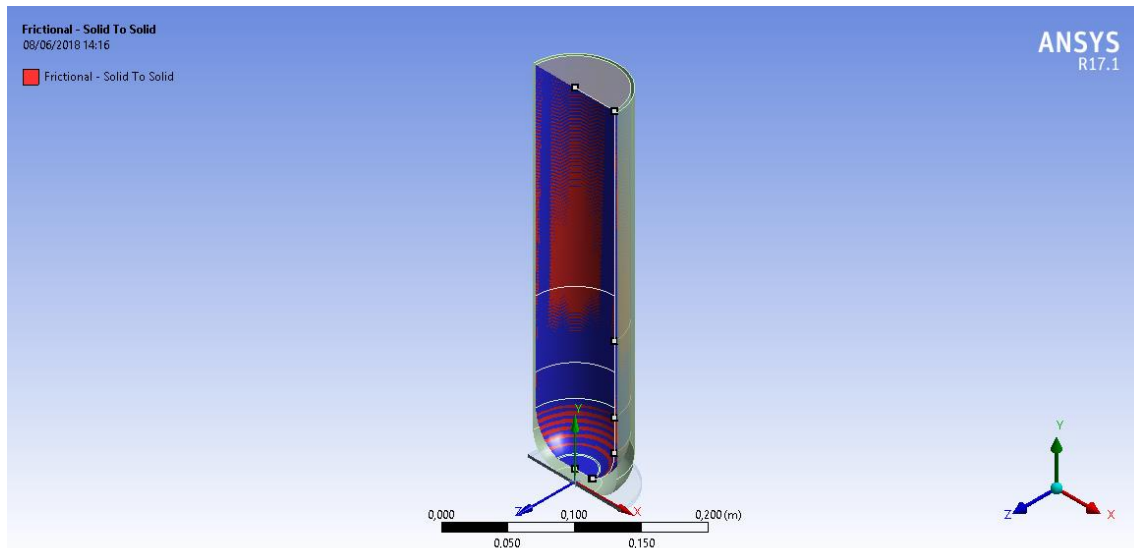


Figure 3.9: Frictional contact, with COF = 0,6.

The other contact is a bonded contact between the liner and the rigid steel plate that doesn't allow separation and sliding.

⁸ Coefficient of friction is calculated with Coulomb's law: $F_{Tangential} \leq \mu F_{normal}$ Where μ is the coefficient of static friction. This way, once the tangential force exceeds this product, sliding will occur.

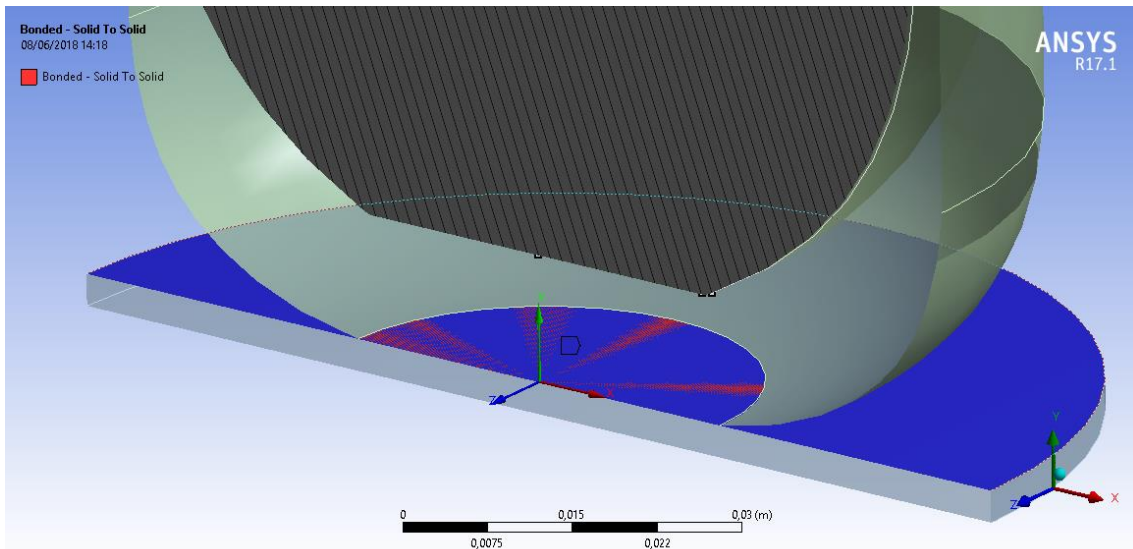


Figure 3.10: Bonded contact between liner and plate.

3.4. Mesh the model - 1st stage⁹

A mesh sensitivity analysis was performed, this means that the mesh size was optimized in such a way that no difference in results in comparison with denser meshes are observed. This way optimizing processing times and having minimal adjustments. The mesh had 32.360 elements and 52.455 nodes. A mesh quality analysis was also made, to choose the size function that would give a better-quality mesh.

⁹ To avoid confusion: In this chapter, the word mesh might have two meanings. One previously described along the document, a reinforcement structure embedded within the matrix (being the matrix in engineering the binder of the composite, in this case silicone). The other, present in this chapter, is a FE mesh. A mesh created by the FE software that is a network formed of elements and nodes, describing the present geometry.

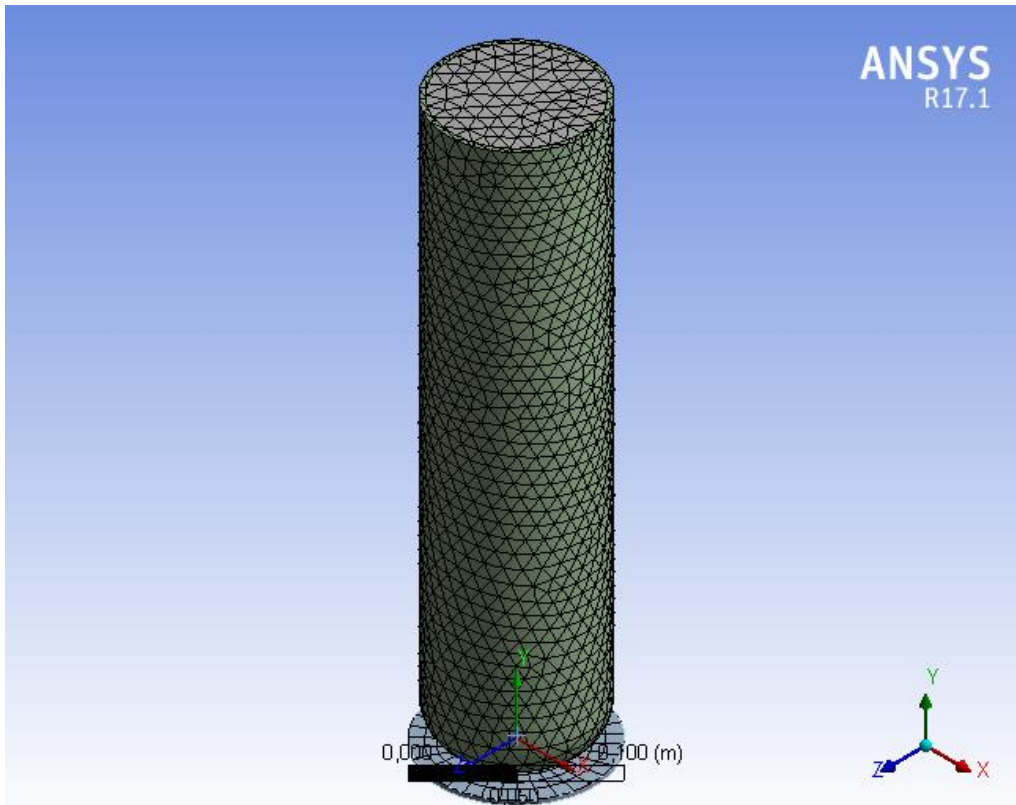


Figure 3.11: Mesh representation

All size functions supplied by Ansys were analysed. This analysis consisted in a run between three main parameters to check mesh quality (element quality, aspect ratio and Jacobian ratio) and to compare which size function provided the best overall quality.

The criteria to evaluate the quality of the mesh according to these three parameters is:

- For the element quality metric: the highest minimum.
- For the aspect ratio: to have the smallest maximum value, as close to 1 as possible.
- For the Jacobian ratio: to have the smaller maximum value.

For the comparison of all size functions with the quality criteria defined by these three parameters, table 3.3 is presented:

Table 3.3: Comparison between the mesh metric and the size functions available. The goal is to find the size function that combines the highest minimum value for element quality, the smallest maximum value for the aspect ratio and smaller maximum value for the Jacobian ratio. Highlighted in bold are the best values according to these criteria, and the size function that have the best match overall.

Size function	Number of elements	Element quality Min value	Aspect Ratio Max value	Jacobian ratio Max value
Proximity and Curvature	97261	0,11621	20	3,4178
Adaptive	19426	0,16071 8	11,818	2,6601
Uniform	32360	0,15145	9,0064	2,645

Proximity	97402	0,12223	19,326	3,4178
Curvature	32262	0,15494	8,9672	2,4385

Proximity and curvature function (table 3.3) wasn't chosen as it showed overall the worst results for each parameter. Proximity function (table 3.3) showed the second-worst value of element quality and its values of aspect and Jacobian ratio were also too high. Adaptive function (table 3.3) showed the best element quality minimum value, however its values for aspect and Jacobian ratio were too high in comparison with Uniform or Curvature function. The next size function with a better value of element quality is the Curvature function (bold in table 3.3) and although the values for this function are very close to Uniform function, they are slightly better. This makes sense as the Curvature size function locally refines the size of the elements based on curvature feature in the geometry.

This way, curvature size function was the chosen one to mesh the model.

3.5. Finite Element Analysis Results - 1st stage

3.5.1. First stage results

On the first stage of the finite element analysis, two parameters were evaluated, the total deformation and the von Mises stress. These two parameters were enough to assess the model viability.

To evaluate this model, a criterion was defined, it being the separation distance between the soft tissue and the liner model (from now on called H). ANSYS doesn't provide a distance between two nodes after deformation. However, it provides information on how much each node deforms. To calculate this information ANSYS uses equation 11:

$$U = \sqrt{U_x^2 + U_y^2 + U_z^2} \quad (11)$$

Where U_x , U_y and U_z are the three individual components for the deformation relative to the coordinate system of reference.

To find out this distance (H), two nodes were selected from the centre of each surface (figure 3.12, 3.13), with the label of the deformation sustained by each node visible. The U_x and U_z component can be neglected in the analysed nodes, as it can be seen from the vector representation in figure 3.13. As so, the distance might be calculated subtracting each deformation vector, as the two nodes at time 0 are in contact, through the following equation:

$$U_l - U_{st} = H \quad (12)$$

Where U_l is the deformation vector value for the interior surface of the liner, parallel and coincident to the soft tissue surface. While U_{st} is the deformation vector value for the lower surface of the soft tissue.

Considering this, the separation distance criterion is achieved, calculated for the hyperelastic model as $H_{\text{hyperelastic}}=16,3$ cm as can be seen in figure 3.12. For the linear model (figure 3.16) this criterion is $H_{\text{linear}}= 2,56\text{cm}$.

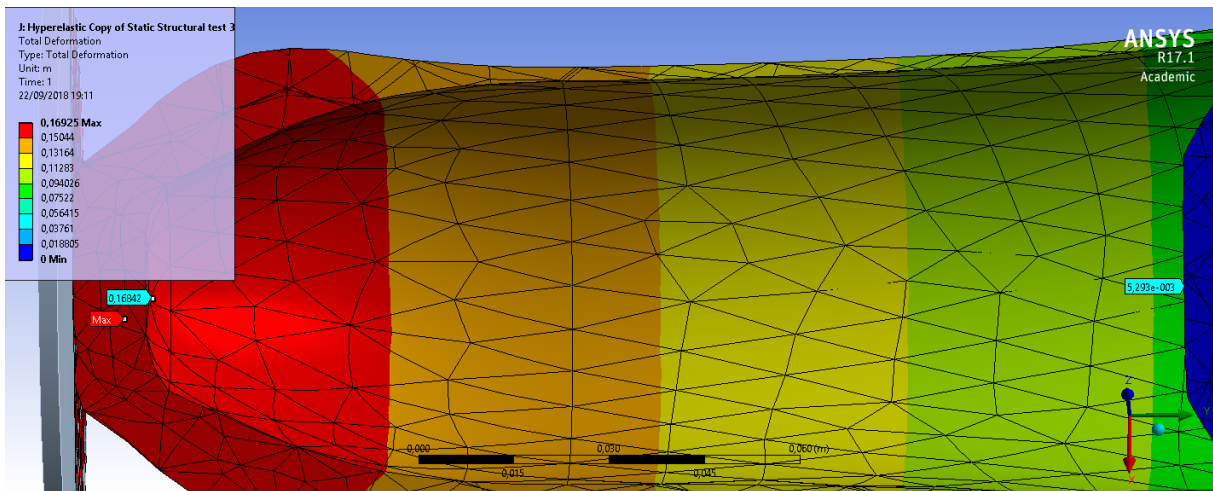


Figure 3.12: Region of interest amplified at the hyperelastic model. The labels on to are the deformation vector values for 2 different nodes at the surface of soft tissue ($U_{st}=5,3$ mm). The label at the liner is the deformation at a single node at the surface of the inside core of the liner ($U_l=16,8$ cm). $H=U_l-U_{st}=16,3$ cm.

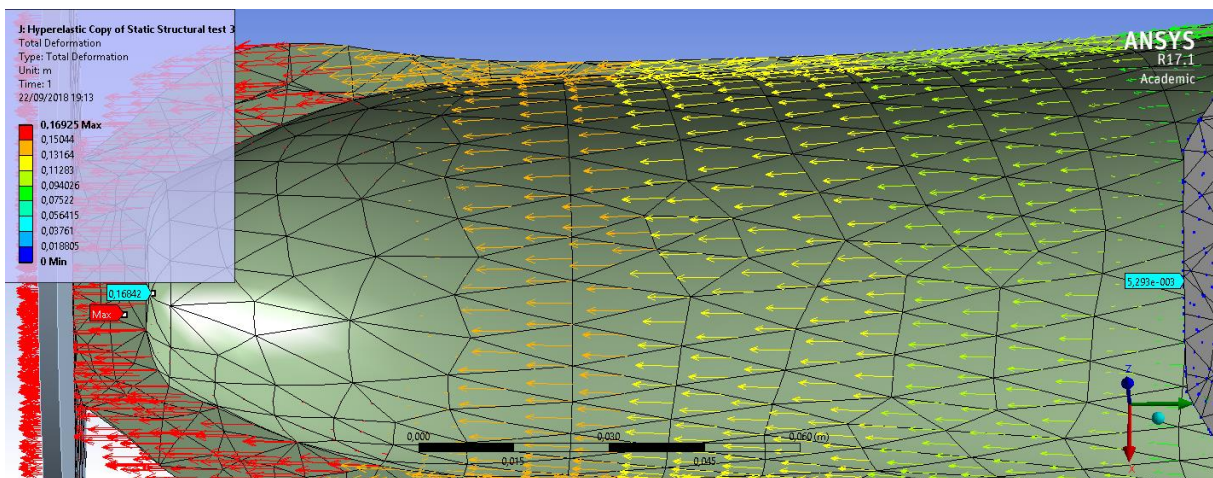


Figure 3.13: Region of interest at the hyperelastic model, with deformation vectors shown in arrows. The blue vectors and red vectors are parallel with the Y axis.

3.5.1.1. Linear Model

The results for the deformation in the linear model can be seen in figure 3.14, 3.15 and 3.16. Figure 3.14 shows the deformation within the soft tissue, while figure 3.15 shows the general deformation pattern of the liner. Figure 3.16 is an amplification of the region of interest, as it is in this region that the separation distance between the liner and the soft tissue can be evaluated. As seen in figure 3.16, the value of U_{st} is 5,7mm and the value of U_l is of 3,13cm, causing the value for the criterion of separation H , to be equal to $H=2,56cm$.

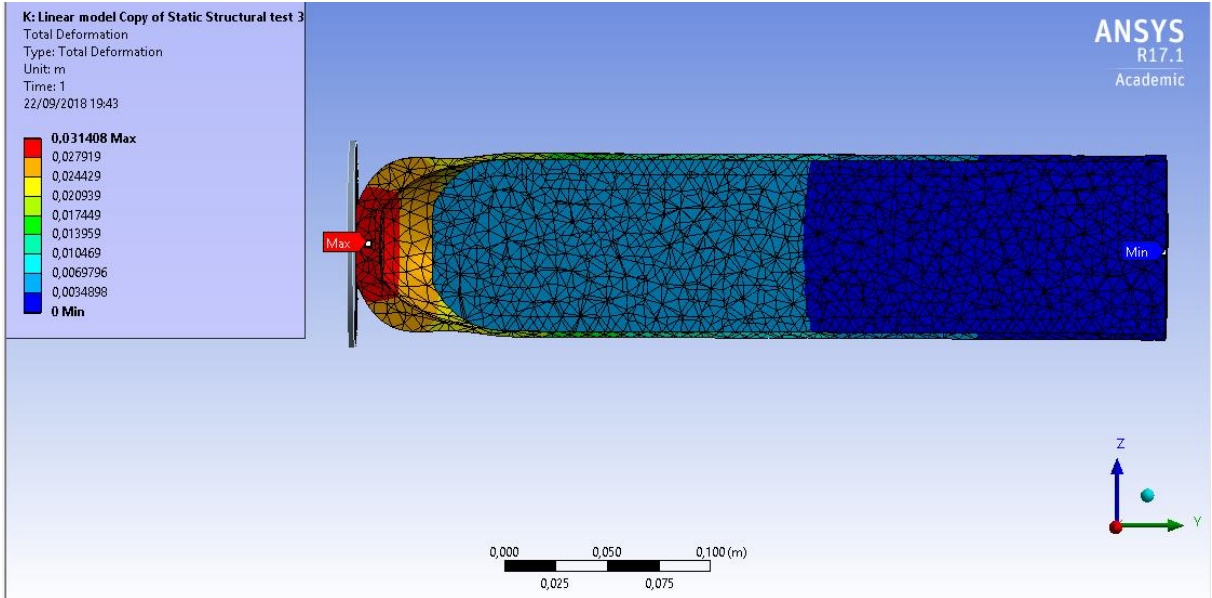


Figure 3.14: Pattern of deformation in the soft tissue. The maximum value of deformation in the soft tissue is of 7mm; An absence of necking is also observed, although separation between soft tissue and liner occurs.

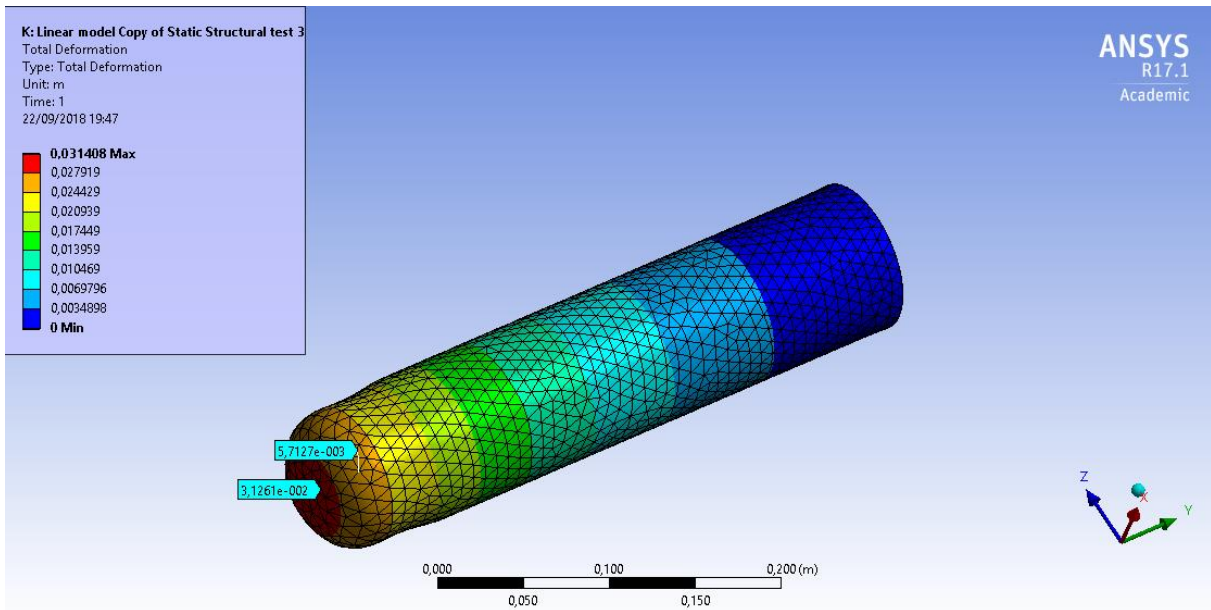


Figure 3.15: Deformation pattern across the liner.

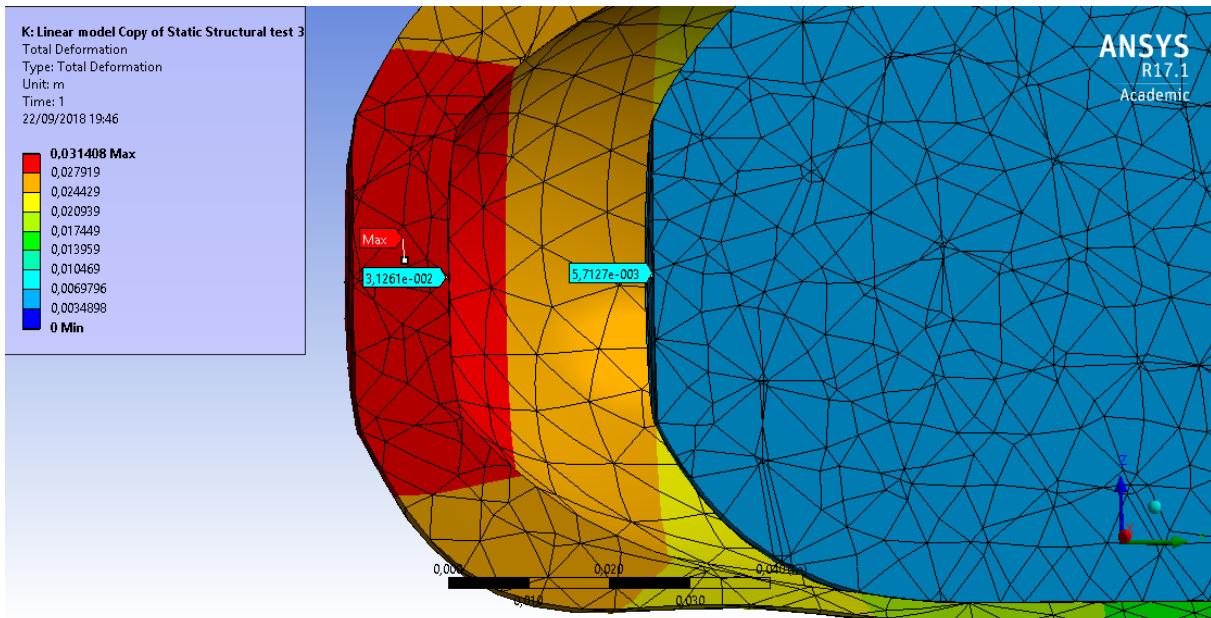


Figure 3.16: Region of interest. Here the values that set the criterion are labelled. On the soft tissue, the $U_{st}=5,7$ mm, and on the liner, the value $U_l=3,13$ cm. The resulting separation criterion is $H=2,56$ cm.

Figures 3.17 and 3.18 show the von Mises stress results. With figure 3.17 showing the stress configuration on the liner and figure 3.18 highlighting the soft tissue core and the stress it sustains.

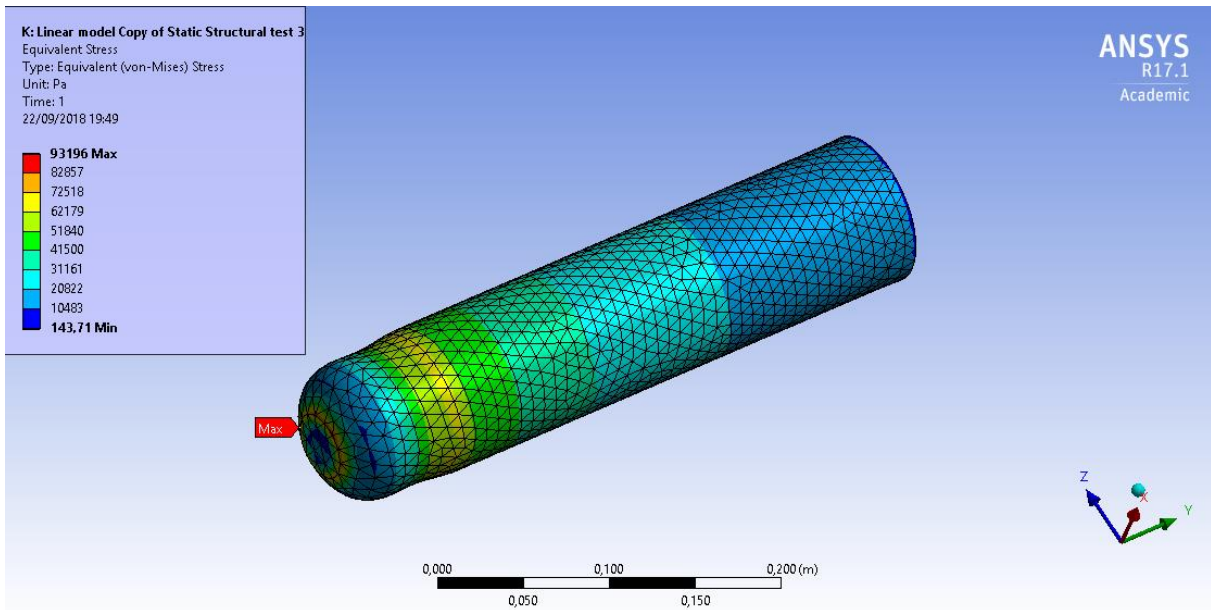


Figure 3.17: Linear model showing Von Mises stress, the stress areas at the silicone liner with maximum value of 93 kPa at the contact region, and the increase in stress at the region where the separation between soft tissue and the liner surface occurs (no necking observed though).

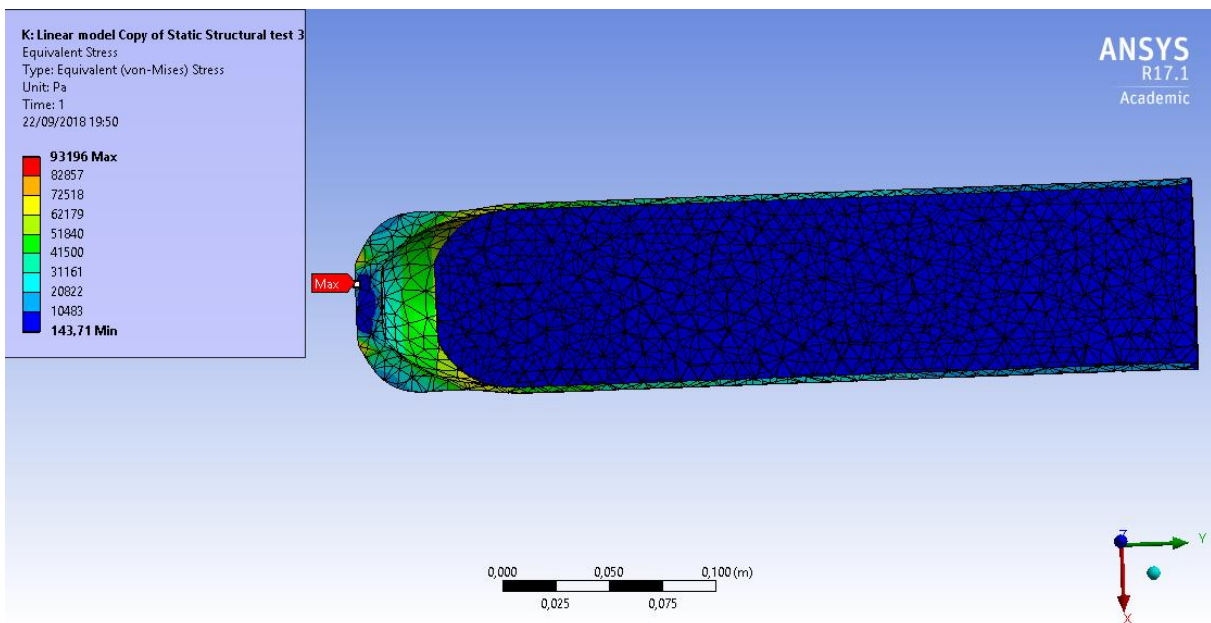


Figure 3.18: Linear model Von Mises stress, showing the stress distribution at the soft tissue with the maximum value of 10kPa and the minimum value of 143 Pa.

3.5.1.2 Hyperelastic/non-linear model

The results for the hyperelastic model deformation are shown in figures 3.19, 3.20 and 3.21. Figure 3.19 shows the liner and soft tissue interior deformation. Through this figure, the displacement criterion can be applied, being that highlighted in figure 3.20, with an amplification of the region of interest. In this figure the value for UI is marked and is of UI=16 cm, while the value for Ust is of Ust=5,3 mm. With these values, the criterion of liner/soft tissue separation established before is H=15,5cm.

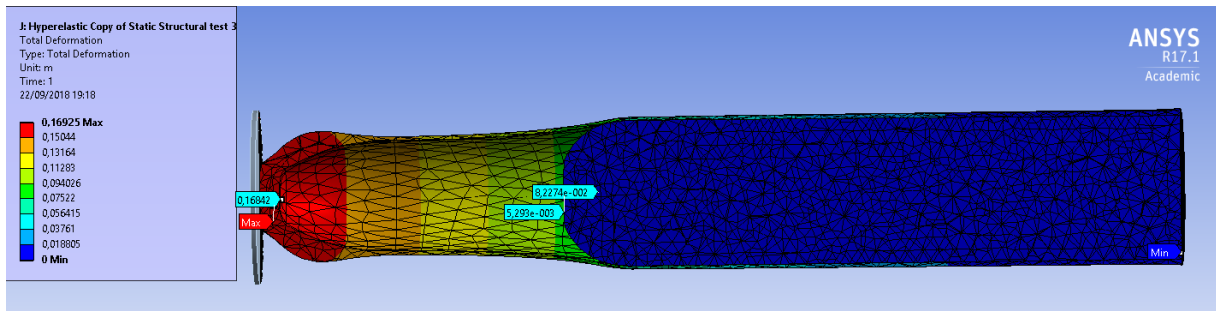


Figure 3.19: deformation pattern at the hyperelastic model liner. The maximum deformation is considerably higher compared to the linear model. Necking of the liner is also observed were the separation between the liner and the soft tissue occurs. Maximum value at the liner approx. 16 cm; Max deformation at the soft tissue approx. 5,3 mm

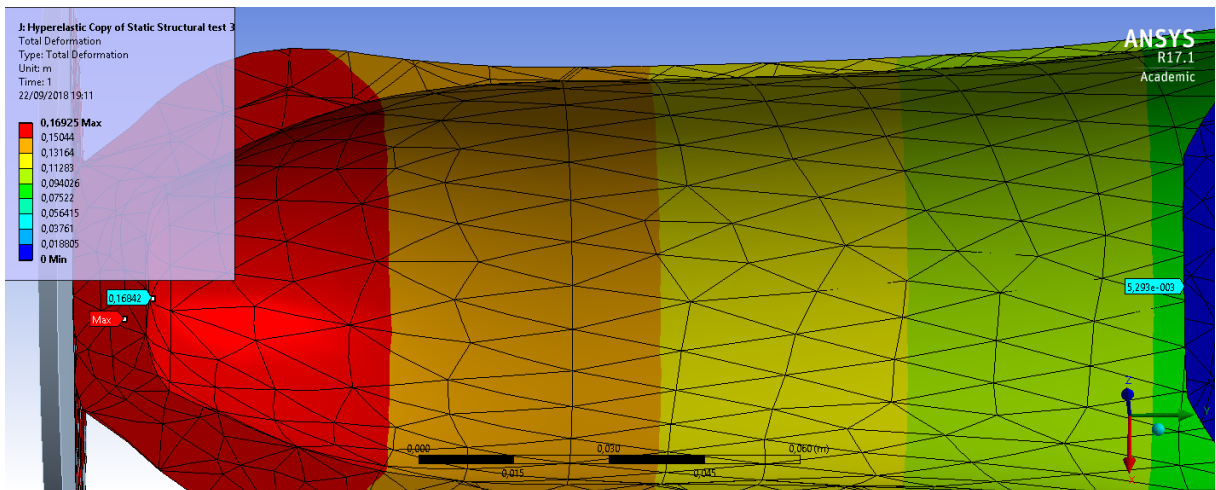


Figure 3.20: Region of interest. Here the values that set the separation criterion can be seen. On the soft tissue, the $U_{st}=5,3$ mm, and on the liner, the value of $U_l=16$ cm. The resulting separation criterion is $H=15,5$ cm.

Figure 3.21 shows the von Mises stress in the soft tissue material. The maximum value of von Mises stress sustained in this material is approximately of 109 kPa. Figure 3.22 highlights the maximum stress region that the liner sustains. It is the region where the displacement from the soft tissue occurs, and where necking is observed. Figure 3.23 shows the general stress distribution sustained in the liner.

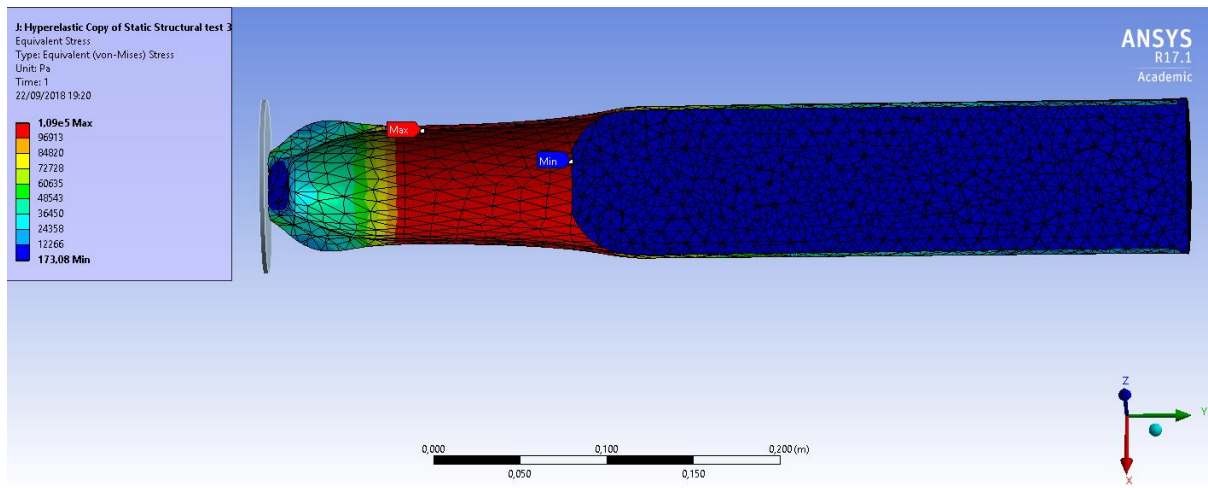


Figure 3.21: Hyperelastic model Von Mises stress, the stress distribution in the soft tissue is homogeneous, it also has a maximum value of 12,3 kPa and a minimum value of 173 Pa.

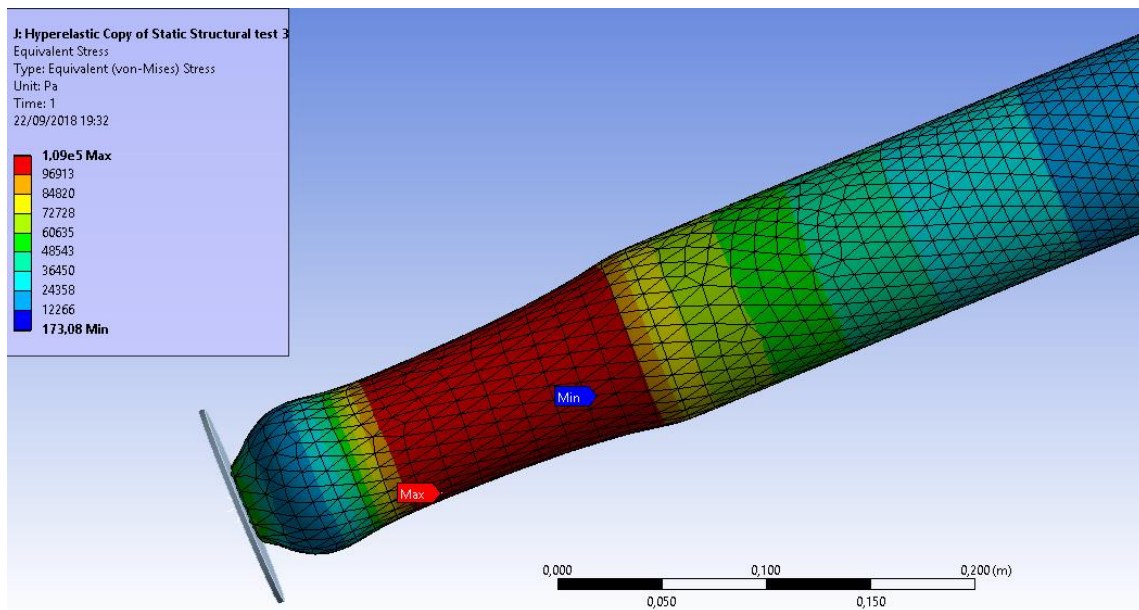


Figure 3.22: Highlight of the necking area, where the maximum von Mises stress is obtained. It shows the stress areas at the silicone liner with maximum value of approx. 109 kPa at the necking region.

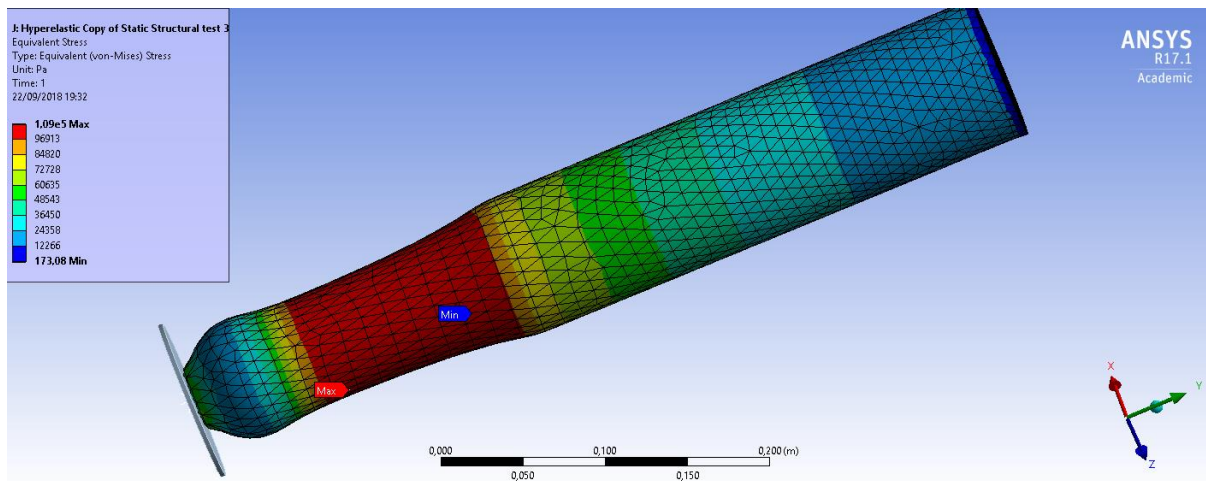


Figure 3.23: Hyperelastic model showing the full von Mises stress pattern across the liner.

3.6. Reinforced liner VS Non-reinforced liner – 2nd Stage

What was done at this second stage of the finite element analysis, was a comparison between the deformation of a reinforced and a non-reinforced silicone liner, during the swing phase of gait cycle. Abaqus and Ansys were both used in this stage. Abaqus for the creation of the reinforced model, and Ansys for the creation of the non-reinforced model. In both softwares the mesh (the computational one) and geometry, the boundary conditions, the silicone’s properties and the analysis conditions were the same. The only difference was the full liner’s length reinforcement fabric mesh assigned in Abaqus with polyester material properties and not assigned in Ansys. The following section describes the main steps taken in this analysis.

3.6.1. Geometry and Mesh

A code capable of generating a mesh with a specific configuration of elements was created by the University of Strathclyde and used in this work (figure 3.24). This way, the methodology in this stage was different from the first stage method. Instead of creating a geometry and asking the software to do the meshing later of that geometry, here a geometry was created from an initial mesh. Ansys showed some limitations due to this change in methodology, this way, Abaqus was also used in this simulation.

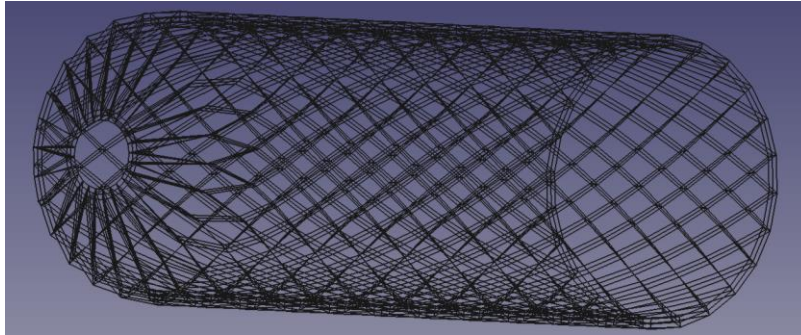


Figure 3.24: Mesh representation in FreeCAD 0.17 software. The liner dimensions are:

- **Height: 36 cm**
- **Distal end opening radius (for the suspension screw insertion): 0,5 cm**

The code developed in FreeCad creates a mesh that has three types of elements: hexahedral, pentahedral (triangular caps for the bottom and top of the liner), and 2 node linear lines (beams, represented in figure 3.25). The beams will be assigned with the reinforcement material (polyester fibres) for the silicone liner and are between two layers of solid elements, 2 mm thick each layer, that will be assigned with silicone. Not only these beams are between the solid elements, as they are coincident with some edges of the solid elements (figure 3.26 and 3.27).

Having concerns about the quality of the elements at the bottom of the liner, an element quality analysis was made. A high aspect ratio was observed for the bottom elements, exactly were a higher deformation was observed. However, the parameters able to manipulate the code supplied by the University of Strathclyde, that would affect this region, without changing the entire mesh configuration, were only the number of nodes around the circumference between the transition from a cylindrical shape to conic shape (see figure 3.29). Three configurations were created, to compare the element quality resulting from the resulting mesh, and the results when applying the same boundary conditions. One configuration had 24 nodes around the circumference of the liner (resulting in the mesh with 1248 elements), another with 28 nodes (resulting in a mesh with 1680 elements) and a third one with 34 nodes resulting in 2448 elements.

A comparison as well as an evaluation were performed between the resulting meshes. Element quality, aspect ratio and Jacobian ratio were evaluated¹⁰. The difference was not significant in any of this

¹⁰ Tables shown in appendix 1.

parameters and this way, for a matter of synthesis, the results presented and analysed from now on, are the ones from the “24-node’s” mesh liner.

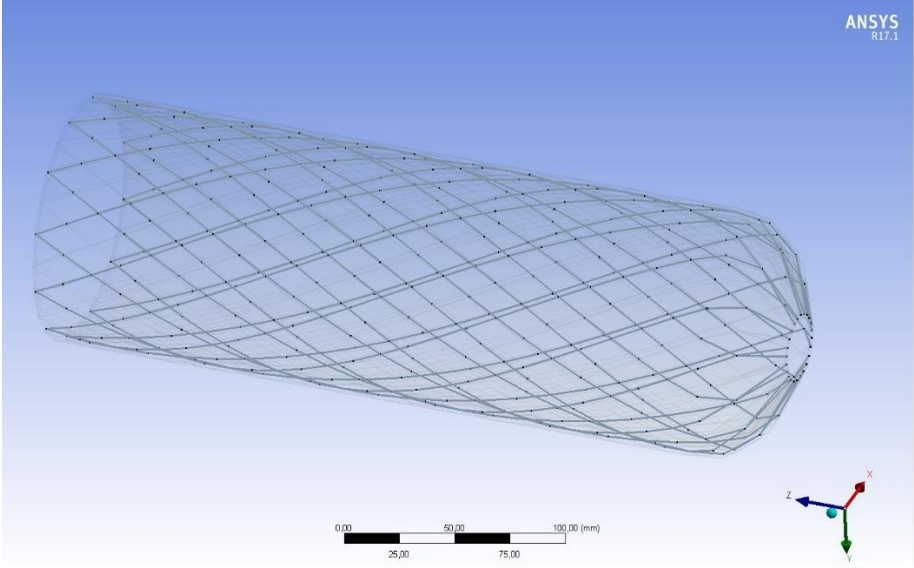


Figure 3.25: Beam elements representation in ANSYS.

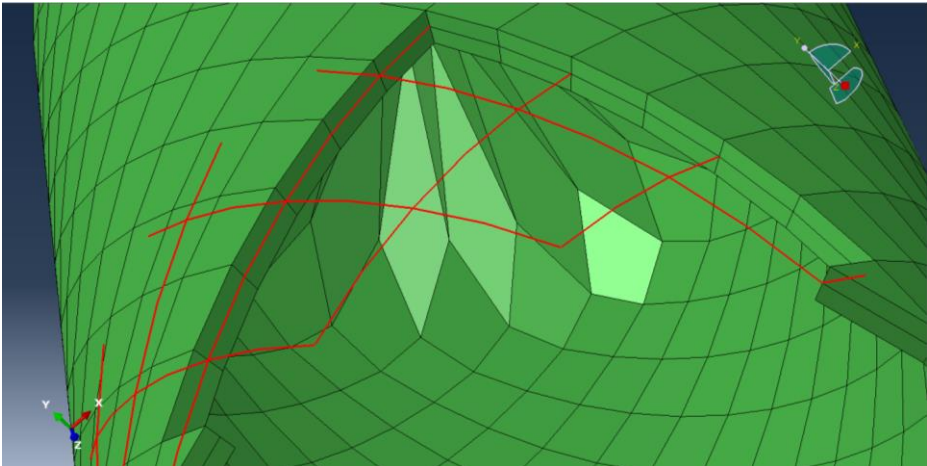


Figure 3.26: Highlighted in red are some (not all) beam elements (the solid elements of this region were removed to visualize the beams). It is visible that they cross the solid elements in the middle of both layers of solid elements.

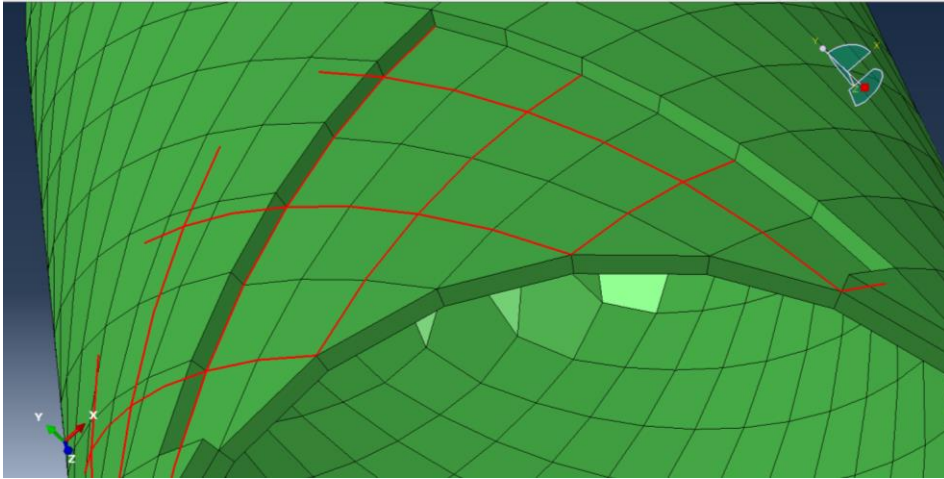


Figure 3.27: Again, highlighted in red are the beam elements, in this figure however the inner layer is shown, to understand the disposition of the beams with the matrix, and that they are coincident with some solid elements' edges.

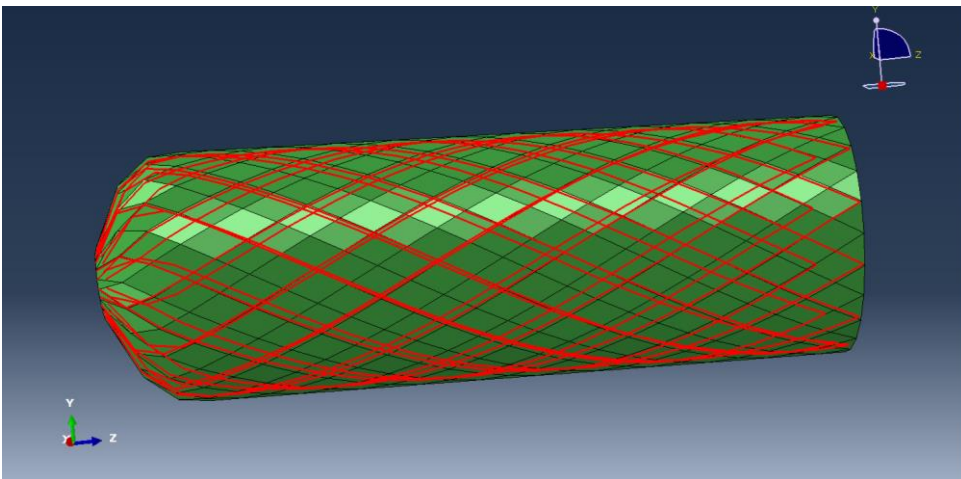


Figure 3.28: Side view of the geometry, with the reinforcement beam elements imbedded in the matrix highlighted in red.

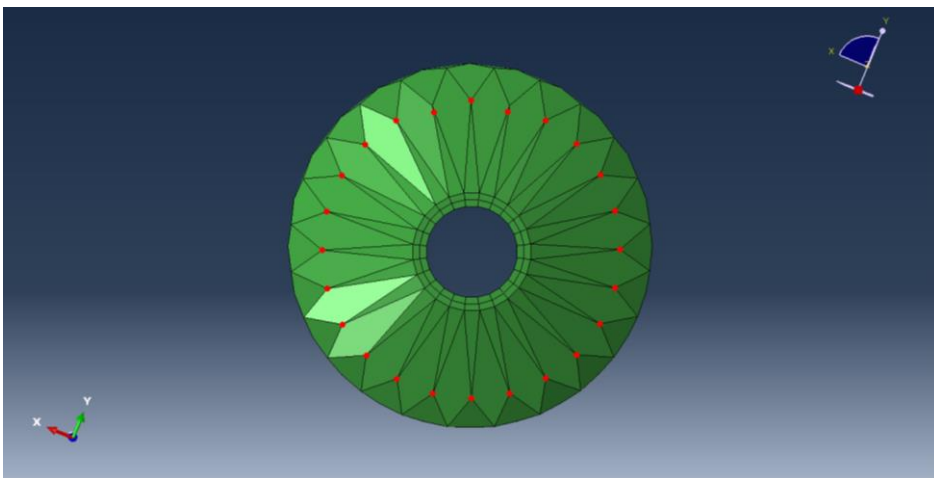


Figure 3.29: Bottom view. Highlighted in red are the nodes that can be manipulated to develop the different mesh configurations. In this case, the "24 node" mesh is visible.

3.6.2. Material Properties

The results from the first stage analysis, show that the linear elastic model shows a displacement closer to the displacement observed with the non-reinforced Majicast prototype liner (results in Chapter 4), while the hyperelastic model, shows a displacement much higher to the one observed in practice. This way, the material chosen for silicone at the second stage analysis was the linear elastic material from the first stage analysis.

Table 3.4: Silicone material properties used for second stage analysis. Linear elastic model used.

Property	Value	Unit
Density	2,3	Kg m ⁻³
Isotropic Elasticity		
Young's modulus	4E+05	Pa
Poisson's Ratio	0,45	
Bulk Modulus	1,333E+06	Pa
Shear modulus	1,3793E+05	Pa

Polyester fibres were the material used for the reinforcement mesh. The properties for the model were retrieved from the university of Michigan material's science department¹¹ and present in the following table.

Table 3.5: Polyester fibres material properties. Linear elastic model.

Property	Value	Unit
Density	1540	Kg m ⁻³
Isotropic Elasticity		
Young's modulus	2,5E+09	Pa
Poisson's Ratio	0,33	

3.6.3. Boundary Conditions

In this stage, there is no insertion of soft tissue inside the liner, although that was put to the test, but as an original mesh was used, both Abaqus and Ansys didn't provide a solution for the insertion of a soft tissue geometry inside the liner. This is not problematic, as the liner effect on the soft tissue due to pistoning was already analysed and shown in the previous section, proving already that the liner with less pistoning causes a smaller tissue stress and stretch.

¹¹ <http://www.mse.mtu.edu/~drjohn/my4150/props.html> - retrieved 13/09/2018

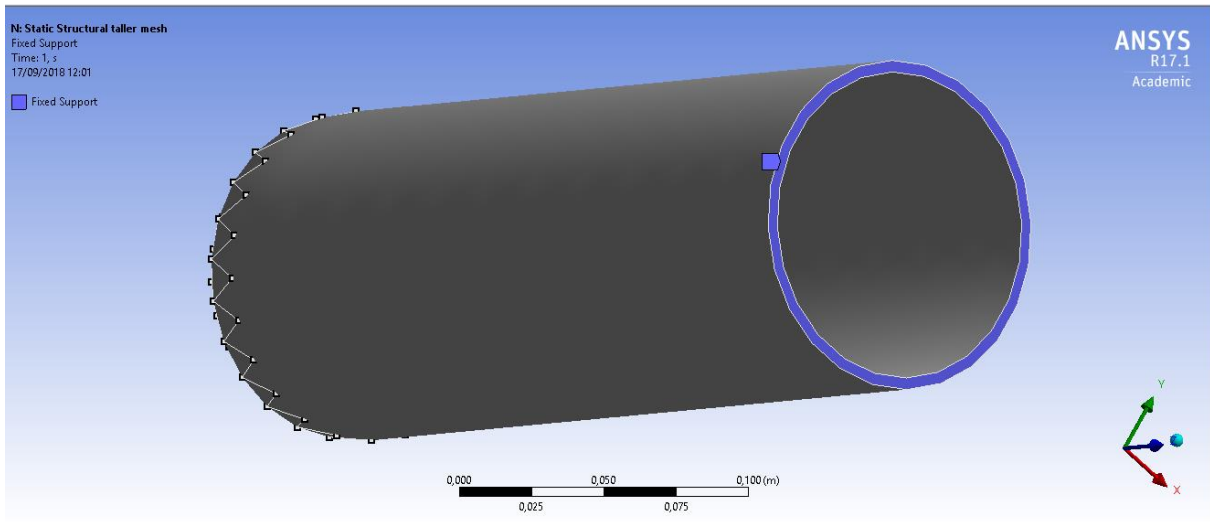


Figure 3. 30: Fixed support on top surface of liner (highlighted area) – Ansys representation

This way, the boundary conditions applied in this analysis were very simple, just enough to compare and prove the effect of the reinforcement. To keep the liner fixed and stable, a fixed support (figure 3.30) was applied at the top surface of the liner, in both Ansys (figure 3.30) and Abaqus (figure 3.32).

To simulate the force exerted by the pin attached to the bottom of the liner, during swing phase of gait, a force was applied at the highlighted area of figure 3.31 and 3.32. Instead of applying this force through a plate, as it was done previously.

In Ansys, the force was applied at the surface, surrounding the distal end opening, where the pin connecting to the prosthesis is placed. The application of a force on a surface in Ansys is made through a force vector. The load is applied by converting the force into pressure, based on the total area of the selected surface. If the face changes its area during the load application, the total load magnitude applied to the face remains the same. However, the force vector directions never change.

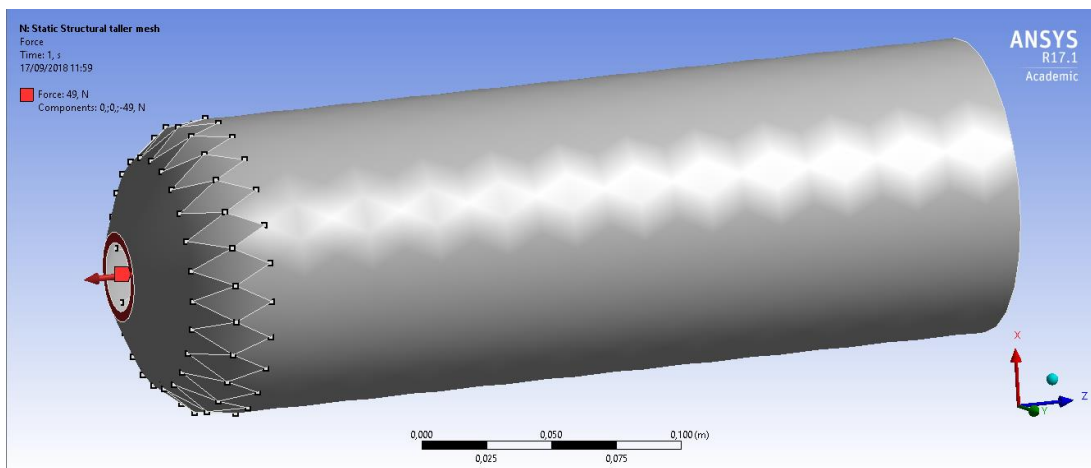


Figure 3. 31: Force representation. 49N applied at the distal end opening of the liner.

In Abaqus, a “general surface traction” (t) force is applied to the same surface (S). The load is computed by integrating t over S:

$$f = \int_S t \, dS = \int_S \alpha \hat{t} \, dS$$

where α is the magnitude (49 N) and \hat{t} is the direction of the load (0, 0, -1).

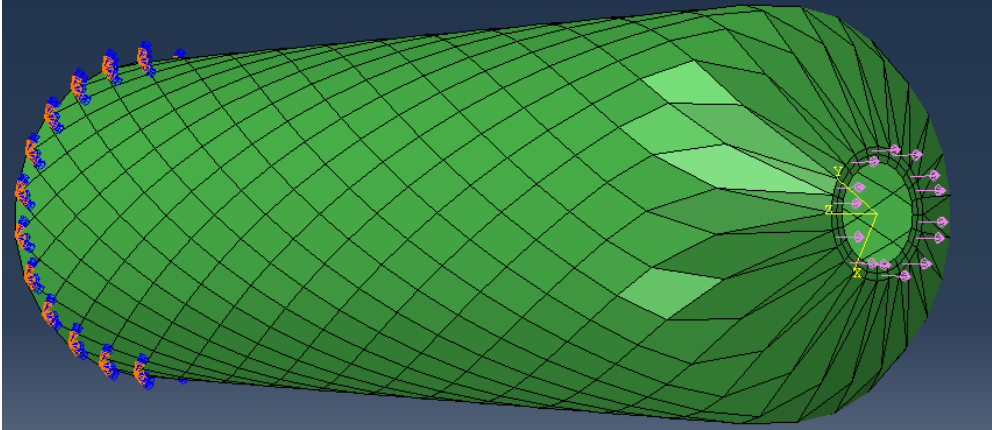


Figure 3.32: Boundary conditions in Abaqus. The top surface is fixed, and the distal end opening as an applied force in the same conditions as reported in Ansys.

With the same boundary conditions applied to the two different models, it is time to analyse the results about the reinforcement effect.

3.6.4. Second Stage Results

3.6.4.1. Reinforced liner – ABAQUS model

As in the first stage, two parameters were accessed: Total Deformation magnitude (figure 3.33) and von-Mises Stress (figures 3.35, 3.36 and 3.37).

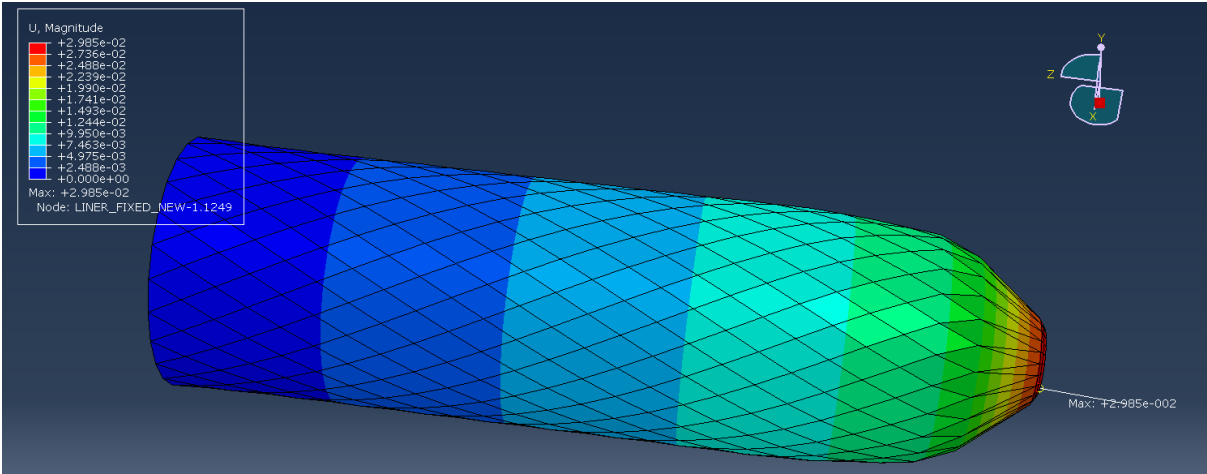


Figure 3.33: Total deformation magnitude at the reinforced liner. Maximum value of node’s deformation at the distal end (≈3cm) equivalent to pistoning value.

Table 3.6: Node magnitude of deformation and liner's region

Node Total Deformation [cm]	Length [mm]
2,99E+00	0
2,74E+00	6
2,49E+00	8
2,24E+00	10
1,99E+00	12
1,74E+00	14
1,49E+00	28
1,24E+00	70
9,95E-01	126
7,46E-01	210
4,98E-01	280
2,49E-01	350
0,00E+00	360

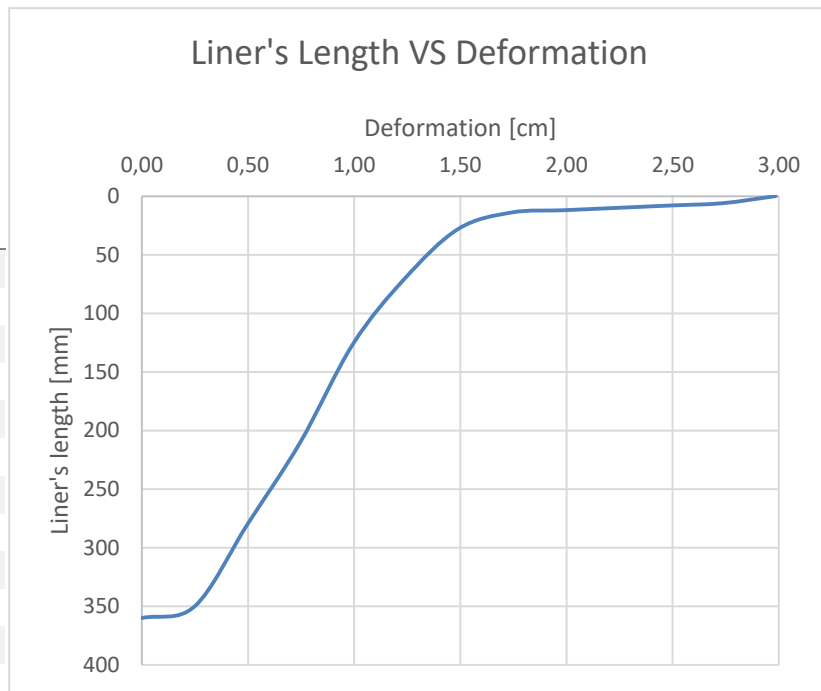


Figure 3.34 Graphical relation between the total node's deformation and the liner's length. A high increase in deformation occurs in the first 25 mm of liner. [0 value of liner's length starts at the distal end].

The maximum value of deformation is almost of 3 cm at the bottom of the liner, where the force is being applied. The deformation range can be divided into two sections. The first is where the deformation is inferior to 1cm, from the dark blue until the lighter green regions, comprising almost the full length of the liner. The second region, where deformation achieves values greater than 1cm is represented from green to red. This last region of higher deformation, starts where the liner's curvature changes and increases rapidly as the bottom's approach. This can be seen in figure 3.34 and table 3.6, the region where deformation was higher than 1,5 cm was in the first 28 cm of liner (considering value 0 at the distal end).

Concerning von Mises stress (figures 3.35-3.37), the maximum value observed was of 278 kPa and the minimum was of 6,8 Pa. The stress is higher in the beams, as it is expected, as the force flows through the stiffest material. Therefore, the entire surface in figure 3.35 is covered in blue, as the silicone is not under high stress. The high stress in the beams can be seen in figures 3.36 and 3.37. Also, it is seen that the beams are under much higher stress at the conic region of the liner (the distal end) and as soon the liner starts to become cylindrical the stress decreases at least one order of magnitude at the beams.

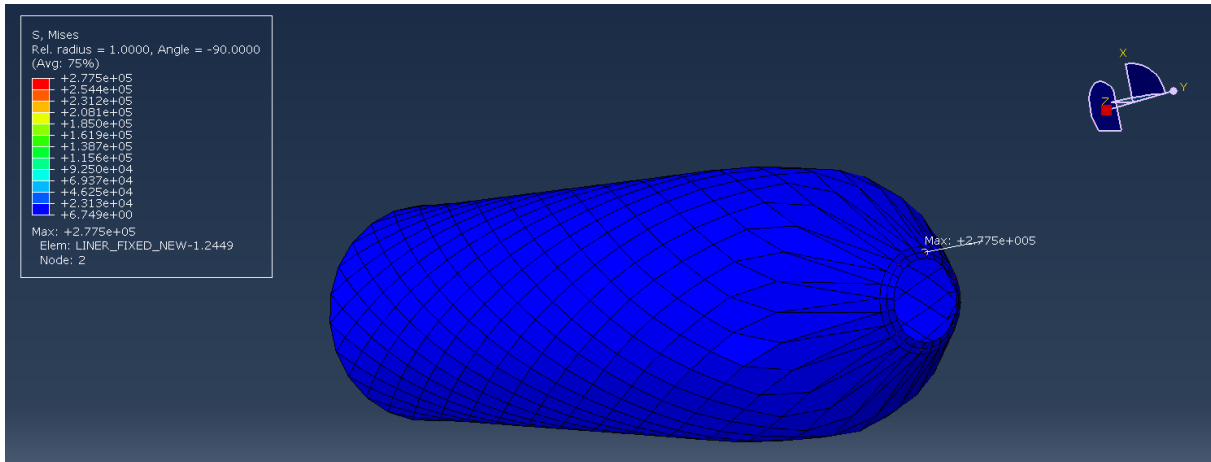


Figure 3.35 Von Mises stress - Exterior view of reinforced liner. Maximum value of stress shown of 278 kPa in a reinforcement beam. The blue colour shows how the silicone doesn't sustain any considerable stress.

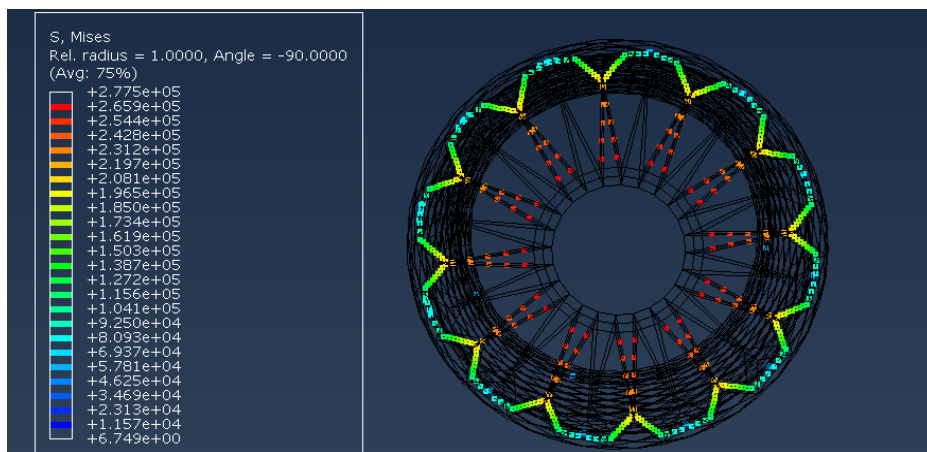


Figure 3.36: Von Mises stress representation at the reinforcement beams – bottom view. Isosurface representation.

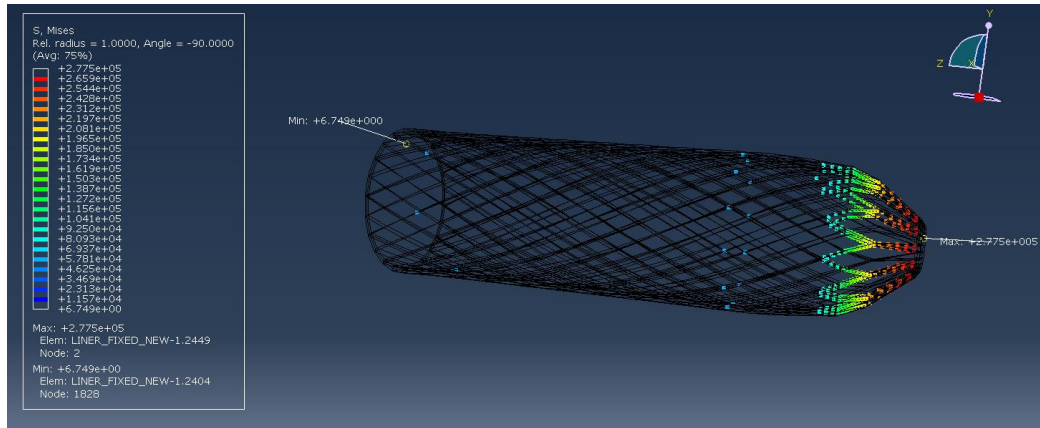


Figure 3.37: Lateral view of Von Mises stress sustained by the beams. Blue dots are visible on the cylindrical region of the liner.

3.6.4.2. Non-reinforced liner – ANSYS model

For the non-reinforced liner, the Von Mises stress and total deformation were also evaluated.

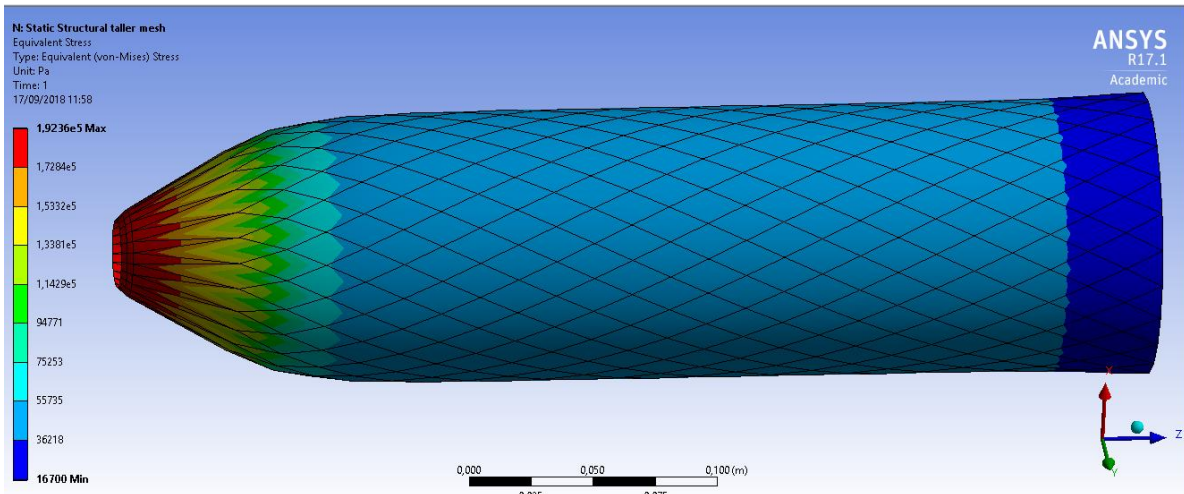


Figure 3.38 Von-Mises stress, lateral view – Non-reinforced liner. Maximum value – 192 kPa.

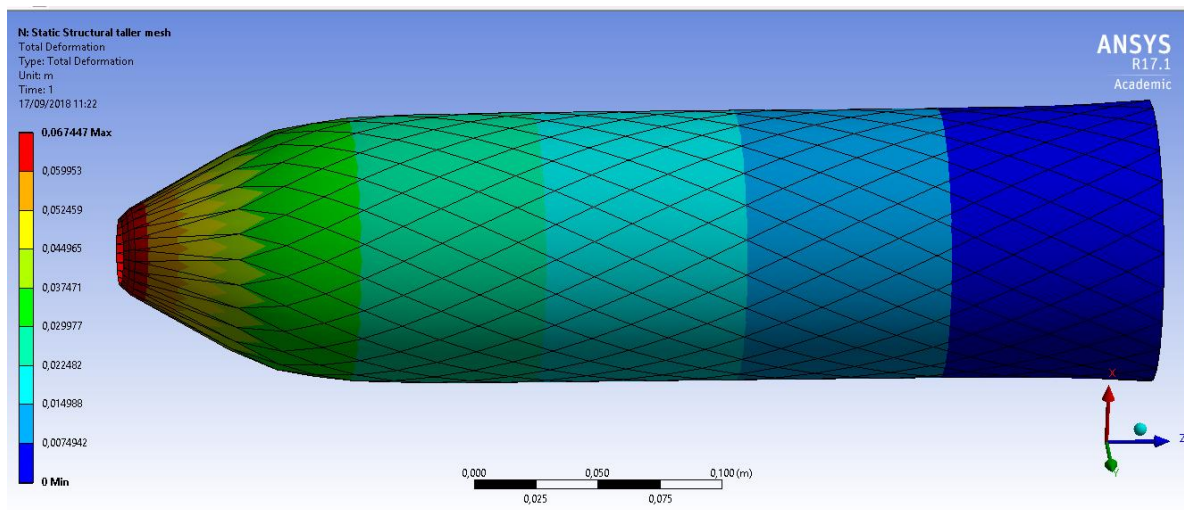


Figure 3.39: Total deformation for Non-reinforced liner, lateral view. Maximum value of total deformation was at the distal end with a value of 6,7 cm. More than twice the value of the reinforced liner.

3.7. Finite Element Analysis Discussion

3.7.1. 1st Stage Discussion – Pistoning effect:

Both models (linear elastic and hyperelastic) observed a clear separation between the soft tissue and the liner, this is expected, because the simulation only concerns the behaviour of non-reinforced silicone liner. With the insertion of a reinforcement mesh, such separation shouldn't occur anymore, or at least should occur to a lesser extent. Comparing the linear model with the hyperelastic model, the H value of liner/soft tissue separation was considerably smaller at the linear model ($H_{\text{linear}}= 2,56\text{cm}$ and $H_{\text{hyperelastic}}=16,3\text{ cm}$) and much closer to reality, according to the non-reinforced Majicast liner test in Chapter 4. The maximum value of deformation in the soft tissue was the same in the non-linear and linear model (figure 3.20 and 3.16 respectively) both having a maximum deformation of approximately 5mm.

The Von Mises stress results have also shown a difference, both in stress areas of sensitivity as well as in maximum values, relative to the two material models used.

In the linear model the maximum stress was of 93 kPa, and it occurred at the bottom of the liner, in the contact region between it and the plate (figure 3.16). In the hyperelastic model, the maximum stress occurs in the region where the liner suffers necking (figure 3.22), the separation region between the liner and the soft tissue. The maximum value of von Mises stress in this model is of 109 kPa, slightly higher than the linear model value.

Both models show the same overall stress configuration, (figure 3.17 for the linear model and figure 3.23 for the hyperelastic model) with an area of higher stress at the region where the separation between liner and soft tissue occurs, even if necking is absent as it is in the linear model, followed by a stress decrease the closer to the bottom of the liner, with another increase at the contact region between the liner and the steel plate that applies the force. It is interesting that the von Mises stress distribution behaves the same in both models, although the separation values (H) between both models are very different, because this indicates that the stress distribution has this pattern.

For both models, the minimum value of von Mises stress occurs in the soft tissue region and in this region, it shows no relevant variation in the range of values through the entire sample. The maximum stress in the soft tissue is higher for the non-linear model than it is for the linear model (12,3 kPa, (figure 3.21) and 10 kPa (figure 3.18) respectively).

These results demonstrate how the pistoning effect of a liner affects the model of a limb. Although the soft tissue model is not sufficiently exact to quantify this effect, it gives some clues of what happens during pistoning, and how the action of a stabilizing mesh fabric imbedded within the silicone matrix is necessary for soft tissue control. In this model it is seen that the concept of surface matching is lost, which will cause the loss of an even pressure distribution, by other words, will cause boundary pressure gradients along the stump and bony prominences, and that will be problematic at full load, during the

stance phase of gait. This pressure gradients will cause shear stress within the soft tissue, compromising the quality of the coupling. It is also seen in this model, that the biggest soft tissue deformation during pistoning occurs at the distal end of the stump. This might cause scar stretching, which should always be avoided.

Comparing the experimental results from Chapter 4, specifically, the results taken from the non-reinforced Majicast liner, the deformation supported by the linear elastic silicone liner model shows closer deformation results than the hyperelastic model. However, the deformation from the linear model is essentially 3 times higher than the real deformation. An explanation for this is the fact that friction is not the main factor responsible for suspension of elastomeric liners. Instead, the correct insertion (donning) of the liner, pushes out the air between the liner and the stump, creating a negative pressure, allowing the atmospheric pressure to apply pressure on the exterior surface of the liner, maintaining suspension. This donning protocol is explained in chapter 2, under the described patent from Klasson and Össur.

So, to a certain degree, this study reflects how the effect of a stabilizing mesh is important to avoid pistoning during swing, as the silicone matrix by itself is not capable of such a thing.

3.7.2. 2nd Stage discussion – Reinforced VS Non-reinforced liner:

The study developed during this stage wants to evaluate the quality of the reinforcement mesh configuration developed by the University of Strathclyde, on pistoning prevention. The goal of evaluating the direct effect of the reinforcement in the soft tissue is left aside in this stage. This because the previous stage of study, concluded that the region under higher deformation when pistoning occurs, was the distal area of the soft tissue. It might be of importance to remember now, that the final goal for this work, is to develop a reinforcement mesh that controls the silicone matrix in such a way that pistoning is avoided, this way maintaining the concept of surface matching during the entire gait cycle.

The data available from the selected linear models:

- For the non-reinforced linear elastic silicone liner with soft tissue (considering friction) – Deformation of 3,13 cm; Separation of 2,56 cm between the liner and the soft tissue;
- Reinforced linear elastic silicone liner without soft tissue, “24-nodes” mesh – Deformation of 3 cm at the distal end;
- Non-reinforced linear elastic silicone liner without soft tissue, “24 nodes” mesh – Deformation of 6,7 cm;

The first consideration to make, is that the reinforcement reduces by more than half, the deformation of the liner.

The main aspect to analyse in this model is the reinforcement mesh configuration. It is seen in the von Mises stress figures, that the stress concentration is present in the conic region at the bottom of the

liner. It is also observed in the deformation figures, that the conic region is the one suffering the highest deformation.

Considering the result of this model and comparing it to the experiment realised in Chapter 4 with the full length reinforced Majicast liner, a major difference is observed, from 3 cm of deformation at the computational model and 3mm of deformation in the experimental model. This computational model doesn't include the friction between the soft tissue and the liner, or does it consider the negative pressure that the liner suffers when donned correctly. However, it already has a deformation of 3 cm, equal to the deformation a non-reinforced computational model liner suffers when friction is considered. Further work necessary to confirm that this reinforcement mesh configuration is good enough to avoid pistoning would be to create a model where soft tissue is inserted but also, where the atmospheric pressure exerted at the liner is applied to the model.

In figure 3.36, referring to the von Mises stress sustained by the reinforcement fibres, it is visible that the cylindrical area sustains a much smaller stress. It is also visible in figure 3.33 and 3.34, that the region with higher deformation are the initial 25mm of the distal region. This suggests that this reinforcement configuration will not require a full-length reinforcement. This is beneficial because a full-length liner is less flexible, and for transtibial amputees, it might constrain the knee movement.

It could be expected that an aspect that would improve this computational model is the FE mesh density, especially around the conic region. However, as seen in the table present in the appendix, to double the number of elements in the mesh, increasing significantly the mesh density in the conic region, doesn't increase significantly the mesh quality parameters of: aspect ratio, element quality and Jacobian ratio. This information tells us that further work is necessary to create a finite element mesh configuration, in such a way that the elements' quality is improved at the bottom of the liner, keeping at the same time the reinforcement beams configuration present here.

One would also expect that, increasing the density of reinforcement beams around the conic area at the bottom of the liner would decrease the displacement observed. This would be of special interest to avoid the "milking" effect, dragging down the soft tissue at the distal end of the stump, possibly causing skin scar stretching. The only drawback of such an increase in density is the increase of difficulty in the donning process for the amputee, something that can be highly considered by patients for the comfort of the liner [80], due to the decrease of flexibility of that area, what would cause a more difficult turn inside out of the liner.

Also, further work would be to construct a liner with the same reinforcement mesh configuration but only reinforcing the first 25mm. This would confirm that this configuration is competitive with the present state of the art commercial reinforced liner configurations.

CHAPTER 4 - Liner's Mechanical Tests

4.1. Objective

- To develop a method that identifies which prosthetic liner shows the smallest longitudinal stretching capacity. In order to verify the one that will reduce pistoning the most and its effect in soft tissue control.

4.2. Materials

The testing setup consists in a model of a transtibial stump and a prosthetic liner sample, inserted in the Instron testing machine.

The stump model consists in a bone replica, covered with a soft tissue model. The soft tissue model was constructed using silicone foam that covered the bone and mimics soft tissue properties. Inside it has a cavity that was filled with a bag, where water can be drained in or out, to simulate the stump volume variations during the day. The cavity was then fulfilled with silicone RTV6166 (from Silicone Solutions Ltd), that mimics the mechanical behavior of soft biological tissue, due to a similar stiffness and viscous behavior [81], and has been used in previous studies for soft tissue testing [82,83]. Finally, the stump model was covered with a silicone membrane, with the thickness of half a liner. This membrane didn't allow air to get between the liner and the stump during the mechanical tests, this way mimicking the behavior when a liner is donned into a residual limb, where the atmospheric pressure keeps the liner in place without air between the liner and the stump.

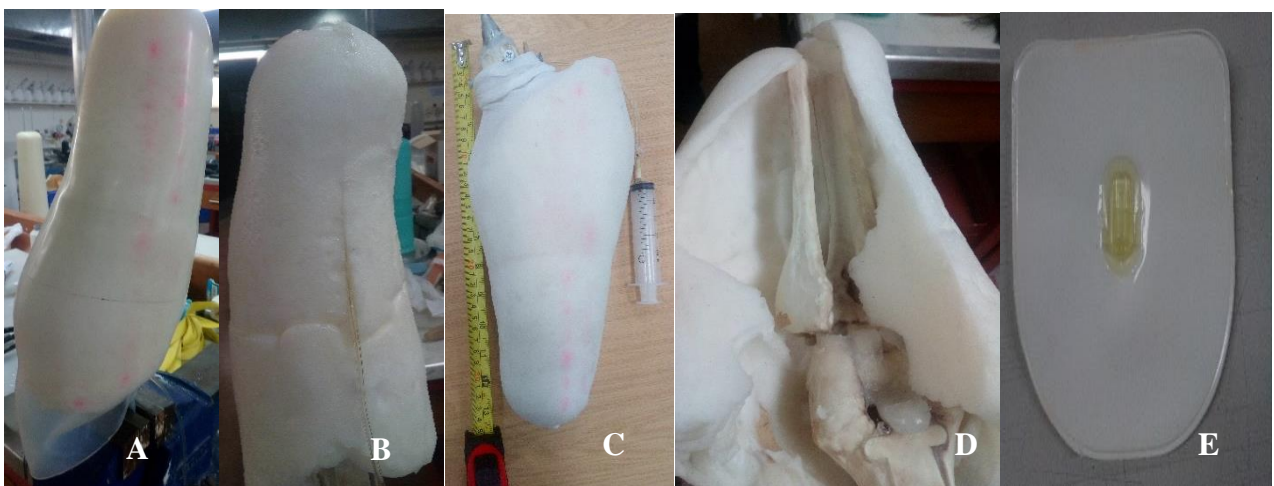


Figure 4.1: A - Silicone membrane covering the model shown. Its purpose is to allow air pushing out when the liner is donned, causing this way a realistic suspension. B - Exterior representation, with tube connecting the syringe to the interior visible; C - Stump model without silicone cover, 35 cm length, with syringe connected to the interior of the model; D - Cavity with transtibial amputation bone replica shown. E - Bag inserted inside the cavity shown in image D, and after that filled with fluid by the syringe.

The liner has an “umbrella” at the end of it, where a pin can be inserted. This pin is meant to fix the liner to the rigid socket in a real embodiment.

Five liners were tested. Two produced at the University of Strathclyde, and three from “Össur hf”. One liner from Strathclyde was a non-reinforced silicone liner, in this thesis called Majicast non-reinforced. The other liner produced at the University of Strathclyde was also composed by a silicone matrix, but reinforced with an imbedded mesh configuration fabric, covering the entire liner. This one is called in this presentation as Majicast reinforced. The three liners from Össur hf were the ICEROSS ORIGINAL, ICEROSS COMFORT and ICEROSS ORIGINAL clear. Iceross original is fully reinforced by a fabric covering the outside and imbedded in the distal area. Iceross original clear is reinforced at the distal area, as can be clearly seen in the figure 4.2. Iceross comfort has the same reinforcement configuration as Iceross original: a fabric covering the entire surface but is mainly reinforced at the distal area, with an imbedded reinforcement in this region (figure 4.2).



Figure 4.2: Liners tested. From left to right: Iceross Original, Iceross Comfort, Iceross Clear, Majicast non-reinforced liner, Majicast reinforced liner.

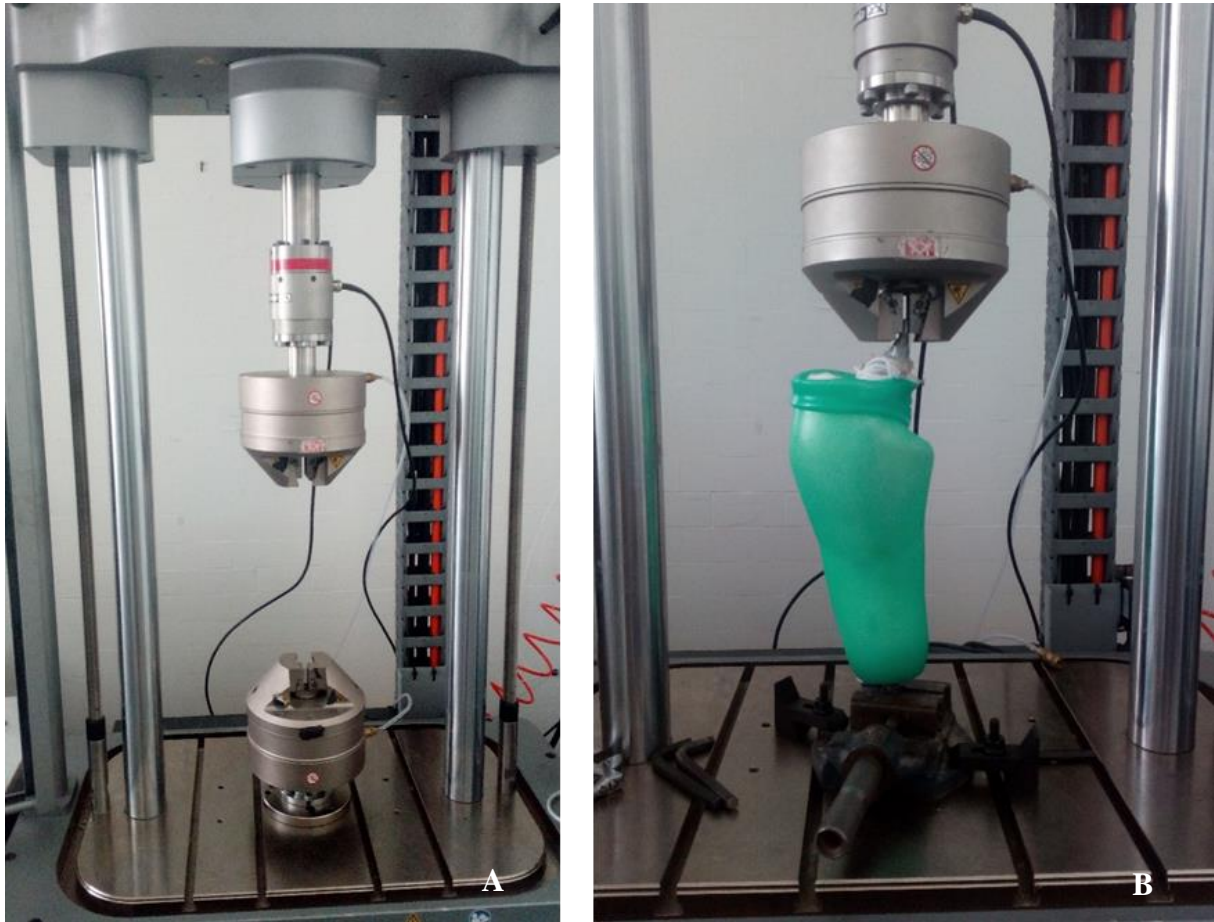


Figure 4.3: Instron machine experimental setup – A - No stump model; B - Stump Model and Non-reinforced Majicast liner prototype.

4.3. Methodology

Thirty tests were conducted. The tests were dynamic and load controlled, mimicking the swing phase of the gait cycle and mimicking a small stump volume variation.

Test Procedure

1. Insert the liner sample in the stump model;
2. Fix the extremity of the bone shown in the Instron machine movable part;
3. Insert the liner's pin at the fixed part of the machine, fixed by a clamp;
4. Set 0 value;
5. Apply test conditions;
6. Analyse the results. The smaller the displacement observed at each liner the more suitable it is for longitudinal soft tissue control.

Table 4.1: Tests description.

Test conditions	Non-reinforced Majicast liner	Reinforced Majicast liner	Iceross Clear	Iceross Original	Iceross Comfort
10 mL mark on the syringe	<ul style="list-style-type: none"> • Dynamic load-controlled tests: Triangular function: 49N max, 0N min, 2 Hz, 30 cycles; • Results: Load and displacement were retrieved at an acquisition rate of 100Hz and 3 graphics were constructed: Displacement vs time; Load vs time and Displacement vs load; • 2 tests for each volume change; 				
15 mL mark on the syringe					
20 mL mark on the syringe					

Test conditions

To measure the influence of a stump volume decrease in the coupling stiffness of a liner, it was decreased the volume of the bag inside the stump model by 5 mL steps, completing 2 steps in total, with a difference of 10mL between the most inflated and most deflated tests. Each time the stump volume changed the tests were conducted two times for each liner placed.

First, for 5 seconds a 0N force was applied to free the system of any pre-stress. Applying a triangular function force with a maximum value of 49N, minimum 0N and a frequency of 2 Hz.

The maximum tensile force was approximated¹² from the calculation of the tension in a simple pendulum, of 15cm length (mimicking the distance between the liner's and the prosthesis center of mass), at the point of maximum velocity, with a mass of 3,5 kg (an approximation of the prosthesis weight) and with a maximum angle of 30°. The frequency was calculated from the number of strides/min given by a transtibial amputee while walking reported by Sanders *et al.* [84] (approximately 70 strides/min). 30 cycles are applied, with constant measurements of load and displacement being taken at an acquisition rate of 100 Hz.

¹² Calculations present in previous chapter.

4.4 Mechanical tests results

Having realized 30 tests, with each one of those tests resulting in three different graphics (“Load vs time”, “Displacement vs time” and “Displacement vs load”), it is not possible to present the 90-graphics showing in detail what happened during each test. Using the same rational as used before at the finite element analysis, the maximum displacement presented in each test was initially chosen as the criteria to evaluate which liner presents a better coupling stiffness with the stump model. Such results are presented in table 4.2.

Table 4.2: Maximum displacement in each test shown, as well as the percental change between each volume variation and the total change between the first volume and the last.

Max Displacement [mm] [±0,05]	Non-reinforced Majicast liner	Variation [%]	Reinforced Majicast liner	Variation [%]	Iceross Clear	Variation [%]	Iceross Original	Variation [%]	Iceross Comfort	Variation [%]
T1 (10 mL mark on the syringe)	8,8		4,4		6,5		6,2		8,8	
T2 (10 mL mark on the syringe)	9		3,8		6,4		5,7		7,5	
T3 (10mL mark on the syringe)										12,3
T1 (15 mL mark on the syringe)	13,6	6%	3,9	2%	8,7	4%	7,3	4%	10,5	6%
T2 (15 mL mark on the syringe)	8,3		4,9		6,5	6,4	9,8			
T1 (20 mL mark on the syringe)	9,5	-17%	3,5	-5%	6,9	-1%	7,9	3%	10,1	-1%
T2 (20 mL mark on the syringe)	8,6		3,5		7,8		7,7		9	
Total % variation		2%		-15%		14%		31%		-1%

To analyse the tendency that the volume change created on the system’s (liner and stump model) behaviour, the percental variation was calculated. It is shown at table 4.3 (maximum displacement table) next to the values of each tests. To calculate this value, an average between Test 1 and Test 2 of each volume variation was used, with the equation:

$$\% \text{ Variation} = \frac{\left(\frac{D1 + D2}{2}\right)_{Vi} - \left(\frac{D1 + D2}{2}\right)_{Vf}}{\left(\frac{D1 + D2}{2}\right)_{Vf}} \times 100$$

Where:

D1 and D2 are respectively the deformations for Test 1 and Test 2;

Vi is the initial volume and Vf is the final volume;

However, before jumping to conclusions based only on this single value, one needs to evaluate if the tests conditions were the same (and constant) for each of the tests. The reason for this is that the Instron machine has some limitations when trying to find the 0N minimum value or the 49N minimum value due to the viscoelastic characteristics of the silicone. To access the tests conditions, other criteria were created:

- The mean maximum tensile force applied. To access the offset from the upper limit;
- The mean maximum compressive force applied. To access the offset from the lower limit of the cycles;
- Average minimum displacement¹³. To be sure that the maximum displacement value is comparable between tests and samples.
- Cycle repeatability – Comparing “Displacement vs load” graphs allows us to see if the cycles are constant or if there are pattern deviations; This criterion ensures that no air is trapped between the liner and the stump model. This occurred during preliminary tests when the stump model didn’t have the silicone membrane enclosing it (figure 4.1-A). The scale to analyse this is:
 1. Very high-density pattern: No cycles leaving the major path;
 2. High density pattern: At least one cycle leaves the path, demanding visualisation of the Load vs time graphic or displacement vs time graphic to be sure that the max and min values are representative for all the cycles

The result of this criterion was “1” for all the tests analysed and presented here, contrary to the results from the preliminary tests. This ensures that the cycles are reliable, and no air got trapped. It also assures us that the maximum and minimum results of load and displacement

¹³ Elastomeric liners are intended to be incompressible, with constant volume deformation under compressive pressure. If a negative displacement occurs, it should not be seen as a liner compression, but as a stump model compression (remember the model has in its composition a foam capable of compression).

are representative (approximated) of the maximum and minimum values of each individual cycle sustained by the liner.

The mentioned criteria are summarized in the following tables: table 4.3 for the average of the minimum displacement in each cycle, table 4.4 shows the mean maximum tensile force applied through all cycles. and table 4.5 shows the mean maximum compressive force in each cycle.

Table 4.3: Mean minimal displacement. Highlighted are the values where the offset was higher than 1mm.

Mean Min Displacement [mm] [±0,05]	Non-reinforced Majicast liner	Reinforced Majicast liner	Iceross Clear	Iceross Original	Iceross Comfort
T1 (10 mL mark on the syringe)	0	1,2	0,5	1,0	-1,3
T2 (10 mL mark on the syringe)	1,6	0,8	1,0	-0,7	-2,7
T3 (10mL mark on the syringe)					3,0
T1 (15 mL mark on the syringe)	0,5	0,5	1,5	1,5	1,7
T2 (15 mL mark on the syringe)	0,1	0,8	0,9	0,6	-0,5
T1 (20 mL mark on the syringe)	-0,2	0,6	1,7	1,0	0,1
T2 (20 mL mark on the syringe)	0,0	0,6	1,6	0,7	-1,5

Table 4.4: Mean maximum tensile force. Highlighted are the values where the offset was higher than 9N, considering the value of 49N as reference.

Mean Max Tensile Force [N] [±0,5]	Non-reinforced Majicast liner	Reinforced Majicast liner	Iceross Clear	Iceross Original	Iceross Comfort
T1 (10 mL mark on the syringe)	59	54	51	50	45
T2 (10 mL mark on the syringe)	54	51	52	44	42
T3 (10mL mark on the syringe)					60
T1 (15 mL mark on the syringe)	78	51	62	58	58
T2 (15 mL mark on the syringe)	48	57	50	51	51
T1 (20 mL mark on the syringe)	59	48	50	60	49
T2 (20 mL mark on the syringe)	51	49	53	54	49

Table 4.5: Mean maximum compressive force. Highlighted are the values where the offset was higher than 10N, considering the value of 0N as reference

Mean Max Compressive Force [N] [±0,5]	Non-reinforced Majicast liner	Reinforced Majicast liner	Iceross Clear	Iceross Original	Iceross Comfort
T1 (10 mL mark on the syringe)	-12	-1	-10	-6	-22
T2 (10 mL mark on the syringe)	-3	-0,5	-4	-21	-27
T3 (10mL mark on the syringe)					7
T1 (15 mL mark on the syringe)	-6	-5	-1	-1	-3
T2 (15 mL mark on the syringe)	-10	-2	-6	-9	-15
T1 (20 mL mark on the syringe)	-12	0	2	-6	-14
T2 (20 mL mark on the syringe)	-10	-2	-1	-9	-23

4.4. Mechanical tests discussion

To have an objective analysis over the 30 tests, some analysis criteria was set up in section 4.3 where the results are described. The goal of the present analysis is to compare the five liners tested, compare the reinforcement present within their silicone matrixes, and to see which one of the liners/reinforcements allows a better pistoning control. As said before, the maximum displacement observed is a good toll to access this. However, after observing that some liners showed a minimal displacement above 1mm (table 4.3), it is better, in order to compare the system behaviour with different liners, to analyse the amplitude of the displacement. For this reason, table 4.6 was created.

Table 4.6: Amplitude of the displacement, using maximum and minimum value of displacement of each test. Also % variation is shown between the immediately previous stump volume tests performed.

Amplitude [mm] [±0,05]	Non-reinforced Majicast liner	% Variation	Reinforced Majicast liner	% Variation	Iceross Clear	% Variation	Iceross Original	% Variation	Iceross Comfort	% Variation
T1 (10 mL mark on the syringe)	8,8		3,2		6		5,2		10,1	
T2 (10 mL mark on the syringe)	7,4		3		5,4		6,4		10,2	

Amplitude [mm] [±0,05]	Non-reinforced Majicast liner	% Variation	Reinforced Majicast liner	% Variation	Iceross Clear	% Variation	Iceross Original	% Variation	Iceross Comfort	% Variation
T3 (10mL mark on the syringe)									9,3	
T1 (15 mL mark on the syringe)	13,1	8%	3,4	5%	7,2	3%	5,8	0%	8,8	0%
T2 (15 mL mark on the syringe)	8,2		4,1		5,6		5,8		10,3	
T1 (20 mL mark on the syringe)	9,7	-4%	2,9	-6%	5,2	-3%	6,9	5%	10	2%
T2 (20 mL mark on the syringe)	8,6		2,9		6,2		7		10,5	
Total % variation	13%		-6%		0%		20%		4%	

Analysing table 4.6, we can divide the amplitude of displacement in three groups:

- In group I (green): the non-reinforced Majicast liner and the Iceross comfort liner, with an amplitude of displacement with a range between 7,4mm and 13,1mm.
- Group II (blue) with the Iceross clear and original, with a range between 5,2-7,2 mm
- Group III (red) with a range between 4,1 and 2,9 mm, where only the Reinforced Majicast liner enters.

It is surprising that Iceross comfort is in the same range of values that the non-reinforced Majicast liner. This because Iceross comfort has an embedded fabric mesh at its distal end, with the purpose of avoiding pistoning (longitudinal displacement), while the Majicast liner doesn't have a fabric mesh embedded and is just composed by the silicone matrix, not having an anisotropic behaviour within its material allowing the liner to stretch longitudinally.

Looking at table 4.4 and 4.5, it is observed that the higher concentration of force offset was in this group (group I), especially for the maximum compressive force applied. The viscoelastic behaviour of both liners was thought to interfere with the Instron machine's ability to control the load. The Majicast for obvious reasons (it has nothing more than silicone), and the Comfort because of its main goal of the

cushioning of bony prominences¹⁴, possible due to a higher silicone concentration, neglecting to a certain extent pistoning control.

In group II are the other two commercial liners studied: Iceross clear and original. The main difference between these two liners is the presence of a covering nylon fabric on the outside of the “Original” liner. The force offset seen (table 4.4 and 4.5) in this group is smaller, pointing to a stiffer behaviour (linear elastic) than a viscoelastic behaviour of the liners, as the Instron machine is more effective at controlling the load. The two fabric reinforcements present within the silicone matrix are the same for both liners (the mesh has the same configuration and density), covering only the distal area of the liner. The fact that both liners present the same behaviour leads us to the conclusion that the nylon fabric cover of the surface of the liner doesn’t have any especial effect on the longitudinal displacement control. Instead, it seems to have only an aesthetic and ergonomic function.

Group III only has the reinforced Majicast liner. This liner shows a stiffer behaviour over all liners tested, showing not only the smaller displacement, but also the smallest force offset. This can be explained by the full-length fabric reinforcement imbedded within the silicone. This fact shows the possibility for a better soft tissue control during swing. Further tests are required to analyse the pressure distribution during stance phase and the bending of the knee.

The reason to analyse the liner’s behaviour variation with the stump volume decrease, is to check if the liner is sensible to the decrease in the stump’s stiffness (caused by the volume decrease), or if the liner can keep the system (soft tissue, bone and liner) to behave in the same way (measured by displacement), even though a part of this system (the soft tissue) clearly losses stiffness.

Analysing table 4.6 and the variation tendency as the volume changes, it can be observed that the displacement amplitude varied more than 10% overall for the systems where the non-reinforced Majicast and the Iceross original liners were used (13% and 20% respectively). It is expected that the non-reinforced Majicast liner demonstrates a higher sensitivity to the stump volume decrease. This liner doesn’t have an embedded fabric mesh within it’s silicone matrix and with the decrease of the volume of the stump model and the resultant stiffness decrease, it does nothing to keep the stiffness of the system. The reinforcement fabric within the silicone matrix is expected to bring a higher stiffness to the liner, especially longitudinally. The larger area the reinforcement covers, the higher the increase in stiffness of the liner will be. This explains why the reinforced Majicast liner shows the smallest variation (-6% overall). Following this rationale, the fact that the reinforcement on the commercial liners is only made on the distal area, might explain the behaviour of the Iceross original liner (20% increase in displacement with 10mL decrease). However, the stump volume variation was very small during the

¹⁴ <https://www.ossur.com/prosthetic-solutions/products/all-products/liners-and-sleeves/iceross-comfort> Consulted on 07/07/2018

performance of the tests (10mL overall) and the number of tests might be too small to make a statistic analysis showing a variation on the liners behaviour as the stump volume decreases.

In the literature review made, no study with a stump volume variation and pistoning measure was found. Pistoning measure has been approached in several ways: FEA [85], camera footage analysis [86] or photoelectric sensors [87]. However, the results observed have a broad range of discrepancy, varying 100mm between the measurements made.

CHAPTER 5 - Conclusions and Future Developments

It is already known that an elastomeric liner locally distributes the pressure around bony prominences, as far as the surface matching concept is acquired, due to the mechanical properties of elastomeric materials. This thesis brings a study on the main aspect that distinguishes elastomeric liners: its reinforcement, with the purpose of developing a new elastomeric liner.

A finite element model (FEM) was created with two main goals: proving the necessity of such a reinforcement, evaluating where the main areas of stress in the reinforcement mesh configuration are present and what was its effect on the liner longitudinal displacement.

In the FEM created, it was proven, by comparing the computational models developed with the mechanical tests performed, that the stress range supported during the swing phase by the silicone allowed the material model chosen to be an isotropic linear elastic silicone material, instead of modelling with a hyperelastic model. This is because on the stress-strain curve of silicone, with the load applied, the material was still behaving linearly, as the deformation result close to the experimental tests proved. However, the deformation from the linear computational model was still too high when compared to the deformation observed in the experimental mechanical model (non-reinforced Majicast liner). The explanation for this is the absence of the atmospheric pressure effect on the computational model, as explained in the discussion of chapter 3.

With the model created with the isotropic linear elastic silicone, and absence of a reinforcement, it was possible to observe the loss of surface matching due to pistoning occurrence, but also, the observation that soft tissue also suffers stretching during pistoning, which might be dangerous if the tissues around the scar are stretched until breakdown. This is especially dangerous in low income countries (this work and Legbank's target), where concerns are raised due to improper surgery [88].

The study developed with the FEM containing the reinforcement mesh configuration, allowed us to evaluate the clear improvement on pistoning control (less than half of the displacement observed in the model without reinforcement). This result shows that the configuration proposed by the University of Strathclyde is effective.

The reinforced FEM have also shown the areas of higher stress concentration. The fact that those areas appear at the distal end of the liner is coincident with the reinforcement areas present in state of the art commercial liners and is in line with what has been developed and claimed in several patents since 1987 (as seen in chapter 2). Further work would be to construct a liner with the same reinforcement mesh configuration but only reinforcing the first 25mm. This would confirm that this configuration is competitive with the present state of the art commercial liners reinforcements configurations.

Further work is necessary to improve the FEM created here. One aspect is to analyse the effect that an increase in the reinforcement density fibres at the distal end would have in the stiffness increase of the liner, and if such an increase would turn the liner too stiff to be used comfortably by the patient at the time of donning the liner.

Another improvement is to increase the similarity between this FEM and reality. To achieve this the model could benefit from several inputs. One improvement is to insert a soft tissue geometry inside the cavity of the liner from the reinforced FEM, as it was done in the first step of the FEA, the more realistic this geometry would be, the better, as different regions of the stump and liner would suffer different stresses. Another improvement, as also said is the atmospheric pressure. In combination with the friction it would create a more realistic boundary condition to the study of pistoning.

The major improvement that can be done to the FEM, other than the ones already presented, is to make the analysis dynamic instead of static. A dynamic analysis with boundary conditions of a full gait cycle, would give a perspective of the maintenance of the coupling stiffness along the number of cycles. Something important, and that can be done previously to any real testing set up.

To compare the reinforcement mesh configuration produced here with the state of the art commercial liners, mechanical tests mimicking the conditions of the swing phase were conducted. The effect of these reinforcements was evaluated when stump volume variations are present, and if the liners were resilient enough to maintain surface matching although the volume decreased.

The mechanical tests resulted in some new discoveries.

The first one is the fact that the non-reinforced Majicast liner shows the same pistoning control as the Iceross Comfort liner. This can be attributed to the low reinforcement of the Iceross Comfort liner. The reinforcement fibres from this liner are only present at the very distal end of the liner. It also shows that the medical grade silicone used by the University of Strathclyde creates a matrix capable of avoiding longitudinal stretch, to a certain extent.

The other main discovery is the fact that the reinforced Majicast liner shows a higher pistoning control than Iceross Clear and Iceross Original. This is positive, because it justifies the mesh configuration used for the reinforcement. Also, connecting this liner with the reinforced FEM liner created in Chapter 3, it is seen that the main stresses are sustained at the distal end, and the reinforcement along the liner is ineffective as it supports a small stress. If, in future work, a testing of a half-length reinforced liner is made, with the same mesh configuration, it is expected that this configuration allows a pistoning control as good as the state of the art liners, once the reinforcement on the top half of the liner is ineffective.

It is still necessary, however, to test the capacity for radial displacement of the reinforced liner. Two movements that the liner needs to do, both in a full-length and half-length reinforced liner, are the knee bending movement and the donning of the liner by an amputee. This should be done in the near future.

To finish, another aspect worthy of mention, is the small variations of pistoning that all liners present with the changes of volume applied to the stump model. Although the volume variations were small, and the number of tests were not statistically relevant, no major difference was observed between any volume mark. This is positive for every liner tested, as it proves that, in this range of volume variation, the surface matching concept and the coupling stiffness is maintained by every liner, independent from volume changes.

References

- [1] – A. Buis, B. Klasson (2006), *Open Learning 94 912 Advanced Prosthetic Science (Manual 3) Prosthetic socket fit; Implications of basic engineering principles*. National Centre for Training and Education in Prosthetics and Orthotics.
- [2] - Paternò, L.,Ibrahimi, M., Gruppioni, E., Menciassi, A., Ricotti, L. (2018). Sockets for limb prostheses: a review of existing technologies and open challenges. *IEEE Transactions on Biomedical Engineering*. PP. 1-1. doi:10.1109/TBME.2017.2775100.
- [3] – Groth, KE. (1942). Clinical observations and experimental studies of the pathogenesis of decubitus ulcers. *Acta Chir Scand* 87 [Suppl 76]:1-209
- [4] – Husain, T. (1953). An experimental study of some pressure effects on tissues, with reference to the bed-sore problem. *The Journal of Pathology and Bacteriology*,66(2), 347-358. doi:10.1002/path.1700660203
- [5] – Kosiak, M. (1959). Etiology and pathology of ischemic ulcers. *Arch Phys Med Rehabil* 40:62-69
- [6] – Kosiak, M. (1961). Etiology of decubitus ulcers. *Arch Phys Med Rehabil* 42:19-29
- [7] – Dinsdale, S.M. (1973). Decubitus ulcers in swine: light and electron microscopy study of pathogenesis. *Arch Phys Med Rehabil* 54:51 – 56
- [8] – Dinsdale, S.M. (1974). Decubitus ulcers: role of pressure and friction in causation. *Arch Phys Med Rehabil* 55:147-152
- [9] – Nola, G.T., Vistnes, L.M. (1980). Differential response of skin and muscle in the experimental production of pressure sores. *Plast Reconstr Surg* 66:728-733
- [10] – Daniel, R.K., Priest, D.L., Wheatley D.C. (1981) Etiological factors in pressure sores: an experimental model. *Arch Phys Med Rehabil* 62:492-498
- [11] – Daniel, R.K., Wheatley D.C., Priest D.L. (1985) Pressure sores and paraplegia: an experimental model. *Ann Plast Surg* 15:41-49
- [12] - Reswick, J. B., & Rogers, J. E. (1976). Experience at Rancho Los Amigos Hospital With Devices and Techniques to Prevent Pressure Sores. *Bed Sore Biomechanics*,301-310. doi:10.1007/978-1-349-02492-6_38
- [13] - Sanders, J. (2005). Stump-socket interface conditions. In *Pressure Ulcer Research: Current and Future Perspectives*. (pp. 129-147). Springer Berlin Heidelberg. doi: 10.1007/3-540-28804-X_9
- [14] – Radcliffe, C.W. (1962). The biomechanics of below-knee prostheses in normal, level, bipedal walking. *Artif Limbs*.;6(2): 16–24. [PMID:13972953]
- [15] – Staats, T.B., Lundt J. (1987). The UCLA total surface bearing suction below-knee prosthesis. *Clin Prosthet Orthot.*; 11(3):118–30.
- [16] – Kristinsson, O. (1993). The ICEROSS concept: A discussion of a philosophy. *Prosthet Orthot Int.* 17(1):49–55. [PMID:8337100] doi: 10.3109/03093649309164354
- [17] – Patterson, S. (2007). Editorial: Experiences with negative-pressure socket design. *The Academy Today*. 3(3): A7-9

- [18] - Finlay, B. (1969): Scanning electron microscopy of the human dermis under uniaxial strain. *Biol. med. Engng* 4 283-348
- [19] - Aukland, K., & Reed, R. K. (1993). Interstitial-lymphatic mechanisms in the control of extracellular fluid volume. *Physiological Reviews*, 73(1), 1-78. doi:10.1152/physrev.1993.73.1.1
- [20] - Sanders, J., Zachariah, S., Jacobsen, A., & Ferguson, J. (2005). Changes in interface pressures and shear stresses over time on trans-tibial amputee subjects ambulating with prosthetic limbs: comparison of diurnal and six-month differences. *Journal of Biomechanics*, 38(8), 1566-1573. doi:10.1016/j.jbiomech.2004.08.008
- [21] - Dickinson, A., Steer, J., & Worsley, P. (2017). Finite element analysis of the amputated lower limb: A systematic review and recommendations. *Medical Engineering & Physics*, 43, 1-18. doi:10.1016/j.medengphy.2017.02.008
- [22] - Tonuk, E., & Silver-Thorn, M. (2003). Nonlinear elastic material property estimation of lower extremity residual limb tissues. *IEEE Transactions on Neural Systems and Rehabilitation Engineering*, 11 (1), 43-53. doi:10.1109/tnsre.2003.810436
- [23] - Portnoy, S., Yizhar, Z., Shabshin, N., Itzchak, Y., Kristal, A., Dotan-Marom, Y., Gefen, A. (2008). Internal mechanical conditions in the soft tissues of a residual limb of a trans-tibial amputee. *Journal of Biomechanics*, 41 (9), 1897-1909. doi:10.1016/j.jbiomech.2008.03.035
- [24] - Portnoy, S., Siev-Ner, I., Yizhar, Z., Kristal, A., Shabshin, N., & Gefen, A. (2009). Surgical and Morphological Factors that Affect Internal Mechanical Loads in Soft Tissues of the Transtibial Residuum. *Annals of Biomedical Engineering*, 37 (12), 2583-2605. doi:10.1007/s10439-009-9801-3
- [25] - Shoham, N., & Gefen, A. (2012). Deformations, mechanical strains and stresses across the different hierarchical scales in weight-bearing soft tissues. *Journal of Tissue Viability*, 21 (2), 39-46. doi:10.1016/j.jtv.2012.03.001
- [26] – Le K.M., Madsen B.L., Barth P.W., Ksander G.A., Angell J.B., Vistnes L.M. (1984) An in-depth look at pressure sores using monolithic silicon pressure sensors. *Plastic and Reconstructive surgery* 74(6):745-753.
- [27] –Stekelenburg, A., Gawlitta, D., Bader, D. L., & Oomens, C. W. (2008). Deep Tissue Injury: How Deep is Our Understanding? *Archives of Physical Medicine and Rehabilitation*, 89(7), 1410-1413. doi:10.1016/j.apmr.2008.01.012
- [28] - S.M. Peirce, T.C. Skalak, G.T. Rodeheaver. (2000). Ischemia-reperfusion injury in chronic pressure ulcer formation: a skin model in the rat. *Wound Repair Regen*, 8, pp. 68-76
- [29] - Sulzberger, M. B., Cortese, T. A., Fishman, L., Wiley, H. S., & Peyakovich, P. S. (1966). Studies on Blisters Produced by Friction. *Journal of Investigative Dermatology*, 47 (5), 456-465. doi:10.1038/jid.1966.169
- [30] – Akers, W. A., & Sulzberger, M. B. (1972). The friction blister. *Plastic and Reconstructive Surgery*, 50(1), 98. doi:10.1097/00006534-197207000-00049
- [31] – Goldstein, B., & Sanders, J. (1998). Skin response to repetitive mechanical stress: A new experimental model in pig. *Archives of Physical Medicine and Rehabilitation*, 79(3), 265-272. doi:10.1016/s0003-9993(98)90005-3

- [32] – Naylor, P. F. (1955). The Skin Surface And Friction. *British Journal of Dermatology*,67(7), 239-248. doi:10.1111/j.1365-2133.1955.tb12729.x
- [33] – Sanders JE, Greve JM, Mitchell SB, Zachariah SG. (1998). Material properties of commonly-used interface materials and their static coefficients of friction with skin and socks. *J Rehabil Res Dev*;35(2):161–176
- [34] - Emrich R, Slater K. (1998). Comparative analysis of below-knee prosthetic socket liner materials. *J Med Eng Technol*;22(2):94–98
- [35] - Covey SJ, Muonio J, Street GM. (2000). Flow constraint and loading rate effects on prosthetic liner material and human tissue mechanical response. *J Prosthet Orthot*;12(1):15–41.
- [36] - Sanders JE, Nicholson BS, Zachariah SG, Cassisi DV, Karchin A, Ferguson JR. (2004). Testing of elastomeric liners used in limb prosthetics: Classification of 15 products by mechanical performance. *J Rehabil Res Dev*;41(2):175–186.
- [37] - Klute, G. K., Glaister, B. C., & Berge, J. S. (2010). Prosthetic Liners for Lower Limb Amputees: A Review of the Literature. *Prosthetics and Orthotics International*,34(2), 146-153. doi:10.3109/03093641003645528
- [38] –Hagberg K., Branemark R.. (2001). Consequences of non-vascular transfemoral amputation: a survey of quality of life, prosthetic use and problems. *Prosthetics Orthotics Int.*, vol. 25, no. 3, pp. 186–194,.
- [39] – Hoaglund, F.T., Jergesen, H.E., Wilson, L., Lamoreux, L.W., and Roberts, R. (1983). Evaluation of problems and needs of veteran lower-limb amputees in the San Francisco Bay Area during the period 1977–1980,” *J. Rehabil. R&D / Veterans Admin., Dept. Med. Surgery, Rehabil. R&D Service*, vol. 20, no. 1, pp. 57–71.
- [40] – Huff EA, Ledoux WR, Berge JS, Klute G.K. (2008). Measuring residual limb skin temperatures at the skin-prosthesis interface. *J Prosthet Orthot*;20(4):170–173.
- [41] – Klute, G.K., Rowe, G.I, Mamishev, A.V., and Ledoux, W.R. (2007). The thermal conductivity of prosthetic sockets and liners. *Prosthetics Orthotics Int.*, vol. 31, no. 3, pp. 292–299,.
- [42] –Shitzer A. and Eberhart, R. (1983). *Heat Transfer in Medicine and Biology: Analysis and Applications. USA: Plenum Press,*
- [43] –Houdas, Y. and Ring, E. (1982). *Human Body Temperature Its Measurement and Regulation. USA: Plenum Press.*
- [44] – Hachisuka K, Matsushima Y, Ohmine S, Shitama H, Shinkoda K. (2001). Moisture permeability of the total surface bearing prosthetic socket with a silicone liner: Is it superior to the patella-tendon bearing prosthetic socket? *J Uoeh*; 23(3):225–232
- [45] – Klute, G. K., Huff, E., & Ledoux, W. R. (2014). Does Activity Affect Residual Limb Skin Temperatures? *Clinical Orthopaedics and Related Research®*, 472(10), 3062-3067. doi:10.1007/s11999-014-3741-4
- [46] – Ghoseiri, K., Zheng, Y. P., Hing, L. L., Safari, M. R., & Leung, A. K. (2016). The prototype of a thermoregulatory system for measurement and control of temperature inside prosthetic socket. *Prosthetics and Orthotics International*,40(6), 751-755. doi:10.1177/0309364615588343

- [47] – Sonck WA, Cockrell JL, Koepke GH. (1970). Effect of liner materials on interface pressures in below-knee prostheses. *Arch Phys Med Rehabil*;51(11):666–669.
- [48] – Lee WC, Zhang M, Mak AF. (2005). Regional differences in pain threshold and tolerance of the transtibial residual limb: Including the effects of age and interface material. *Arch Phys Med Rehabil*;86(4):641–649.
- [49] – Gholizadeh, H., Osman, N. A., Eshraghi, A., Ali, S., & Razak, N. (2013). Transtibial prosthesis suspension systems: Systematic review of literature. *Clinical Biomechanics*,29(1), 87-97. doi:10.1016/j.clinbiomech.2013.10.013
- [50] - Linde, H. V., Hofstad, C. J., Geurts, A. C., Postema, K., Geertzen, J. H., & Limbeek, J. V. (2004). A systematic literature review of the effect of different prosthetic components on human functioning with a lower-limb prosthesis. *The Journal of Rehabilitation Research and Development*,41(4), 555. doi:10.1682/jrrd.2003.06.0102
- [51] – Dasgupta, A. K., McCluskie, P. J., Patel, V. S., & Robins, L. (1997). The performance of the ICEROSS prostheses amongst transtibial amputees with a special reference to the workplace a preliminary study. *Occupational Medicine*,47(5), 323-323. doi:10.1093/occmed/47.5.323-a
- [52] – Wheeler, J., Mazumdar, A., Marron, L., Dullea, K., Sanders, J., & Allyn, K. (2016). A pressure and shear sensing liner for prosthetic sockets. *2016 38th Annual International Conference of the IEEE Engineering in Medicine and Biology Society (EMBC)*. doi:10.1109/embc.2016.7591124
- [53] – Sanders, J.E., Lam, D., Dralle, A.J., and R. Okamura. (1997). Interface Pressures and Shear Stresses at Thirteen Socket Sites on Two Persons with Transtibial Amputation, *Journal of Rehabilitation Research and Development*, 34(1).
- [54] – Bo Klasson, Ossur Kristinsson (1987), Sleeve-shaped article, particularly for amputation stumps. *U.S Pat No 4,923,474*
- [55] – Aldo A. Laghi, Donald R. Fox (1996) Elastomer reinforcement of an elastomer interface membrane for residual limb of an amputee. *US Pat No 5,728,168A*
- [56] – Össur Kristinsson and Hilmar Br. Janusson (1997), Dual durometer silicone liner for prosthesis, *US Pat No 6136039A*
- [57] – Olafur Freyr Halldorsson (2009), Suspension liner having multiple component system. *US Patent No 20110118854A1*
- [58] – Fay, J; (2001) Prosthetic liner having longitudinal inelasticity. *U.S. Patent No. US6231617B1*
- [59] - H. Gholizadeh, N.Osman, A. Eshraghi, S. Ali (2014). The Effects of Suction and Pin/Lock Suspension Systems on Transtibial Amputees' Gait Performance. doi: <https://dx.doi.org/10.1371%2Fjournal.pone.0094520>
- [60] – Luder Mosler, Christian Muller, Thomas Kettwig (2012). Liner for a prosthesis, and prosthesis. *US Patent No 20150250624A1*.
- [61] – J. Colvin, C. Kelley (2011). Fabric covered polymeric prosthetic liner. *US Pat No 9265629B2*
- [62] – J.L. Doddroe, C.T. Kelley, L. Rowe, JR. (2010) Polymeric prosthetic liner with controlled stretch characteristics. *US Pat No 20130331951A1*
- [63] – C. A. Caspers (1990). Prosthetic polyurethane liner and sleeve for amputees. *US Patent No US5534034A*

- [64] - A.Buis, N. Mathur, I.Glesk (2016). Skin Temperature Prediction in Lower Limb Prostheses. *IEEE journal of biomedical and health informatics*, VOL. 20, NO. 1. doi: 10.1109/JBHI.2014.2368774
- [65] – Lin, C., Chang, C., Wu, C., Chung, K., & Liao, I. (2004). Effects of liner stiffness for trans-tibial prosthesis: A finite element contact model. *Medical Engineering & Physics*, 26(1), 1-9. doi:10.1016/s1350-4533(03)00127-9
- [66] - Yeoh, O. H., (1993). Some forms of the strain energy function for rubber. *Rubber Chemistry and technology*, Volume 66, Issue 5, Pages 754-771.
- [67] –Cagle, J.C. , Reinhall P.G., Allyn K. J., McLean J., Hinrichs P., Hafner B.J. & Sanders J.E. (2017). A finite element model to assess transtibial prosthetic sockets with elastomeric liners. *Medical & Biological Engineering & Computing*; 56(7):1227-1240. DOI: 10.1007/s11517-017-1758-z.
- [68] – Silver-Thorn M.B.; Steege J.W.; Childress D.S. (1996) *A review of prosthetic interface stress investigations, Journal of Rehabilitation Research and Development Vol . 33 No . 3, Pages 253-266*
- [69] – Steege JW, Childress DS. (1988). Finite element modeling of the below-knee socket and limb : phase II . In: *Modeling and control issues in biomechanical systems, ASME*:121-9.
- [70] – Silver-Thom MB. Prediction and experimental verification of residual limb/prosthetic socket interface pressures for below-knee amputees (Dissertation). Chicago: Northwestern University, 1991.
- [71] — Silver-Thorn MB, Childress DS. (1992). Use of a generic, geometric finite element model of the below-knee residual limb and prosthetic socket to predict interface pressures. In: *Proceedings of the 7th World Congress of ISPO*,:272.
- [72] - Torres-Moreno R, Solomonidis SE, Jones D .(1992). Threedimensional finite element analysis of the above-knee residual limb. In: *Proceedings of the 7th World Congress of ISPO*,:274.
- [73] - Vannah WM. (1990). Indentor tests and finite element modelling of bulk muscular tissue in vivo (Dissertation). Chicago: Northwestern University.
- [74]- Stephen J.P., Scott L.D., (1996). The influence of muscles on knee flexion during the swing phase of gait”, *Journal of Biomechanics*, Volume 29, Issue 6, Pages 723-733
- [75] – Radcliffe, CW. (1962). The Biomechanics of Below-Knee Prostheses in Normal, Level, and Bipedal Walking. *Artificial Limbs*, Vol. 6, No. 2, pp. 16-24.
- [76] – Kadaba MP, Ramakrishnan HK, Wootten ME. (1990). Measurement of lower extremity kinematics during level walking. *Journal of orthopaedic research: official publication of the Orthopaedic Research Society*.;8(3):383–92.
- [77] – Selles RW, Bussman JBJ, Wagenaar RC, Stare HJ. Effects of prosthetic mass and mass distribution on kinematics and energetics of prosthetic gait: a systematic review. *Arch Phys 'Med Rehabil* 1999;80:1593-9.
- [78] – M.ZhanG, A Mak, (1999). In vivo friction properties of human skin. *Prosthetics and Orthotics International*, 23, 135-141
- [79] – Cagle J. (2016). “A Computational Tool to Enhance Clinical Selection of Prosthetic Liners for People with Lower Limb Amputation”. (Doctoral dissertation) University of Washington.
- [80] – K.L. Coleman; D. Boone; L. Laing; D. Mathews; D. Smith. (2004) Quantification of prosthetic outcomes: Elastomeric gel liner with locking pin suspension versus polyethylene foam liner with 84

neoprene sleeve suspension. *Journal of Rehabilitation Research & Development*, Volume 41, Number 4, Pages 591–602.

[81] – Valtorta, D. (2007). Dynamic torsion test for the mechanical characterization of soft biological tissues (Doctoral dissertation). Zürich, ETH, Diss.

[82] – Ottensmeyer, M.P. (2002). Tempest I-D: An instrument for measuring solid organ soft tissue properties. *Exp Techniques* 26, 48–50. doi: <https://doi.org/10.1111/j.1747-1567.2002.tb00069.x>

[83] – Kalanovic, D., Ottensmeyer, M. P., Gross, J., Gerhardt, B., and Dawson, S. L. (2003) Independent testing of soft tissue viscoelasticity using indentation and rotary shear deformation. *In Medicine Meets Virtual Reality, IOS Press*, pp. 137–143.

[84] – J.E. Sanders, S.G.Zachariah, A.B.Baker, J.M.Greve, C.Clinton (2000). Effects of changes in cadence, prosthetic componentry, and time on interface pressures and shear stresses of three trans-tibial amputees. *Clinical Biomechanics*, Volume 15, Issue 9, 684 – 694.

[85] – Commean PK, Smith KE, Vannier MW. (1997). Lower extremity residual limb slippage within the prosthesis. *Arch Phys Med Rehabil*; 78:476-85.

[86] – Gholizadeh, H., Abu Osman, N., Lúvíksdóttir, Á., Eshraghi, A., Kamyab, M. and Wan Abas, W. (2011). A new approach for the pistoning measurement in transtibial prosthesis. *Prosthetics and Orthotics International*, 35(4), pp.360-364.

[87] – Sanders JE, Karchin A, Ferguson JR, Sorenson EA. (2006). A noncontact sensor for measurement of distal residual-limb position during walking. *Journal of Rehabilitation Research & Development*;43:509–516.

[88] – C.S Harkins, & A. McGarry, & A. Buis. (2013). Provision of prosthetic and orthotic services in low-income countries: A review of the literature. *Prosthetics and orthotics international*. 37(5):353-61. Doi: 10.1177/0309364612470963.

Appendix A – Mesh analysis

Table A. 1: Parameters evaluating the quality of three different meshes for the reinforced model.

Mesh	Number of elements	Element quality Min value	Aspect Ratio Max value	Jacobian ratio Max value
24-node	1248	1,37E-02	32,96	1,317
28-node	1680	1,36E-02	31,55	1,296
34-node	2448	1,34E-02	29,88	1,274

It is wanted:

- A high minimum value of element quality
- A low maximum value of aspect ratio
- The closest possible Jacobian ratio to 1.